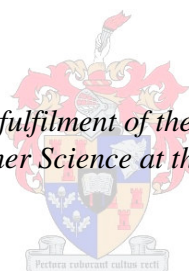


Organic-inorganic hybrid graft copolymers of polystyrene and polydimethylsiloxane

by
Aimée Celestè Sutherland

*Thesis presented in partial fulfilment of the requirements for the degree
Master of Science in Polymer Science at the University of Stellenbosch*



Supervisor: Prof Peter Edward Mallon
Department of Chemistry and Polymer Science

March 2010

Declaration

By submitting this dissertation electronically, I declare that the entirety of the work contained therein is my own, original work, that I am the owner of the copyright thereof (unless to the extent explicitly otherwise stated) and that I have not previously in its entirety or in part submitted it for obtaining any qualification.

March 2010

Copyright © 2010 Stellenbosch University

All rights reserved

Abstract

Hybrid graft copolymers of polystyrene (PSty) and polydimethylsiloxane macromonomers (PDMS) were synthesised. PSty-*g*-PDMS was synthesised employing the grafting through technique via a conventionally free radical polymerization (FRP) using a polydimethylsiloxane macromonomer. In this series the amount of PDMS incorporated into the copolymer was varied by varying the macromonomer to styrene ratios as well as the length of the PDMS side chain. This allows for the study of the effect that the macromonomer content and the branching length has on the efficiency of the grafting process. A second series of PDMS-*g*-PSty was also synthesized where the PDMS forms the backbone and the PSty the grafts. Two synthetic techniques were employed for the formation of these polymers. Firstly, the grafting onto approach was used where functional polystyrene prepolymers with either an allyl or vinyl end-groups were synthesised anionically (living anionic polymerization) prior to the coupling of a functional prepolymer using a hydrosilylation reaction with a Karstedt platinum catalyst. This technique was successful and gave insight to the effect of the polystyrene prepolymer graft length has on the grafting efficiency as well as the functional groups needed on the PDMS backbone. Furthermore, the effect of the viscosity (of the PDMS macromonomer) plays on the grafting efficiency was also elucidated. Lastly, the grafting from approach was employed for the formation of PDMS-*g*-PSty. ATRP, atom transfer radical polymerization, of styrene using a bromoisobutyrate functional PDMS macroinitiator was used for the synthesis of these copolymers. This was accomplished by reacting commercial silane functional PDMS molecules via a hydrosilylation reaction (using a Karstedt catalyst) with allyl-2-bromo-2-methyl-propionate to give a PDMS macroinitiator with bromoisobutyrate functional groups. This will allow for the initiation and growth of polystyrene branches from the PDMS backbone (employing ATRP with a suitable catalyst and ligand). The formation of the end-product, PDMS-*g*-PSty, via this route proved to be extremely difficult and largely unsuccessful. Liquid chromatography (LC) at the critical point (LCCC) of polystyrene was used to separate the graft material from homo-polymers which might have formed as well as from the PDMS macromonomer. This technique allows for a very fast chromatographic analysis of the grafting reaction. Under the critical conditions of PSty it was found that the graft copolymer eluted at a lower retention time than the unreacted macromonomer and PSty homopolymer. Two-dimensional chromatography, where LCCC (1st dimension) was coupled to size exclusion chromatography (2nd dimension), was used for the evaluation of the CCD and MMD (molecular mass distribution) of the graft material. LC was furthermore coupled off-line to FTIR and TEM using an LC interface. LC-FTIR gave insight to the microstructure of the material, whilst LC-TEM gave insight to the morphological nanostructure of the material.

Opsomming

Hibried ent-kopolimere is gesintetiseer uit polistireen (PSty) en poldimetieilsiloksaan (PDMS). PSty-g-PDMS is gesintetiseer deur gebruik te maak van die ent-deur tegniek via 'n konvensionele vrye radikaal polimerisasie proses (VRP). In die reeks is die hoeveelheid PDMS wat geïnkorporeer is, gevarieer deur die hoeveelheid PDMS tot PSty verhouding te verander asook die lengte van die PDMS sytak. Gevolglik het dit toegelaat vir die studie van die effek wat die makromonomeer inhoud, sowel as die taklengte het op die effektiwiteit van die ent-proses. 'n Tweede reeks is ook gesintetiseer, waar die PDMS die ruggraat vorm van die ko-polimeer, en die stireen die takke vorm van die ko-polimeer. Dus is PDMS-g-PSty gesintetiseer. Twee sintetiese tegnieke is benut vir die vorming van die kopolimere. In die eerste geval is daar van die ent-op tegniek gebruik gemaak waar funksionele polistireen prepolimere met 'n alliel of 'n silaan end-groep gesintetiseer is deur gebruik te maak van 'n anioniese lewendige polimerisasie voor die koppeling van die PDMS makromonomeer deur 'n hidrosililasie proses met 'n Karstedt platinum katalisator. Die tegniek was suksesvol en het in diepte insig gegee van die effek wat die molekulêre lengte van die polistireen prepolimeer het op die effektiwiteit van die ent-proses, sowel as die minimum hoeveelheid funksionele groepe wat teenwoordig moet wees op die PDMS ruggraat. Verder is die effek wat die viskositeit (van die PDMS makromonomeer) op die ent-proses het, bekend gemaak. Laastens is daar ook van die ent-vanaf tegniek gebruik gemaak vir die vorming van PDMS-g-PSty. AORP, atoom oordrag radikale polimerisasie, van stireen, deur gebruik te maak van 'n bromoisobutiraat funksionele PDMS makro-inisieerder, is gebruik vir die sintese van die kopolimere. Die makro-inisieerders is bekom deur gebruik te maak van kommersiële silaan funksionele PDMS, en dit is gereageer deur middel van 'n hidrosililasie proses met alliel-2-bromo-2-metiel-propionaat. Dit het PDMS makroinisieerders tot gevolg gehad met bromoisobutiraat funksionele groepe. Gevolglik kon stireen takke vanaf die PDMS ruggraat gegroei word deur gebruik te maak van AORP met 'n geskikte katalisator en ligand. Die vorming van die end-produk, PDMS-g-PSty, deur middel van hierdie roete was onsuksesvol. Vloeistof chromatografie by die kritiese punt van polistireen was gebruik om die ent-produk te skei van die homo-polimere en PDMS makromonomeer. Gevolglik kon die chemiese samestelling van die ent-produk geëvalueer word. Twee-dimensionele chromatografie, waar vloeistof chromatografie by die kritiese punt van polistireen in die eerste vlak gekoppel was aan grootte uitsluitings chromatografie in die tweede vlak, was benut om die chemiese komposisie sowel as die molekulêre massa verdeling van die ent-produk te verkry. Verder was vloeistof chromatografie indirek aan Fourier-oordrag infrarooi en transmissie elektron mikroskopie (TEM) gekoppel. Eergenoemde het insig gegee tot die mikrostruktuur van die materiaal, terwyl laasgenoemde insig gegee het tot die morfologiese nanostruktuur van die materiaal.

Dedicated to my brother, Steven – “Pain is momentarily, quitting lasts forever”

Acknowledgements

This thesis would not have been possible without the funding from the NRF.

Thank you Prof Mallon for all your guidance throughout the thesis process.

Mom and Dad, for your encouraging words and great understanding.

Donna, my partner in crime, and holding my hand.

Gareth and Wael, teaching me everything I know about polymer in the lab.

Lebo and Rueben for giving advice.

Jaques-antoine Raust for showing me all of the ropes for 2-D analysis.

Flatmates over the two years; Charl, Elsa, Storm and Jannie. Thank you for endearing my growing pains.

Special thank you to Storm for keeping me grounded.

My foreign friends, Nico, Osvaldo, John, Mat for keeping times interesting (especially Nico).

Wade, for his wise words, for always listening and telling me to breathe.

Emanti team, especially Grant, Philip, Beryl and Nicolene for being very supportive.

The staff at Polymer Science; Oom Hennie, Erinda, Aneli, Deon, Jim and Kelvin. Special thank you to Kelvin for all his assistance.

Andy, for the use of his lab during ridiculous times.

Mohammed Jaffer at UCT for his TEM assistance. Finding that one golden sample.

Elsa Malherbe at NMR. Rerunning my samples a million times.

Erica girls, Anja, Mia, Lanmari and Carien, for the endless discussions about love life and everything else.

Table of contents

Glossary	iv
List of figures	viii
List of schemes	xii
List of tables	xiii

Chapter 1: Introduction and objectives

1.1	Introduction	2
1.2	Objectives	3
1.3	Thesis outline	4
1.4	References	5

Chapter 2: Historical and literature review

2	Introduction	7
2.1	Hybrid materials	7
2.1.1	General overview	7
2.2	Copolymers	9
2.2.1	General overview	9
2.2.2	Branched polymers	9
2.2.3	Graft copolymers	10
2.2.4	Hybrid graft copolymers	11
2.3	Polymerization techniques – focus on copolymerization	13
2.3.1	Free Radical Polymerization – FRP	13
2.3.1.1	Free radical copolymerization with macromonomer	14
2.3.2	Living polymerization – Anionic polymerization	15
2.3.2.1	Initiation by nucleophilic addition	17
2.3.2.2	Propagation	18
2.3.2.3	Termination	20
2.3.3	Controlled Radical Polymerization – CRP	21
2.3.3.1	Atom Transfer Radical Polymerization- ATRP	22
2.4	Synthesis of graft copolymers	25
2.4.1	Grafting onto	25
2.4.2	Grafting through	27

2.4.2.1	Macromonomers	28
2.4.3	Grafting from	29
2.5	Chromatography – focus on analysis of graft copolymers	31
2.5.1	Size Exclusion Chromatography – SEC	32
2.5.2	Liquid Adsorption Chromatography – LAC	33
2.5.3	Liquid Chromatography at the Critical Point – LCCC	34
2.5.4	Two-Dimensional Chromatography – 2-D	36
2.5.5	Coupling techniques with chromatography	38
2.6	References	41

Chapter 3: Experimental

3.1	Synthesis	45
3.1.1	Materials	45
3.1.2	Purification of solvents	45
3.1.3	Purification of monomers	46
3.1.4	Synthesis of PSty- <i>g</i> -PDMS – Grafting through	46
3.1.5	Synthesis of PDMS- <i>g</i> -PSty – Grafting onto	47
3.1.5.1	Anionic polymerization of polystyrene	47
3.1.5.2	Hydrosilylation of polystyrene and polydimethylsiloxane	48
3.1.6	PDMS- <i>g</i> -PSty – Grafting from	50
3.1.6.1	ATRP macroinitiator method	50
3.1.7	Extraction of homo-polymers	51
3.2	Characterization of polymers synthesised	52
3.2.1	Chromatography analysis	52
3.2.1.1	Size Exclusion Chromatography – SEC	52
3.2.1.2	SEC for materials containing PDMS segments	53
3.2.1.3	Liquid Chromatography at Critical Conditions – LCCC	54
3.2.1.4	Two-dimensional chromatography – 2-D	54
3.2.2	Off-line coupling of chromatography	56
3.2.2.1	Off-line coupling of chromatography to FT-IR	56
3.2.2.2	Off-line coupling of chromatography to TEM	57
3.2.3	Nuclear Magnetic Resonance – NMR	58
3.3	References	59

Chapter 4: Results and Discussion

4.	Introduction	61
4.1	Grafting through – PSty-g-PDMS	61
4.1.1	NMR results of the grafting reactions	62
4.1.2	SEC results of the grafting reactions before extraction – RI detector	63
4.1.3	SEC results of the grafting reactions before extraction – ELSD detector	66
4.1.4	SEC results of the grafting reactions after extraction – ELSD detector	68
4.1.5	HPLC analysis	70
4.1.5.1	Liquid chromatography at the critical point of styrene	70
4.1.5.2	Two-dimensional chromatography results	76
4.1.5.2.1	PSty-g-PDMS: Short 25	76
4.1.5.2.2	PSty-g-PDMS: Medium 25	77
4.1.5.2.3	PSty-g-PDMS: Long 25	80
4.16	Coupling of LC-CC to FT-IR	82
4.17	Morphological analysis	85
4.1.7.1	LCCC coupled to TEM via indirect deposition	85
4.2	Grafting onto – PDMS-g-PSty	88
4.2.1.1	Synthesis and analysis of PSty prepolymer – Allyl functionality	88
4.2.1.2	Hydrosilylation –PDMS-g-PSty	90
4.2.1.2.1	SEC results for the grafting reactions – ELSD detector	91
4.2.1.2.2	HPLC results of PDMS-g-PSty	95
4.2.1.2.3	LCCC-FTIR and two-dimensional chromatography results	99
4.2.2.1	Synthesis of PSty prepolymer – Silane functionality	101
4.2.2.2	Hydrosilylation – PDMS-g-PSty – LCCC results	103
4.2.2.2.1	LCCC results	103
4.3	Grafting from – PDMS-g-PSty	106
4.3.1	Synthesis of PDMS macroinitiator	106
4.3.2	ATRP – PDMS-g-PSty	108
4.4	References	110

Chapter 5: Conclusions and Recommendations

5.1	Conclusions	112
5.2	Recommendations and future work	113

Glossary

Abbreviations

2-D:	Two-dimensional chromatography
ACDMS:	Allyl-chlorodimethylsilane
AIBN:	2,2'-azobis(isobutyronitrile)
APCI:	Atmospheric pressure chemical ionization
ATRA:	Atom transfer radical addition
ATRP:	Atom transfer radical polymerization
BuLi:	Butyllithium
CCD:	Chemical composition distribution
CDCl ₃ :	Deuterated chloroform
CDMS:	Chlorodimethylsilane
CEEC:	Condition of entropy-enthalpy compensation
CRP:	Controlled radical polymerization
CuCl:	Copper(I)chloride
dNbipy:	4,4'-di-(5-nonyl)-2,2'-bipyridine
dRI:	Differential refractive index
ELSD:	Evaporative light scattering detector
ESI:	Electro spray ionization
FRP:	Free radical polymerization
FTD:	Functional type distribution
FTIR:	Fourier transform infra-red
GE-LC:	Gradient elution liquid chromatography
HMS:	Methyl-hydrosiloxane
homo-PDMS:	Polydimethylsiloxane homopolymer
homo-PSty:	Polystyrene homopolymer
HPLC:	High performance liquid chromatography
IR:	Infra-red
KOH:	Potassium hydroxide
LAC:	Liquid adsorption chromatography
LC:	Liquid chromatography
LCCC:	Liquid chromatography at the critical conditions
LC-CAP:	Liquid chromatography at the critical point of adsorption

LC-LCA:	Liquid chromatography under limiting conditions of adsorption
LC-LCD:	Liquid chromatography under limiting conditions
LC-PEAT:	Liquid chromatography at the point of exclusion-adsorption transition
NMP:	Nitroxide mediated living radical polymerization
NMR:	Nuclear magnetic resonance
Nu:	Nucleophile
N ₂ :	Nitrogen
M ⁺ :	Metal counterion
MAD:	Molar architecture distribution
MCR:	mono-methacryloxypropyl terminated polydimethylsiloxane
Methanol:	Methanol
MgSO ₄ :	Magnesium sulphate
MMD:	Molar mass distribution
MS:	Mass spectrometer
MW:	Molecular weight
PDI:	Polydispersity index
PDMS:	Polydimethylsiloxane
PnBuA:	Poly(n-butylacrylate)
PMMA:	Poly(methylmethacrylate)
PSty:	Polystyrene
RAFT:	Radical addition fragmentation chain transfer
RI:	Refractive index
SEC:	Size exclusion chromatography
SFRP:	Stable free radical polymerization
STD:	Structural type distribution
Sty:	Styrene monomer
TEM:	Transmission electron microscopy
THF:	Tetrahydrofuran
TMEDA:	N,N,N',N'-tetramethylethylenediamine
UV:	Ultraviolet
UV-Vis:	Ultraviolet-viscometer
VDT:	Vinylmethylsiloxane

Notations

[A]:	Concentration of monomer A
[B]:	Concentration of macromonomer B
<i>b</i> :	Block
DP_n :	Number average degree of polymerization
DP_n^0 :	Instantaneous number-average degree of polymerization
<i>f</i> :	Initiation efficiency
<i>g</i> :	Graft
ΔG :	Change in Gibbs free energy
ΔH :	Change in enthalpy
[I]:	Concentration of initiator
K:	Kelvin
k_{act} :	Rate of activation
k_{app} :	Apparent or observed propagation rate constant
K_d :	Distribution coefficient/Separation coefficient
k_d :	Rate constant of initiator decomposition
k_{deact} :	Rate of deactivation
k_p :	Rate constant of propagation
k_t :	Rate constant of termination
L_m :	Complexing ligand
[M]:	Monomer concentration
M_n :	Number average molecular weight
M_w :	Weight average molecular weight
M_t^n -Y:	Transition metal complex
<i>N</i> :	Degree of polymerization
P_n :	Polymer chain
r_A :	Reactivity ratio of monomer A
r_B :	Reactivity ratio of macromonomer B
R_p :	Rate of propagation
ΔS :	Change in entropy
V_m :	Total volume
V_r :	Retention volume
V_p :	Pore volume
T_g :	Glass transition temperature

X:	(pseudo)Halogen
Y:	Ligand or counterion
χ	Segment-segment interaction parameter/ Flory-Huggins Parameter
λ	Number of branches per graft copolymer
v :	Average number of monomer units
w :	Weight fraction
δ :	Chemical shift in NMR
Φ_{cr} :	Fraction of strong solvent at the critical point
Φ_{sol} :	Fraction at the point of complete solubility

List of Figures

Chapter 2

Figure 2.1:	Different architectural structures of hybrid materials.	7
Figure 2.2:	Architectures of highly branched molecules.	10
Figure 2.3:	Illustration of a unfavoured propagation reaction of a poly(macromonomer) radical with a macromonomer and a hindered termination reaction due to the steric hindrance.	15
Figure 2.4:	Possible distribution of branches resulting from the copolymerization technique employed.	24
Figure 2.5:	Scheme of different methods to synthesize graft copolymers.	25
Figure 2.6:	Various branched architectures obtained via the macromonomer technique.	28
Figure 2.7:	Illustration of the structural complexity of macromolecules, indicating the different possible distributions.	31
Figure 2.8:	Different modes of separation, molecular weight versus retention time.	31
Figure 2.9:	Schematic illustration of block-copolymer <i>AB</i> under critical conditions.	35
Figure 2.10:	Schematic illustration for the analysis of a complex polymer system.	37
Figure 2.11:	Schematic illustration of liquid chromatography coupled to FTIR spectroscopy.	39

Chapter 3

Figure 3.1:	Graphical illustration of the indirect deposition of the polymeric fraction onto a TEM grid.	58
-------------	--	----

Chapter 4

Figure 4.1:	¹ H-NMR spectra obtained for mono-methcryloxypropyl PDMS (MCR PDMS), PSty- <i>g</i> -PDMS and Sty monomer respectively.	63
Figure 4.2:	SEC graph obtained for short 25.	64
Figure 4.3:	Short SEC graphs overlaid, RI response.	64
Figure 4.4:	SEC graph obtained for medium 25.	65
Figure 4.5:	Medium SEC graphs overlaid, RI response.	65
Figure 4.6:	SEC graph obtained for long 25.	65

Figure 4.7:	Long SEC graphs overlaid, RI response.	65
Figure 4.8:	25 wt% series SEC graphs overlaid, RI response.	66
Figure 4.9:	25 wt% series SEC graphs overlaid, UV response.	66
Figure 4.10:	Short series graphs overlaid-ELSD response.	67
Figure 4.11:	Short series graphs overlaid-UV response.	67
Figure 4.12:	Medium series graphs overlaid ELSD response.	67
Figure 4.13:	Medium series graphs overlaid, UV response.	67
Figure 4.14:	Long series graphs overlaid, ELSD response.	68
Figure 4.15:	Long series graphs overlaid, UV response.	68
Figure 4.16:	SEC chromatogram of long 25, showing the unsuccessful removal of homo-PDMS.	69
Figure 4.17:	LCCC chromatogram of medium 25, showing the unsuccessful removal of homo-PDMS.	69
Figure 4.18:	An example of the determination of the critical point by varying the mobile phase composition.	71
Figure 4.19:	Chromatogram of short 10.	71
Figure 4.20:	Chromatogram of short 25.	71
Figure 4.21:	Chromatogram of short 35.	72
Figure 4.22:	Overlaid chromatograms, short series ELSD response.	72
Figure 4.23:	Chromatogram of medium 10.	72
Figure 4.24:	Chromatogram of medium 25.	72
Figure 4.25:	Chromatogram of medium 35.	73
Figure 4.26:	Overlaid chromatograms medium series, ELSD response.	73
Figure 4.27:	Chromatogram of long 10.	73
Figure 4.28:	Chromatogram of long 25.	73
Figure 4.29:	Chromatogram of long 35.	74
Figure 4.30:	Overlaid chromatograms long series, ELSD response.	74
Figure 4.31:	25 wt% series graphs overlaid, ELSD response.	74
Figure 4.32:	25 wt% series graphs overlaid, UV response.	74
Figure 4.33:	2-D chromatogram of short 25.	76
Figure 4.34:	2-D chromatogram for medium 25.	77
Figure 4.35:	Three dimensional view of medium 25's 2-D plot.	79
Figure 4.36:	2-D chromatograms overlaid: short 25 and medium 25.	79
Figure 4.37:	2-D chromatogram for long 25.	80

Figure 4.38:	Stacked waterfall plot of short 25. The absorption bands indicated by the arrows were used for the determination of the PSty-g-PDMS chain composition.	82
Figure 4.39:	Ratio of PDMS/PSty overlaid with LCCC chromatogram: short 25.	83
Figure 4.40:	Ratio of PDMS/PSty overlaid with LCCC chromatogram: medium 25.	84
Figure 4.41:	Ratio of PDMS/PSty overlaid with LCCC chromatogram: long 25	84
Figure 4.42:	LCCC chromatogram (a) of short 25 with chemigram overlay, TEM image of the material in region A (b) and region B (c).	86
Figure 4.43:	LCCC chromatogram (a) of medium 25 with chemigram overlay, TEM image of the material in region A (b) and region B (c).	87
Figure 4.44:	Typical ¹ H-NMR spectrum for PSty with an allyl endgroup.	89
Figure 4.45:	SEC chromatogram of HMS_071_30 overlaid with prepolymer PSty_vs_3_30.	91
Figure 4.46:	SEC chromatogram of HMS_031_30 overlaid with prepolymer PSty_vs_3_30.	91
Figure 4.47:	SEC chromatograms of HMS_013 series, ELSD response.	92
Figure 4.48:	SEC chromatograms of HMS_013 series, UV 254 nm response.	92
Figure 4.49:	SEC chromatogram of HMS 301_20.	92
Figure 4.50:	SEC chromatogram of HMS 301_10.	92
Figure 4.51:	SEC chromatogram of HMS 301_5.	93
Figure 4.52:	SEC chromatogram of HMS 071_20.	93
Figure 4.53:	SEC chromatogram of HMS 071_10.	93
Figure 4.54:	SEC chromatogram of HMS 071_5.	93
Figure 4.55:	SEC chromatogram of HMS 031_20.	94
Figure 4.56:	SEC chromatogram of HMS 031_10.	94
Figure 4.57:	SEC chromatogram of HMS 031_5.	94
Figure 4.58:	Chromatogram obtained for HMS 301_10.	96
Figure 4.59:	Chromatogram obtained for HMS 301 series, ELSD response.	96
Figure 4.60:	Chromatogram obtained for HMS 071_10.	96
Figure 4.61:	Chromatogram obtained for HMS 071 series, ELSD response.	96
Figure 4.62:	Chromatogram obtained for HMS 031_10.	97
Figure 4.63:	Chromatogram obtained for HMS 031 series, ELSD response	97
Figure 4.64:	Ratio of PDMS/PSty overlaid with LCCC chromatogram: HMS 071_20.	99
Figure 4.65:	Ratio of PDMS/PSty overlaid with LCCC chromatogram: HMS 071_10.	99
Figure 4.66:	2-D chromatogram for HMS 071_5.	100

Figure 4.67:	Typical ^1H -NMR spectrum for PSty with a silane endgroup.	102
Figure 4.68:	LCCC chromatogram of VDT 954_20.	103
Figure 4.69:	Magnified LCCC chromatogram of VDT 954_20.	103
Figure 4.70:	LCCC chromatogram of VDT 954 series.	103
Figure 4.71:	LCCC chromatogram of VDT 731_20.	104
Figure 4.72:	Magnified LCCC chromatogram of VDT 731_20.	104
Figure 4.73:	LCCC chromatogram of VDT 731 series.	104
Figure 4.74:	LCCC chromatogram of VDT 131_10.	104
Figure 4.75:	Magnified LCCC chromatogram of VDT 131_10.	104
Figure 4.76:	^1H -NMR spectra obtained for bromoisbutyrate PDMS macroinitiator for the ATRP of styrene and silane functional PDMS before hydrosilylation respectively.	107
Figure 4.77:	SEC chromatogram of PDMS- <i>g</i> -PSty.	108
Figure 4.78:	LCCC-chromatograms of PDMS- <i>g</i> -PSty.	108

List of Schemes

Chapter 2

Scheme 2.1: Conventional free radical polymerization of styrene; possible reaction which can arise.	13
Scheme 2.2: Charge delocalization of styrene.	17
Scheme 2.3: Initiation step for anionic polymerization.	17
Scheme 2.4: Propagation step for anionic polymerization.	18
Scheme 2.5: Ion pair associations with alkyl-lithium initiators in THF.	19
Scheme 2.6: Termination using a suitable electrophile.	20
Scheme 2.7: A general functionalization methodology for chain-end functionalization using chlorosilane functionalization followed by hydrosilylation.	21
Scheme 2.8: General illustration of the three main controlled radical polymerization reactions.	22
Scheme 2.9: Mechanism of metal complex-mediated ATRA and ATRP.	23
Scheme 2.10: General mechanism of transition-metal catalyzed ATRP.	23
Scheme 2.11: Synthesis of graft copolymers with PSty as backbone; employing the grafting onto method.	26
Scheme 2.12: Polystyrene macromonomer prepared anionically.	29
Scheme 2.13: Anionic polymerization utilized for the grafting from approach, synthesis of PI-g-PSty.	30
Scheme 2.14: Synthesis of poly(methylphenylsilane)-g-PSty via ATRP by means of the grafting from method.	30

Chapter 3

Scheme 3.1: Synthesis of PSty-g-PDMS; free radical polymerization of styrene monomer with PDMS macromonomer.	46
Scheme 3.2: Anionic polymerization and termination of functionalised polystyrene.	47
Scheme 3.3: Proposed structure of Karstedt's catalyst.	48
Scheme 3.4: Modified Chalk-Harrod mechanism.	49
Scheme 3.5: Two different routes using hydrosilylation coupling reaction to synthesize graft copolymers.	49
Scheme 3.6: Modification of silane terminal PDMS to ATRP macroinitiator.	50
Scheme 3.7: Polymerization of PDMS-g-PSty by means of ATRP with PDMS as macroinitiator.	51

List of Tables

Chapter 4

Table 4.1:	Formulation of reactions performed – PSty- <i>g</i> -PDMS.	62
Table 4.2:	Experimentally obtained molecular weights of the graft copolymers obtained – ELSD detector.	66
Table 4.3:	Molecular weights obtained for the different products for short 25.	77
Table 4.4:	Molecular weights obtained for the different products for medium 25.	78
Table 4.5:	Molecular weights obtained for the different products for long 25.	80
Table 4.6:	Summary of the effect of chain length on the formation of the graft co-product.	81
Table 4.7:	Feed ratio and molecular weights obtained for PSty prepolymer terminated with ACDMS.	88
Table 4.8:	Summary of the PDMS prepolymers with MeHSiO functional groups.	89
Table 4.9:	Termination efficiency of PSty allyl functional prepolymers calculated from ¹ H-NMR.	90
Table 4.10:	Summary of M_n , M_w , and PDI's values obtained for the coupling reaction.	95
Table 4.11:	Influence of molecular weight of PSty prepolymer and functional groups of PDMS prepolymer on the grafting efficiency.	97
Table 4.12:	Molecular weights obtained for the different products for HMS 071_5.	100
Table 4.13:	Feed ratio and molecular weights obtained for PSty prepolymer terminated with CDMS.	101
Table 4.14:	Summary of information of the PDMS prepolymers with vinylmethylsiloxane groups.	101
Table 4.15:	Termination efficiency of PSty silane functional end-groups.	102
Table 4.16:	Termination efficiency of PSty allyl functional prepolymers calculated from ¹ H-NMR.	107

Chapter 1

Introduction and Objectives

"It was the best of times, it was the worst of times; it was the age of wisdom, it was the age of foolishness; it was the epoch of belief, it was the epoch of incredulity; it was the season of Light, it was the season of Darkness; it was the spring of hope, it was the winter of despair; we had everything before us, we had nothing before us.." – Charles Dickens

1.1 Introduction

In recent years, the focus of producing new monomers at low costs has been shifted to rather create specialised, high performance materials from their existing monomer counterparts. One such type of material are hybrid materials consisting of organic and inorganic segments^[1]. Combining the active inorganic and organic components, into a single material, at a nanosize level, have extraordinary implications in the development of polymeric materials^[2]. Furthermore, the attractiveness in hybrid materials lies in the fact that the properties of the disparate components are combined into a single material which will exhibit unique properties^[3].

These materials have promising and potentially an astounding wide variety of applications in many different areas such as optics, nanotechnology, membranes, electronics, coatings, biology and many more^[2].

In this study hybrid materials were synthesised which consisted of PSty, polystyrene (organic) and PDMS, polydimethylsiloxane (inorganic). These two components have extremely dissimilar properties. PSty is a glassy, brittle material at room temperature, whilst PDMS (even at very high molecular weights) is a viscous liquid at room temperature^[4]. The segments can be joined to produce a hybrid material with a wide range of architectural structures such as block-, star-, miktoarm- and graft copolymers^[5]. The latter mentioned, graft copolymers, are certainly the most attractive of the branch polymers.

Graft copolymers, which consist of two different polymer units, are similar to polymer blends *but* are covalently bonded which leads to nanophase separation and consequently remarkable properties are displayed^[6-8]. Three different methods, grafting onto, grafting through and grafting from, are employed for the synthesis of graft copolymers. The grafting onto method implies the coupling reaction between the main backbone (which have suitable functional groups) and the branches. These prepolymers are synthesised separately via a living polymerization mechanism. The grafting from technique entails the growth of branches from the backbone which has active sites that can initiate the polymerization of the branches. Lastly, the grafting through, also better known as the macromonomer method, implies the copolymerization of the macromonomer with functional end-groups with another monomer.

Complex graft copolymers can be synthesised with controlled synthetic techniques, which will allow for the control over the molecular architectures of the polymer^[9]. Such techniques are living polymerization and more recently developed controlled radical polymerization techniques such as ATRP, RAFT and NMP^[10].

The grafting reaction will necessarily lead to a complex mixture of products; that of the graft copolymer, the formation of homo-polymers as well as unreacted macromonomers. To obtain

complete information about the MMD and CCD of the polymer, it is necessarily to separate the graft material from the homo-materials. Although various methods are readily employed for the removal of homo-polymers, this is extremely difficult with the material studied in this project owing to their similar polarities making conventional solvent extraction methods inadequate. With this said, the development of analytical techniques for the greater understanding of the material is of utmost importance.

Liquid chromatography has been used as a primary technique for the analysis and characterisation of complex materials which are distributed in more than one molecular direction^[11]. The chemical composition is readily evaluated by means of gradient elution chromatography or liquid chromatography at the critical point of adsorption. When such a technique, which separates according to chemical composition, are combined with conventional size exclusion chromatography which evaluates the molar mass distribution a complete understanding of the graft polymer in the CCD and MMD direction will be elucidated^[12]. This is a 2-D chromatography technique. Advances in analytical techniques have opened the possibility of coupling LC to another specialised technique, such as TEM, which will lead to a wealth of information and a greater understanding of the material under question.

1.2 Objectives

The objectives for this research topic were as follow:

1. The employment of three different synthetic routes for the development of a hybrid graft material which consists of PSty and PDMS molecular units.
 - The evaluation of the synthesis of the hybrid material, PSty-g-PDMS, by means of a conventional free radical polymerization using the grafting from technique.
 - Synthesising a series of PSty-g-PDMS copolymers with various PDMS macromonomer content by the variation of the graft density as well as the graft lengths.
 - The evaluation of the synthesis of the hybrid material, PDMS-g-PSty using controlled polymerization techniques.
 - The synthesis of PSty prepolymers with either an allyl or silane functional group with different molecular lengths via anionic polymerization. Thereafter employing a hydrosilylation (using a Karstedt platinum catalyst) coupling method to synthesise a series of PDMS-g-PSty using the grafting onto technique.
 - The synthesis of PDMS macroinitiators for the ATRP of styrene to synthesise PDMS-g-PSty employing the grafting onto technique.
-

2. The development of chromatographic techniques for the analysis of the complex material.
 - The development of LCCC analysis at the critical point of PSty for the evaluation of the CCD of the polymeric materials.
 - The development of two-dimensional chromatography for a comprehensive understanding of the CCD and MMD, where LCCC is used in the first dimension of separation and SEC as the second dimension of separation.
 - Coupling chromatographic techniques offline to FTIR and TEM as to understand the microstructure and phase morphology of the materials synthesised in this project.

1.3 Thesis outline

Chapter 2 gives the historical and theoretical background of this project. The polymers synthesized in this study are classified as hybrid materials

Chapter 3, which is the experimental part of the thesis, will give a concise description of the synthesis of the graft copolymers as well as the analytical techniques used for characterization.

Chapter 4 present the results for the PSty-g-PDMS and PDMS-g-PSty series synthesised. This will be illustrated and discussed. A final conclusion is drawn from this and summarized in chapter 5 together with recommendations and possible future work.

1.4 References

- [1] G. Kickelbick, *Hybrid Materials. Synthesis, Characterization and Application* (Wiley-VCH Verlag GmbH & Co, Germany, 2007).
- [2] C. S. Pedro Gomez-Romero, *Functional Hybrid Materials* (Wiley-VCH Verlag GmbH & Co. KGaA, 2004), pp. 417.
- [3] H. Shinoda, P. J. Miller, K. Matyjaszewski, *Macromolecules* **34**, 3186 **2001**.
- [4] E. H. I. J. Brandrup, *Polymer Handbook* (John Wiley & Sons Inc, New York, ed. second edition, 1975).
- [5] J. Pyun, Matyjaszewski, K., *Chemistry of Materials* **13**, 3436 **2001**.
- [6] M. Pitsikalis, S. Pispas, J. W. Mays, N. Hadjichristidas, *Advances in Polymer Science* **135**, 2 **1998**.
- [7] K. Ito, S. Kawaguchi, *Advances in Polymer Science* **142**, 130 **1999**.
- [8] K. Ito, *Progress in Polymer Science* **23**, 581 **1998**.
- [9] V. Castelvetro, C. De Vita, *Advances in Colloid and Interface Science* **108-109**, 167 **2004**.
- [10] Matyjaszewski K., *Statistical, Gradient, Block and Graft Copolymers by Controlled/Living Radical Polymerizations* (Springer-Verlag Berlin Heidelberg, New York, 2002).
- [11] H. J. A. Philipsen, *Journal of Chromatography A* **1037**, 329 **2004**.
- [12] H. Pasch, *Advances in Polymer Science* **128**, 2 **1997**.

Chapter 2

Historical and Literature Review

(1879-1955), Germany

(To a student)

Dear Miss

I have read about sixteen pages of your manuscript ... I suffered exactly the same treatment at the hands of my teachers who disliked me for my independence and passed over me when they wanted assistants ... keep your manuscript for your sons and daughters, in order that they may derive consolation from it and not give a damn for what their teachers tell them or think of them. ... There is too much education altogether – Albert Einstein

2 Introduction

In this chapter the concept of hybrid materials and particular graft copolymers which are classified as hybrid materials will be discussed. Emphasis will be placed on the different synthetic techniques which are readily used in the polymer science field to synthesise these polymers. As these polymers are intricate in their nature, advanced analytical techniques are required. These analytical techniques will be discussed in detail in this chapter.

2.1 Hybrid materials

The scope and demand of hybrid materials are increasing rapidly, mainly due to technology breakthroughs and the desire to generate high performance, superior materials. Hybrid materials are considered to be innovative and advanced in the material field, forming a unique branch of material science.

2.1.1 General overview

Hybrid materials can broadly be defined as materials that include two moieties blended on the molecular scale^[1] and that consist of inorganic- and an organic components. Hybrid materials are by no means a new concept to the scientific world. Their origins are found in nature but it is only in the latter part of the 20th century that a great deal of interest has focused on these materials. The reason for this interest can be ascribed to the development of synthetic- as well as analytical techniques. The growth of different synthetic techniques, particular controlled synthetic routes, will essentially allow one to have some control over the material, whilst the development of analytical techniques will provide new insight to these materials.

The main advantages of inorganic-organic hybrid materials speak for themselves, the disparate properties of the organic and inorganic components can be combined into a single material. The different moieties are usually incompatible, and consequently a di-phasic morphology will be obtained. However, if one decreases the size of the organic and inorganic units to the same level, one can easily obtain a homogenous material that allows for fine tuning of the materials' properties on the molecular scale and even more importantly on the nano-scale. This will lead to two scenarios: the homogenous materials will exhibit properties in between the two original phases or will exhibit completely unique properties^[2]. As previously mentioned, the growth of superior, versatile synthetic routes allows for greater possibilities for the formation of hybrid materials and will enable one to alter *and* control the shape, morphology and topology of hybrid materials^[3].

The four main topics for the synthesis of these inorganic-organic materials can be divided as follows: molecular engineering, nano- and micrometer sized organization, functional to

multifunctional hybrids and lastly the combination with bioactive components. As reported by J.Pyun and K.Matyjaszewski^[4], these materials can have a wide range of architectural structure (Figure 2.1): copolymers; such as graft-, star-, block, particles, surfaces, glassy networks and interpenetrating polymer networks^[2].

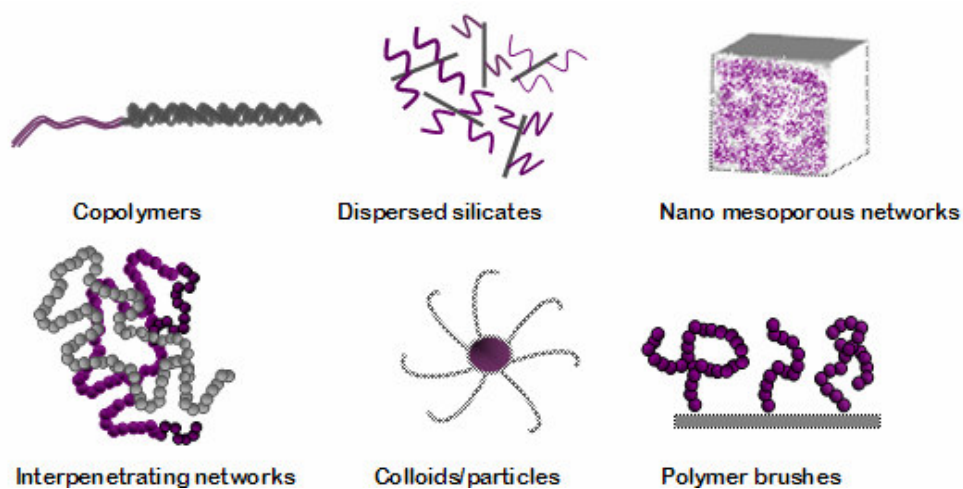


Figure 2.1: Different architectural structures of hybrid materials (redrawn from reference^[4, 5]).

It is very clear that hybrid materials that are multi-functional, can be altered in a desired way by means of synthetic routes. They have novel properties, different topologies and shapes are possible, and so forth. With this said, it is evident that there is a multitude of possibilities for the formation of hybrid materials as there is an unlimited combination of inorganic and organic components. The unlimited combinations necessarily lead to a wide range of applications.

2.2 Copolymers

2.2.1 General overview

There has been an overwhelming amount of research done on copolymers, and with good reason. The development of copolymers arises from academia and industry striving for novel materials which will balance the properties of their homopolymer counterparts. Furthermore, copolymers are superior to their blended counterparts, as a vast majority of polymers that are blended together are mutually immiscible leading to a thermodynamically unstable state.

Copolymers, which are defined in literature as having more than one type of monomer unit in the polymer chain^[6], have vast topologies: statistical or otherwise known as periodic, gradient, and segmented copolymers. Moreover, the topology of the polymer chain can also be further varied: comb, multi-arm, dendrimers etc. leading to an even greater definition of copolymers.

The possible variations of copolymers' topology and overall molecular structure allows for copolymers to have a variety of applications. However, their ill-defined composition leads to failure in the material, which is not always apparent. This has led to a greater focus on the development of well-defined copolymers synthesised using advanced techniques and analysed using superior techniques. Controlled synthetic techniques allow for a greater correlation between parameters and properties, thereby a structure-property correlation can be developed.

In the following section the focus will be on branched polymers, and more particularly graft branched polymers and the different methodologies of synthesising these polymers.

2.2.2 Branched polymers

The growing interest in branched polymers is understandable. Branched polymers have a higher concentration of terminal groups and numerous possible architectural structures leading to significant chemical and physical changes relative to their linear equivalents. The complex molecular architecture of branched polymers plays a significant role in the determination of the phase behaviour of the polymer^[7]. Branching will unavoidably affect crystallinity, crystalline melting point, viscoelastic properties, solution viscosities, glass transition temperature (T_g), free volume as well as the melt viscosities (this will be lower compared to linear polymers with exactly the same molar mass). The latter mentioned is an advantageous property for extrusion, coating or other manufacturing processes^[8, 9].

The most common branched architectures are schematically represented in Figure 2.2. These architectures have a reactive central part which can have different dimensions, i.e. backbones, single groups, nano-particles etc. This central reactive part serves as the attachment point for

different types of branches. The branches again, can also have different architectures, contributing to an *even* more complex polymer. Furthermore, these branches can have terminal groups, exhibiting polar, hydrophobic properties, which can be reactive, or bulky.

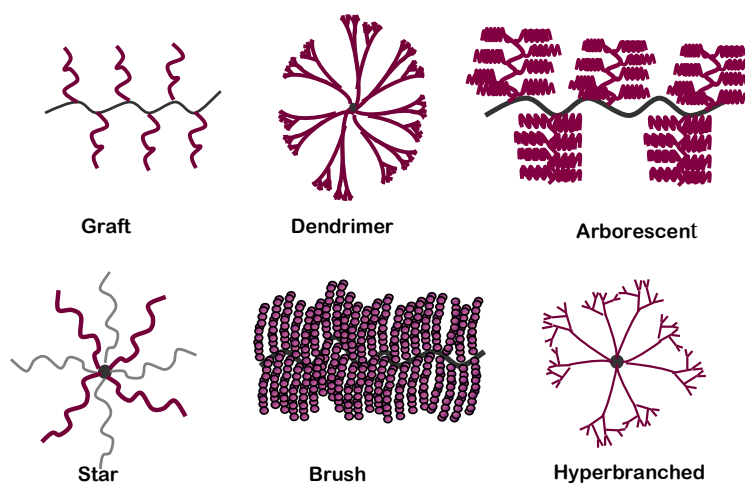


Figure 2.2: Architectures of highly branched molecules^[8].

2.2.3 Graft copolymers

Graft polymers are also known in literature as molecular brushes or comb-like polymers. The latter refers to polymers where the side chains are relatively short. We shall focus our attention on graft polymers with a comb-like structure i.e. a polymer which comprises of identical type of side chains and a different polymer main chain. Owing to their particular architectures (a main chain with pendant grafts) the possibility exists to synthesise comb-like graft copolymers with well defined structures.

The attractiveness of graft copolymers lies with the variety of functional groups that can be imparted to the polymer, leading to boundless varieties and applications. One of the key properties is the phase separation which these polymers demonstrate, making them very attractive in applications such as impact resistant plastics, thermoplastic elastomers, drug delivery polymers and very importantly gas permeation membranes.

Graft polymers, generally, are easier to synthesize than block copolymers *and* generally still exhibit the properties of their block copolymer counterparts^[10]. Applications of block and graft copolymers have already established their importance in different biomedical fields: tissue engineering, implantation, artificial organs, and most interestingly in drug delivery^[11]. It has been reported that graft hybrid copolymers have advantages over block hybrid materials, as these polymers allow for the possibility of tailoring their properties for potential biomedical applications^[11].

2.2.4 Hybrid graft copolymers

The different architectural possibilities of hybrid materials have been discussed in the previous section. The focus of this study is specifically on hybrid graft polymers constituting polystyrene (organic) and polydimethylsiloxane (inorganic) segments.

PSty-*g*-PDMS and PDMS-*g*-PSty, the two polymeric compounds synthesised in this study, will necessarily lead to a material which will convey the many desirable properties of both the constituting components. The noticeable difference between the constituent groups, PSty and PDMS, is that of their glass transition temperatures, T_g 's. PSty has a known T_g of 373 K^[12], whilst PDMS has a T_g of 146 K^[12]. In essence this implies that PDMS will remain a viscous liquid material at room temperature, even at extraordinary high molecular weights (Mw's), whereas PSty will be a glassy brittle material at room temperature. Other desirable properties of PDMS are its elastomeric behaviour; thermal-, UV- and oxidative stabilities; biocompatibility, good electrical properties, hydrophobic surface properties and of course its low surface energy^[13-15].

It has been formerly mentioned that hybrid materials will exhibit segregated phase morphologies as these materials consist of disparate segments. These phase separated materials' surfaces will tend to be covered with one of the components i.e. the component with a lower surface energy will accumulate on the surface^[16-18]. This surface segregation behaviour of hybrid copolymers is extremely attractive as this property is very advantageous in fields of adhesives, lubricants, coatings and surface modifications^[18]. It is quite possible to predict this type of phase behaviour as polymer-polymer interactions in graft systems are comparable to that of di-block copolymers governing meso-structural ordering. Of course one has to take into account that graft copolymers are structurally more complex and therefore won't exactly phase separate as di-blocks do. Phase-separation can be calculated by knowing χN , where χ is the segment-segment interaction parameter and N the degree of polymerization for the di-block as a whole. However, for graft copolymers the amount and placement of the branches also have to be taken into consideration, in other words the number of branches per graft chain needs to be known: $\chi N/\lambda$ where λ is the number of branches per graft copolymer. It has been reported^[15] if $\chi N/\lambda > 100$, then the polymeric system will lead to nano-phase separation.

PDMS has the propensity to nano-phase segregate in inorganic-organic systems as PDMS will most likely exhibit a lower surface energy than its counterpart. Work done by Lee *et al.*^[16, 18], Wu *et al.*^[17], Chen *et al.*^[19] and Maynard *et al.*^[15] all conclude that the PDMS segment segregates to the free surface as this is a thermodynamic favourable process: minimizing the total free energy of the copolymer segments. This propensity of PDMS to phase segregate, and thus have a nano-phase segregated system, is extremely useful especially for membrane applications.

The complex architectural structure of these materials requires advanced synthetic routes to allow control over the parameters of the materials. In the next sections the focus will be on the theory behind the synthesis as well as on the advanced analytical techniques required to wholly understand the behaviour of these complex materials.

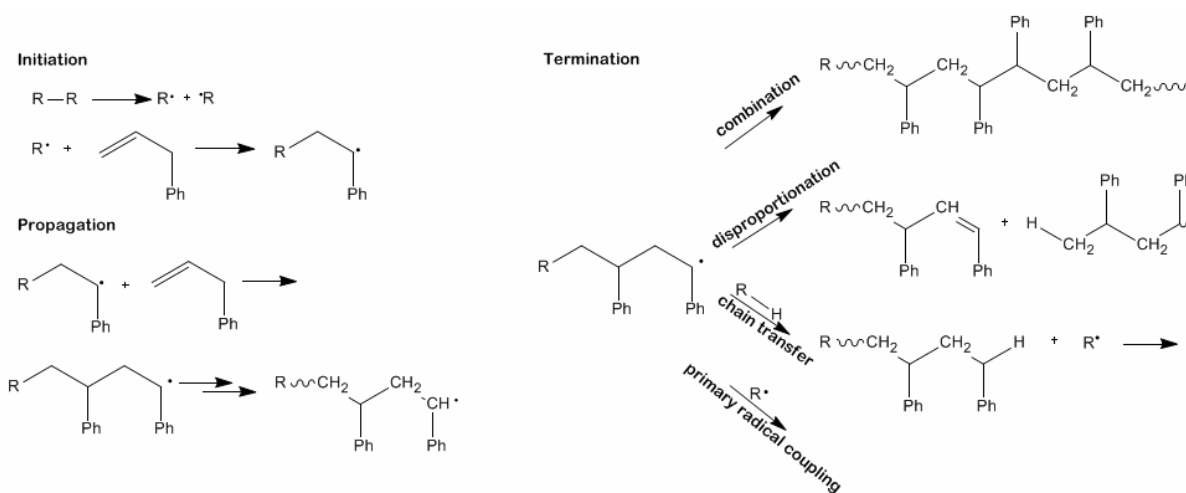
2.3 Polymerization techniques – focus on copolymerization

Three different methodologies; grafting onto, grafting from and grafting through can be approached by either free radical, ionic (such as living anionic polymerization) or controlled living polymerization techniques (NMP, nitroxide mediated living radical polymerization; ATRP, atom transfer radical polymerization; RAFT, radical addition fragmentation chain transfer).

2.3.1 Free radical polymerization - FRP

Free radical polymerization has been widely employed for the synthesis of copolymers. Although synthetically proven to be facile, it has numerous disadvantages. The most problematic factor is the intermediate reactive radical. This reactive radical can undergo fast reactions, rendering bimolecular chain terminating reactions which implies very low selectivity. This contributes in the lack of control over the polymerization, and hence a lack of control in chain length^[20].

Although free radical polymerization does not allow one to control the polymerization and thus the formation of the desired species, it is highly tolerant to impurities such as water, polar hydroxyl or amino functional groups which will in an ionic polymerization lead to termination of the active species. This implies that the technique can be conducted under less stringent conditions, making it an economically attractive process^[6]. Scheme 2.1 shows the main chemical processes associated with free radical polymerization. Initiation and propagation occurs within seconds, termination can occur via combination disproportionation, chain transfer and radical coupling. Since the formation of radicals and the termination process cannot be controlled, this will unavoidably lead to different molecular structure inhomogeneities.



Scheme 2.1: Conventional free radical polymerization of styrene; possible reactions which can arise^[20, 21].

2.3.1.1 Free radical copolymerization with macromonomers

Free radical polymerization is a very useful technique for the copolymerization of graft copolymers via the grafting through approach using a macromonomer. It should be recognized that macromonomers will have a different reactivity during polymerization or copolymerization than the corresponding conventional monomer^[22, 23]. A few considerations regarding the properties of a macromonomer need to be considered as this will directly influence the polymerization and copolymerization^[24]:

- Macromonomers have a high viscosity, influencing the diffusion-controlled step of the polymerization.
- Entanglement formation is highly possible
- The concentrations of the polymerizable end-groups are low compared to their monomer counterparts.
- Diffusion of reactants is reduced.

It is, therefore, evident that the kinetics of macromonomer polymerization will differ from that of the monomer counterpart owing to the macromonomers sensitivity to diffusion-controlled kinetic events, the high segment density, and the dimension of the macromonomer leading to entanglements. Furthermore, it has been revealed that propagation is somewhat unfavoured and that termination does not occur as readily resulting in polymerization rates which are comparable or even higher than those for the corresponding monomers (see Figure 2.3)^[22] hence the polymerization of macromonomers compared to their monomer counterparts exhibit much lower k_t and k_p values^[23].

Copolymerization, involving macromonomers, have been invariably treated according to the Mayo-Lewis equation (terminal model)^[23]. The model relates the instantaneous compositions of the monomer mixture to the copolymer composition:

$$\frac{d[A]}{d[B]} = \frac{1 + r_A \frac{A}{B}}{1 + r_B \frac{B}{A}} \quad [2.1]$$

$d[A]/d[B]$ is the molar ratio of the monomers A and macromonomer B , $[A]/[B]$ is the concentration of monomer A and macromonomer respectively, r_A and r_B is the reactivity ratio of monomer A , and macromonomer B respectively. From literature^[22, 23, 25] it has been reported that the kinetics of macromonomers for free-radical polymerization follows the conventional square-root equation for the overall rate of polymerization:

$$R_p = k_p \left(\frac{2k_d f}{k_t} \right)^{1/2} [I]^{1/2} [M] \quad [2.2]$$

k_p and k_t are the rate constants of propagation and termination respectively, k_d is the rate constant of initiator decomposition, f is the initiation efficiency, $[I]$ and $[M]$ are the concentrations of the initiator and monomer correspondingly. The kinetic chain length (ν) is defined as the average number of monomer units that are polymerized by each initiating radical:

$$\nu = R_p / R_t = \frac{k_p [M]}{(2k_d f k_t)^{1/2} [I]^{1/2}} = \frac{(1+x)}{2} DP_n^0 \quad [2.3]$$

where:

$$R_t = 2k_d f [I] \quad [2.4]$$

assuming a steady state. DP_n^0 is the instantaneous number-average degree of polymerization with the assumption of no chain transfer, and x is the fraction of disproportionation during termination.

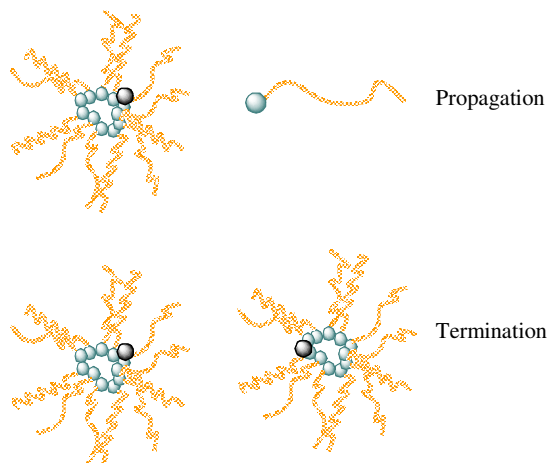


Figure 2.3: Illustration of a unfavoured propagation reaction of a poly(macromonomer) radical with a macromonomer and a hindered termination reaction due to the steric hindrance.

Although free radical copolymerization with macromonomers has numerous limitations, such as low reactivity ratios owing to incompatibility of the macromonomer with the monomer, low molecular weight of the grafts, and many others, it *still* provides a method to obtain graft copolymers with a well-defined structure^[26].

2.3.2 Living polymerization – Anionic polymerization

In 1956 the first account of ‘Living’ polymers was reported by Szwarc and this caused a revolution in polymer science^[27]. It was regarded as the birth of a number of synthetic techniques to prepare a realm of polymers with novel, well-defined molecular architectures and nano-structured morphologies. Szwarc’s discovery not only had importance from the point of view of designing

novel polymers, but also had intellectual impact as it opened an avenue for synthetic scientists to search for conditions where termination and transfer could be eliminated or suppressed.

Living polymerization implies a reaction where chain-breaking does not occur, or in other words chain polymerization proceeds in the absence of the kinetic steps of termination and chain transfer. The formation of undesired species by means of free radical polymerization inevitably led to the development of controlled and living polymerization^[20, 27, 28]. Assuming spontaneous termination does not take place (hence optimal and adequate reaction conditions exist), the molecular weight can easily be controlled, *if* initiation is fast with respect to propagation. The number average degree of polymerization can therefore be equated as the monomers consumed to initiator molar ratio:

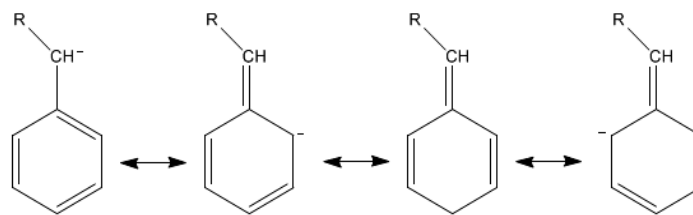
$$DP_n = \frac{\Delta[M]}{[I]} \quad [2.5]$$

Based on early theoretical work of Flory, the reaction scheme implies that an ideal living anionic polymerization should yield a polymer with a molecular weight distribution that is Poisson-like^[20, 29].

$$w_i = \frac{i v^{i-1} e^{-v}}{(v+1)(i-1)!} \quad [2.6]$$

where w_i stands for the weight fraction of the i -mer and v stands for the number average degree of polymerization. Polydispersities will remain narrow, provided solvation/desolvation and ionic dissociation/association processes are fast. Active species will inevitably collide, however they will not annihilate themselves.

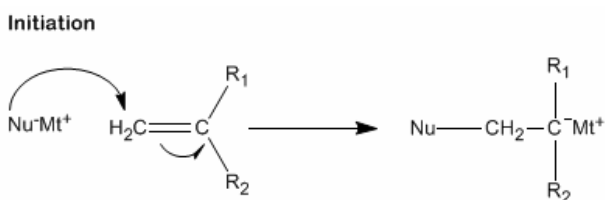
Anionic polymerization can be considered as the epitome of living polymerization as it personifies the defining characteristics of living polymerizations and has been successfully employed to synthesise polymers with well-defined, narrow molecular weight distributions and compositional heterogeneity. The active species is formally an anion, i.e., an atom or group with a negative charge and an unshared pair of electrons. Monomers which are susceptible to this type of polymerization are those that can form stable carbonionic species. Such monomers include styrenic, dienic, and cyclic monomers as they can react with nucleophiles which leads to ring-opening. Furthermore, the double bond must have substituents that can stabilize the negative charge, thus these groups need to be charge withdrawing which will make the anions stable to possible nucleophilic attack from other species. Aromatic rings, double bonds, carbonyl, ester, cyano, sulfone groups etc., will stabilize the negative charge and promote the anionic polymerization. This can clearly be illustrated with styrene as monomer:



Scheme 2.2: Charge delocalization of styrene.

2.3.2.1 Initiation by nucleophilic addition

The general initiation step is illustrated in Scheme 2.3. Nu is a nucleophile, which is anionically charged, and M^+ is the associated metal counterion. Alkyl-lithium compounds are the most useful class of initiators for vinyl polymers^[30]. Organolithium compounds are unique as the C-Li bond exhibits properties of both covalent and ionic bonds. The high solubility of organolithium compounds can be ascribed to the covalent character of C-Li bond along with the strong aggregation of the ion pairs^[30].



Scheme 2.3: Initiation step for anionic polymerization.

These initiating compounds associate into dimers, tetramers or hexamers in a hydrocarbon solution. This degree of association is directly related to the steric requirements of the alkyl group, implying that the degree of association decreases as the steric requirements of the alkyl group increases. *n*-Butyl lithium will form hexameric aggregates in a hydrocarbon solution. If the alkyl group has a branching point at an α - or β -carbon, i.e. *t*-butyl lithium or *sec*-butyl lithium, then the aggregates will change to tetrameric aggregates^[30]. The relative reactivities of alkylolithiums are linked to their degree of association, thus the less associated alkylolithiums are, the more reactive they are as initiators. For styrene polymerization the following holds true^[31]:



Alkyl-lithiums are extremely reactive with oxygen, carbon dioxide and moisture; hence if these compounds are remotely present they will destroy the initiator and prevent further initiation from taking place.

The initiation kinetics of styrene using an alkyl-lithium initiator in a hydrocarbon solvent has been studied extensively. Styrene polymerization with *n*-BuLi in benzene was studied by the classic work of Worsford and Bywater^[30, 31]. It led to the development of the following relationship:

$$R_i \propto [n - BuLi]^{1/6} [Sty] \quad [2.7]$$

hence:

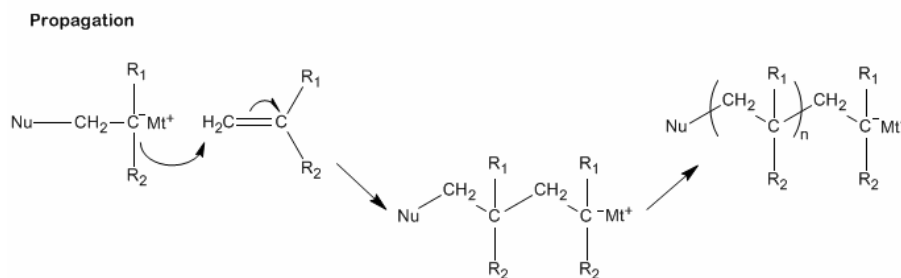
$$R_i = k_i (K_d / 6)^{1/6} [n - BuLi]_0^{1/6} [Sty] \quad [2.8]$$

As *n*-BuLi predominantly aggregate into hexamers in hydrocarbon solutions, the fractional kinetic order of the initiation rate on the total initiator concentration implies that the unassociated *n*-BuLi is the initiating species as formed by the following equilibrium:



One can conclude from this that an incomplete or stepwise dissociation exists which leads to aggregates with lower degrees of association. However, these aggregates are not completely inactive towards the polymerization of the monomer.

2.3.2.2 Propagation



Scheme 2.4: Propagation step for anionic polymerization.

From the initiation step, the anionic centre is a strong base which can incorporate further monomer via nucleophilic attack. Propagation (Scheme 2.4) continues as more monomers are attacked, adding to the growing chain.

The propagation kinetics for styrene polymerization, where the counterion is lithium, has been studied extensively in aromatic and aliphatic solvents leading to an unambiguous equation^[28]

$$R_p \propto [PStyLi]^{1/2} [Sty] \quad [2.10]$$

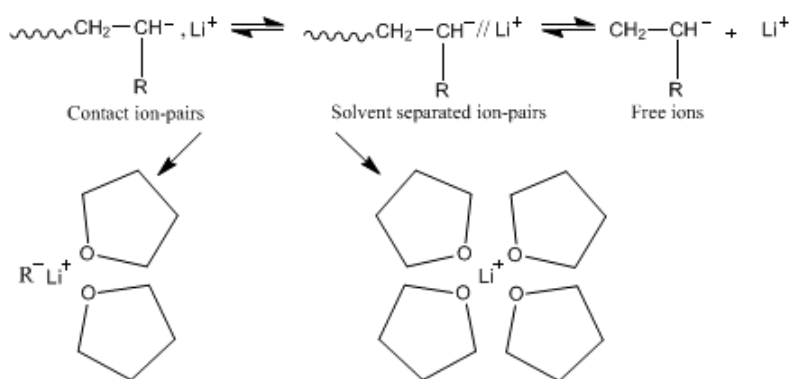
hence:

$$R_p = k_{app} [PStyLi]^{1/2} [Sty] \quad [2.11]$$

where $[PSty]$ is the living polymer concentration and is the monomer concentration. k_{app} is the apparent or observed propagation rate constant^[32]. From this it must be made apparent that much higher polymerization rates will occur in anionic methods opposed to free-radical polymerization. This is due to the higher concentration of propagation species and the lack of termination reactions.

The mode of anionic propagation is severely affected by the nature of the initiator as the counterion remains associated with the growing active site (Scheme 2.5). These active propagating groups may exist as ion-pairs which can be solvated and even dissociated into free ions. All of these species are in equilibrium with one another. The manner of association of the anion with counterion cannot be overemphasized, as this plays a critical role in propagation. A too strong association will hinder the addition of monomers to the chain, if the counterion is too loosely associated with anion, side reactions can occur.

The active propagating group may exist as ion-pairs, which in turn can be solvated and dissociated into free ions. Hence, a mixture of free or solvent separated ion pair active centres and contact ion pairs will always exist. Therefore, the kinetics and mechanism of polymerization depend on their relative content in the reaction medium^[20]. The solvent separated ion-pairs are by far more reactive, and a small increase in their relative concentrations will lead to a definite increase in propagation rates^[33]. Chiefly the goal should be to have a solvent separated ion-pair which will allow the molecules in solution to insert themselves between the anion active centre and the counterion. This will increase the activity and decrease the time for full conversion.

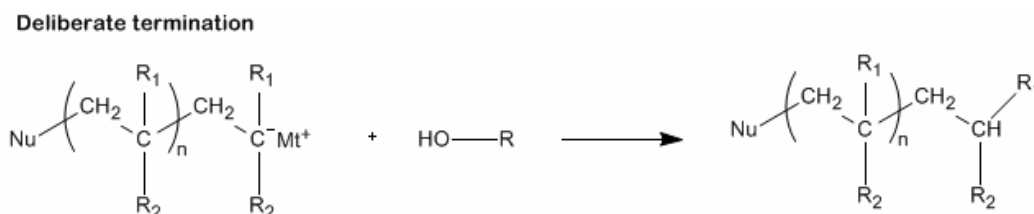


Scheme 2.5: Ion pair associations with alkyl-lithium initiators in THF.

The counterion will necessarily play a role in the rate of propagation. In polar solvents it is observed that the free ion concentration will increase along the series. Hence: $Cs^+ < Rb^+ < K^+ < Na^+ < Li^+$. This is a consequence of the fact that lithium has the smallest radius and highest electronegativity, thus Li^+ anions are solvated more readily than Cs^+ . However, there is a reversal

in the series when non-polar solvents are used, as the solvation effect does not play a role: $\text{Cs}^+ > \text{Rb}^+ > \text{K}^+ > \text{Na}^+ > \text{Li}^+$. Propagation will now be dependent on the species with the weakest bond between the anion and counterion^[33].

2.3.2.3 Termination

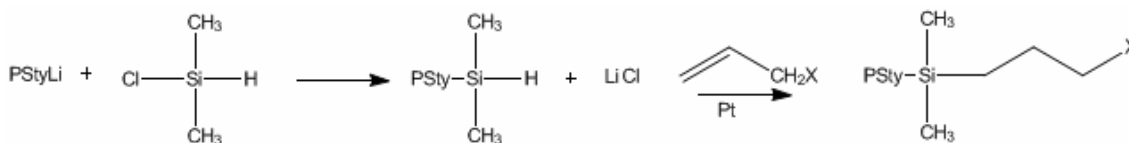


Scheme 2.6: Termination using a suitable electrophile.

If proper precaution is taken, termination will not occur spontaneously. This is of extreme importance as it allows one to synthesize a macromonomer with specific end-chain functionality, a unique feature of living polymerization. Under ideal conditions, every chain should have a similar length, hence all chains will have an active anionic end-group, enabling one to end-group functionalize the polymer chains. Thus after complete monomer consumption, the resulting polymeric organolithiums (in an alkyllithium-initiated polymerization) can react with electrophiles to form an end-functionalized polymer^[34] (see Scheme 2.6). These end-groups can further initiate polymerization with other monomers or can couple and link reactive groups on other oligomers/polymers. Terminating agents can either be living or non-living. Non-living agents neutralize the active centres, whilst living agents will create a new anionic active centre. Morton^[35] showed the first non-living linking reaction for the synthesis of 3- and 4-arm star polystyrenes by means of trichloromethylsilane/tetrachlorosilane. A realm of branched polymers via this method has since been developed for the creation of well-defined branched polymers.

In a review N. Hadjichristidis *et al.*^[36] it was shown that one can synthesise a multitude of polymers with complex branched architectures by means of anionic polymerization. Star polymers, asymmetric and miktoarm stars; comb and α,ω -branched polymers; cyclic polymers and combinations of cyclic polymers with linear chain as well as hyperbranched polymers were all successfully polymerized with well-defined structures.

R. Quirk^[34] reported the use of a combination of living anionic polymerization and hydrosilylation chemistry. Polystyryllithium was terminated with chlorodimethylsilane to prepare chain-end, silyl hydride-functional polymers (Scheme 2.7). These ω -silyl hydride functionalized polymers can react with numerous substituted alkenes.



Scheme 2.7: A general functionalization methodology for chain-end functionalization using chlorosilane functionalization followed by hydrosilylation^[34].

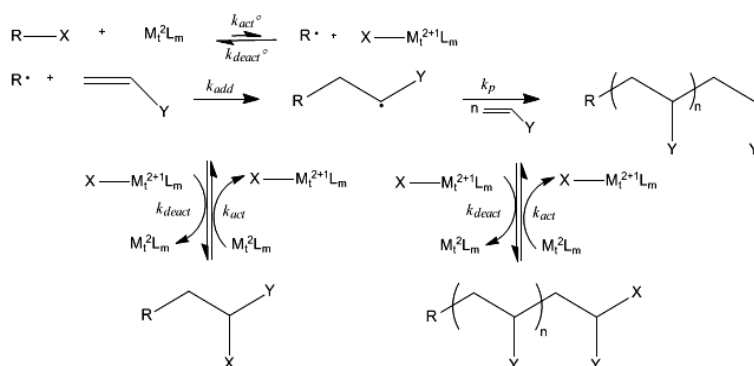
To conclude, living polymerization is an extremely advantageous and desirable technique as it allows for the preparation of macromolecules with well-defined structures which will have a low degree of compositional heterogeneity. It offers the possibility to create a methodology to synthesize macromolecular compounds which will have a specific molecular weight distribution, copolymer composition, microstructure, stereochemistry, branching, and chain-end functionality. However, living polymerizations are not immortal as Szwarc reported. It is incomprehensible that propagation will exist without any form of termination or chain transfer reactions. As Szwarc pointed out, with time any living chain will eventually decompose, isomerize or react with its surroundings.

2.3.3 Controlled Radical Polymerization – CRP

It cannot be overemphasised that there is a great need to produce polymers with well-defined compositions, architectures, and functionalities^[37]. Living polymerization techniques such as anionic polymerization does allow for a methodology to synthesis such polymers as this type of polymerization proceeds in the absence of irreversible chain transfer and chain termination. However, anionic polymerization is extremely intolerant of impurities, making it difficult from a synthetic point of view. This led to the development of controlled radical polymerization, CRP techniques.

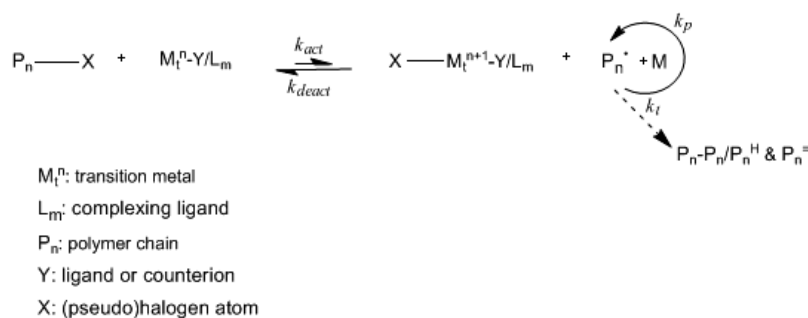
CRP has the main advantage over other living polymerizations, such as cationic and anionic polymerizations in that it is more tolerant of functional groups and impurities. CRP techniques are based on the concept of active and dormant species. In the mid 1990's, the idea of an equilibrium between active and dormant species were established. The most successful CRP techniques are as follows:

1. SFRP, stable free radical polymerization and NMP, nitroxide mediated process. Control of the system is made possible via a reversible homolytic cleavage of a weak covalent bond. This leads to a propagating radical and a stable free radical – reaction 1 in Scheme 2.8



Scheme 2.9: Mechanism of metal complex-mediated ATRA and ATRP^[37].

The normal schematic of the ATRP equilibrium which emphasizes the repetitive nature of activation and deactivation is shown below (Scheme 2.10).



Scheme 2.10: General mechanism of transition-metal catalyzed ATRP^[38].

Basically the radicals which are the active species are generated through a reversible redox process which in turn is catalyzed by a transition metal complex, $M_t^n\text{-}Y/\text{Ligand}$ where Y may be another ligand or the counterion. This complex undergoes a one-electron oxidation with concomitant abstraction of a halogen atom from dormant species, $R\text{-}X$. $R\text{-}X$, the added initiator can be a multifunctional initiator, in other words it can either possess more than one initiating functionality, it can be used to introduce additional functionality into the α -chain end or it can be a macroinitiator. Active radicals are formed at a rate of activation, k_{act} , propagate with a rate k_p and reversibly deactivate, k_{deact} and also terminate, k_t . Polymer chains will grow by the addition of the intermediate radicals to monomers, very similar to conventional free radical polymerization. During this process termination reactions are inhibited as oxidized metal complexes, $X\text{-}M_t^{n+1}$ are generated as persistent radicals, minimizing the contribution of termination. Termination reactions occur predominately via radical coupling and disproportionation, but in an adequate, well-controlled system, only a minute percent of polymer chains will undergo termination. For ATRP to

be successful as a polymerization technique, fast initiation (initiator is consumed rapidly) and fast deactivation of the active species by higher oxidation state metal is required.

ATRP as a superior technique became evident when H. Shinoda *et al.*^[2] employed different synthetic techniques for the development of PMMA-*g*-PDMS (as illustrated in Figure 2.4). Free radical polymerization gave a graft polymer which was heterogeneously branched, the copolymer prepared by RAFT, gave a tapered structured which was intermediately homogeneously branched whilst ATRP produced a copolymer which was homogeneously branched. Graft copolymers' bulk and surface properties are greatly affected by the copolymer morphology, composition and branch length; hence it is of the utmost importance that an adequate synthetic route is chosen.

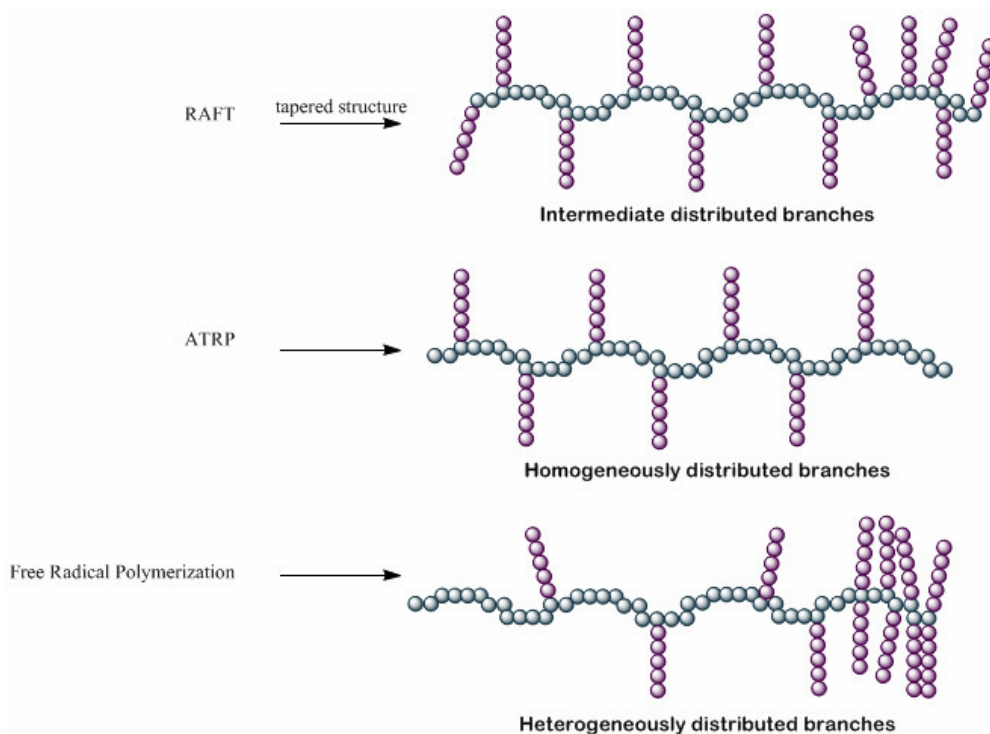


Figure 2.4: Possible distribution of branches resulting from the copolymerization technique employed^[2].

2.4 Synthesis of graft copolymers

Molecular parameters such as the nature and degree of polymerization of the backbone *and* the length and density of the side chains will greatly affect the properties of the graft copolymer. The composition, backbone length and branch length can easily be controlled by the choice of synthetic route. However, the control over branch spacing length as well as the grafting positions of the side chains has proven to be extremely difficult, even when employing living polymerization techniques^[39]. Thus to acquire the desired product^[39] advanced strategies in synthetic routes are required.

Branched polymers have been successfully synthesised with the grafting onto, grafting from and grafting through techniques, from monomers and macromonomers. Each of these methods have their pros and cons, but it should be highlighted that all three methods are affected by the steric hindrance of the reactive centre, greatly affecting the grafting efficiency^[6]. Figure 2.5 illustrates the three different synthetic routes to acquire a graft copolymer. These methods will be discussed in greater detail.

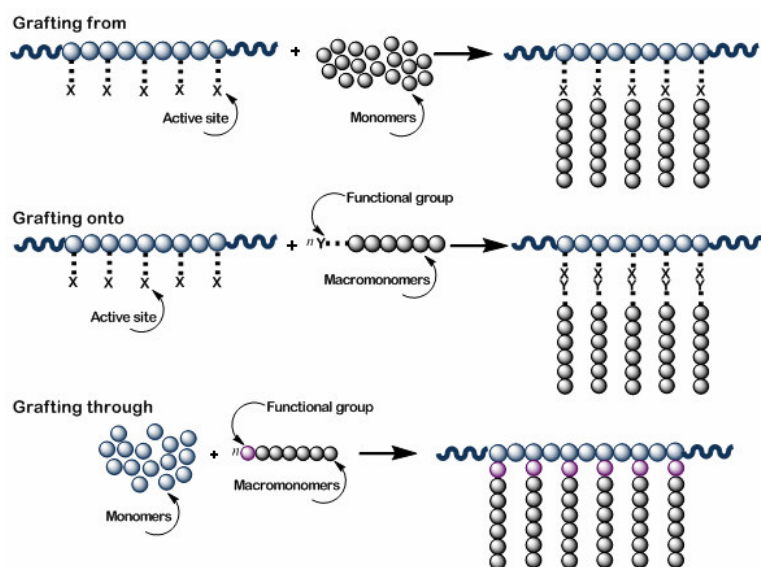


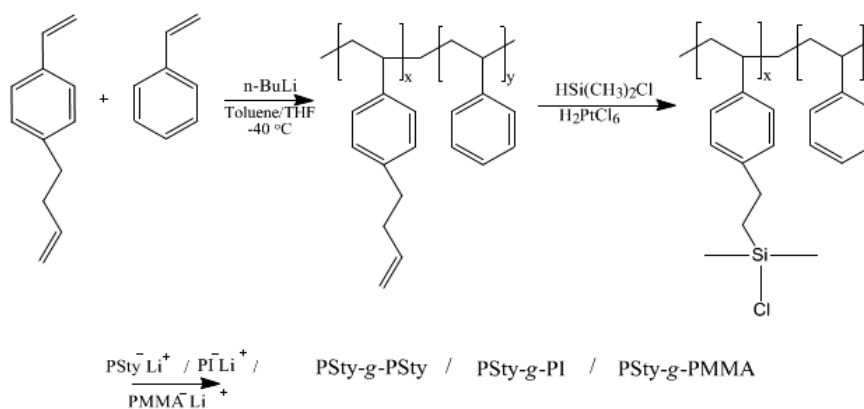
Figure 2.5: Scheme of different methods to synthesize graft copolymers^[6, 40].

2.4.1 Grafting onto

The approach in this technique is to make use of preformed, terminally functionalized polymer chains, and requires the presence of complimentary functionalities^[6]. These functionalized chains react with a multifunctional molecule that will form the core of the macromolecules. The difference in this technique over other grafting techniques has to do with the chain growth. In the grafting from technique, grafted chains are grown from the backbone by the continual addition of the

monomer. The grafting onto technique implies covalent bonding between two different homopolymers, hence the addition of the chain end of a particular polymer to the backbone of the other polymer on a particular active site^[25]. Thus, it involves the synthesis of end-functional polymers together with the synthesis of a complimentary polymer backbone precursor. This type of synthetic strategy is based on the supramolecular assembly approach, making use of secondary interactions: hydrogen bonding, coordination and ionic interaction^[41]. This route is extremely attractive as it allows one to synthesise the backbone and side chains independently, allowing more control over the system^[42]. Another advantage of this method is that the polymer backbone, as well as the attachable chains/ branches, can be synthesised by various living polymerization techniques, allowing control over the molecular weight and allowing narrow polydispersities. This method, however, is not without problems; low grafting efficiency and complicated purification methods contribute to its limitation as a technique. The low grafting efficiency can be attributed to the limiting diffusion of attachable chains to reactive centres of the backbone, as well as steric hindrance of the functional macromonomer^[8, 39].

Anionic polymerization has been successfully utilized for the grafting onto technique. This method allows one to control the molecular weight; molecular dispersity and the chemical composition of the backbone as well as the branches (to be discussed in greater detail in the following section). As mentioned before, this method allows for the modification of the main chain introducing functional groups which can undergo reactions with preformed polymers. Polystyrene is commonly synthesised anionically and subsequently terminated by making use of chloromethylation. To avoid the well-known side reactions which can occur during chloromethylation with a $-\text{CH}_2\text{Cl}$ group, $-\text{SiMe}_2\text{Cl}$ is rather introduced for termination^[42] Ruckenstein and Zhang^[36] used the grafting onto technique by employing anionic polymerization for the synthesis of numerous graft copolymers with polystyrene as a backbone (Scheme 2.11).



Scheme 2.11: Synthesis of graft copolymers with PSty as backbone; employing the grafting onto method^[36].

4-vinylphenyl-1butene was reacted with styrene, allowing for selective polymerization of the vinylic bond. Thereafter the polymer was subjected to hydrosilylation, introducing a Si-Cl group at the olefinic double bond. This functional group acted as a grafting site for the linking of PSLi, PILi or PMMALi groups. Hawker *et al.*^[6] employed NMP, nitroxide mediated polymerization, for the grafting onto reaction of N-oxysuccinimide 4 vinylbenzoate with styrene. This block copolymer contained an active ester moiety which could react with an amino-functional dendron to form a branched copolymer.

2.4.2 Grafting through

This technique, which is also better known as the macromonomer approach, implies the radical copolymerization of a macromonomer with a low molecular weight comonomer, or otherwise stated; the polymerization of macromonomers *through* their terminal functionality^[6]. In principle the macromonomers forms the branches of the copolymer with the backbone formed in situ. These macromonomers are linear polymer or oligomeric species that contain a copolymerizable moiety at the chain end. Graft polymers are formed by either homo- or copolymerization with another monomer. This method is attractive in the sense that macromonomers are prepared separately prior to polymerization. Consequently the graft copolymer can have a well-defined grafting density (the number of branches per backbone can be controlled via the ratio of the molar concentrations of the macromonomer and comonomer) and side chain length, as the macromonomers can be analyzed prior to copolymerization. Much attention has been paid to this technique as these polymers are promising for a variety of applications.

However, polymers synthesised via this route are rather ill-defined as this route leads to side products and is contaminated with residual macromonomers^[39], requiring fractionation or dialysis for the removal of the macromonomer^[41]. Another disadvantage of this technique is the degree of polymerization of the backbone; the backbone being dependent on the macromonomer length and type^[9, 41]. With this said, it is clear that one has to take the reactivity ratios of the species into consideration: these ratios will vary during the course of polymerization as macromonomer and comonomer incorporation occurs in the graft copolymer and will lead to randomness. The variation in ratios can be ascribed to the fact that the concentration of the species will alter as a function of time. Besides random placement which can occur, phase separation also takes place owing to the formation of the copolymers. All of these factors lead to compositional heterogeneity.

As formerly stated in this section, the grafting through method is also termed the macromonomer approach, since preformed macromonomers are used for the copolymerization with another monomer. Therefore, it is worthwhile elaborating on this concept of macromonomers.

2.4.2.1 Macromonomers

The term macromonomer (macromolecular monomer, a polymer and monomer at the same time^[22]) has been defined in literature^[23] as any polymer or oligomer monomer with functional end groups that can undergo polymerization. Macromonomers were introduced as a trademark by a study group at ICI, synthesising well-known, high solids in non-aqueous dispersions^[43]. A macromonomer serves as a building block to form arms or branches. It should be apparent that macromonomers can differ in type (different monomer repeating unit) and have different end-groups, allowing for a vast range of branched polymers differing in architecture, compositions and combinations. Two of these architectures that are possible is a comb-shape polymer which have regular dense attached branches (via homopolymerization), and graft copolymers that have randomly, loosely, distributed branches (via copolymerization). Figure 2.6^[23] shows the various branched architectures which can be acquired with the macromonomer technique: a, d are comb-like; b, e are star-like; f brush-like and c flower-like. a, b, c are graft copolymers from copolymerization and d, e, f are poly(macromonomers) from homopolymerization.

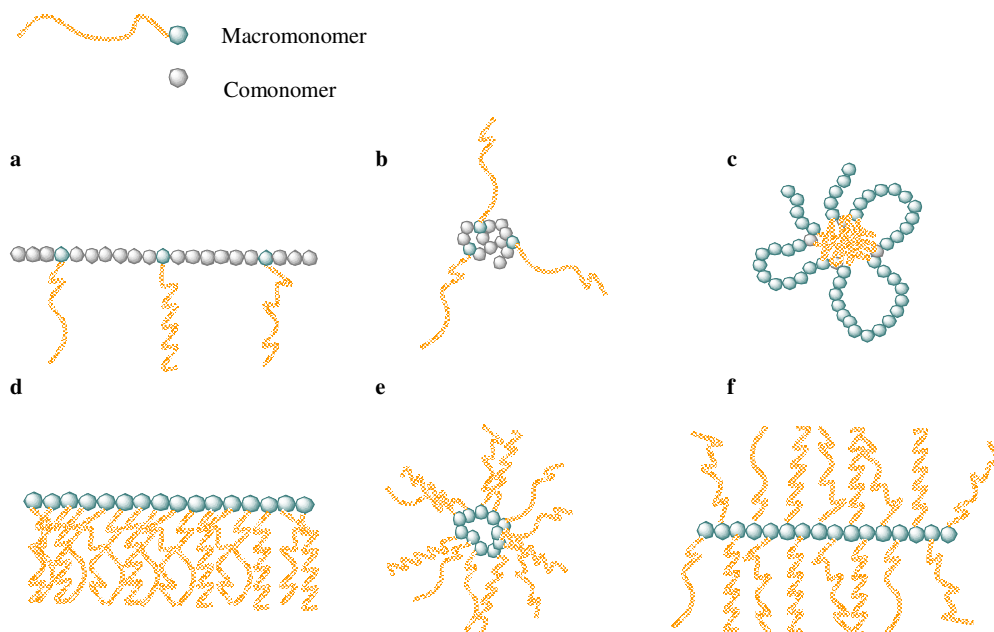
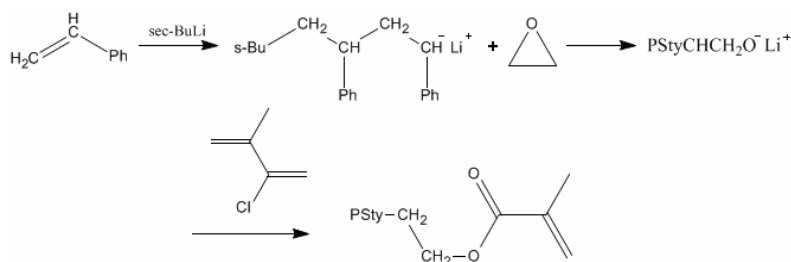


Figure 2.6: Various branched architectures obtained via the macromonomer technique (redrawn from reference^[23]).

Macromonomers can be prepared by almost any possible polymerization technique. Of course living polymerization and controlled radical polymerization allows for control over the molecular weight, and consequently the molecular weight distribution as well as specific chain-end functionalities. This chain-end group that can copolymerize with another appropriate functional

monomer/comonomer can be achieved by various methods: the termination method - end-capping of a living polymer; initiation method - initiation of living polymerization; transformation of the end-group and polyaddition^[23]. The latter method involves polyaddition reactions between a vinyl and silane group (hydrosilylation).

Anionic polymerization has been proven to be one of the best methods for the synthesis of well-defined macromonomers with functional, polymerizable end-groups. Milkovich developed a method for the synthesis of PSty macromonomers which is widely used^[36, 40, 42]. Styrene monomer is polymerized with *sec*-BuLi, and thereafter end-capped with an excess ethylene oxide. This end-capped living polymer is then reacted with methacryloyl chloride to form the desired PSty macromonomer (Scheme 2.12).



Scheme 2.12: Polystyrene macromonomer prepared anionically.

Similarly controlled radical polymerization has been used by various study groups to prepare styrene macromonomers. Hawker *et al.*^[44] used NMP, nitroxide mediated living radical polymerization, to polymerize macromonomers with styrene to form the desired graft copolymer with well-defined structures. ATRP, atom transfer radical polymerization, was employed by K. Matyaszewski^[6], showing that well-defined macromonomers can also be formed via this route.

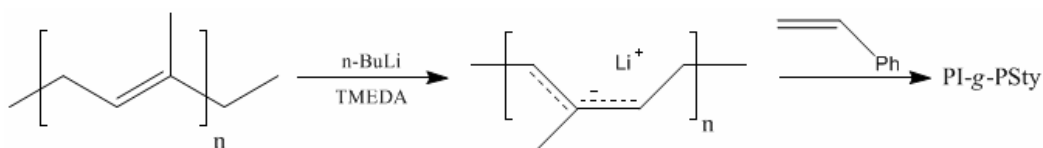
To conclude, the formation of graft copolymers via the grafting through technique is very promising and advantageous, as endless possibilities for the formation and control of macromonomers exist.

2.4.3 Grafting from

This technique overcomes many of the limitations mentioned for the previous methods, such as steric hindrance as the core only has to react with monomers and not macromonomers. This technique utilizes a functional backbone, i.e., the backbone contains reactive sites. Initiation and growth will occur at these sites, by introducing the desired monomer, which will result in the formation of branches and ultimately the graft copolymer. The density of graft chains can be

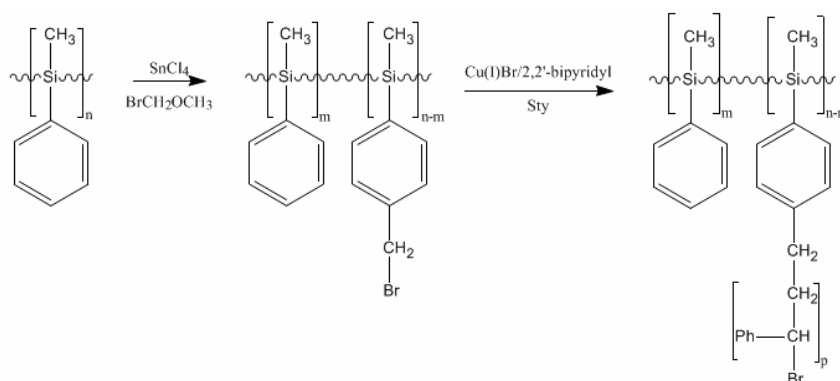
controlled by means of the active sites generated along the backbone, but this only holds true if one assumes each of the active sites participates in the formation of a branch^[36, 40].

When using ionic polymerization in the grafting from method, multiple charged initiators are necessary, which in turn results in poor solubility and a broad molecular weight distribution^[8]. Nevertheless, anionic polymerization has been successfully utilized for the grafting from method. To generate active sites for anionic polymerization, metallation of allylic, benzylic or aromatic C-H bonds in the backbone can occur by means of an organometallic compound in the presence of a strong chelating agent. Scheme 2.13 shows the synthesis of PI-g-PSty and PBd-g-PSty; PI and PBd was formed through metallation of *n*-BuLi in the presence of the strong chelating agent, TMEDA (N,N,N',N'-tetramethylethylenediamine). Employing anionic polymerization, the polymer exhibited well-defined molecular characteristics^[36, 40].



Scheme 2.13: Anionic polymerization utilized for the grafting from approach - synthesis of PI-g-PSty.

Controlled radical polymerization techniques have also been successfully used in the grafting from approach. Hawker *et al.*^[44] pioneered this after establishing that a unimolecular TEMPO-based initiator controlled the polymerization of styrene. Based on this work done, K. Matyjaszewski^[6] copolymerized numerous polymers via this method, and showed that this technique can provide a route to graft copolymers via ATRP. Scheme 2.14 shows how ATRP can be employed in the grafting from method to synthesise an inorganic-organic graft copolymer: poly(methylphenylsilane)-g-PSty.



Scheme 2.14: Synthesis of poly(methylphenylsilane)-g-PSty via ATRP by means of the grafting from method^[40].

2.5 Chromatography – focus on analysis of graft copolymers

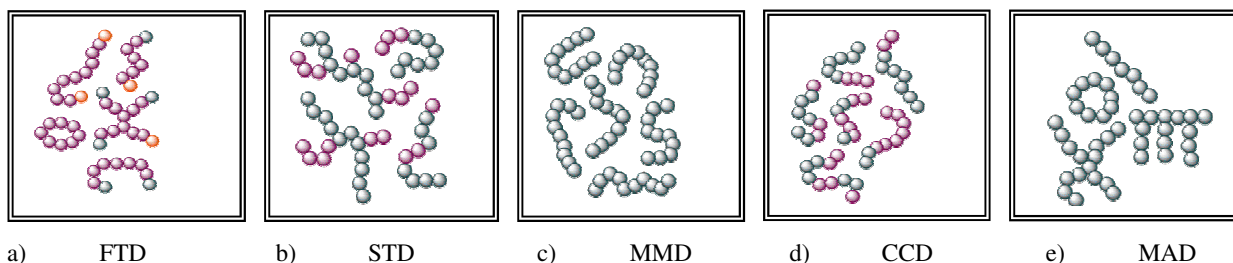


Figure 2.7: Illustration of the structural complexity of macromolecules showing the different possible distributions^[45].

Branched polymeric materials, such as the graft copolymers under this study, are complex polymers. An intricate product is obtained in grafting reactions due to the synthesis method. The polymeric systems will more than likely comprise of a mixture of the graft copolymer, residual ungrafted polymer backbone as well as the homopolymer. In addition, the distribution of graft and graft length results in the copolymer having distributions in more than one direction of molecular heterogeneity. Figure 2.7 shows the general structural complexity of macromolecules: functionality type distribution (FTD), structural type distribution (STD), molar mass distribution (MMD), chemical composition distribution (CCD) and architecture distribution (MAD)^[45-47]. To complicate matters further, the different molecular heterogeneity distributions can be superimposed on one another, i.e. polymers can be block or graft, which can also be mono- or bi-functional^[45, 47].

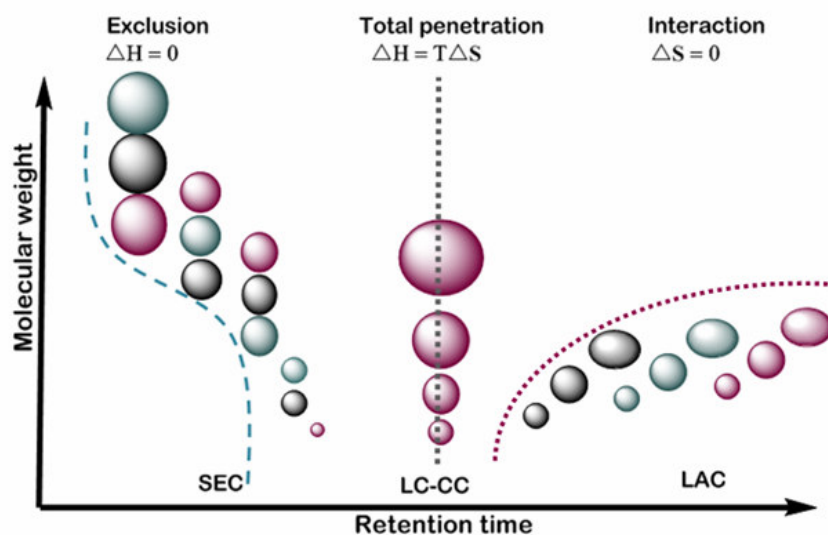


Figure 2.8: Different modes of separation, molecular weight versus retention time^[45].

Chromatography relates to the selective distribution of an analyte between the mobile and stationary phase^[47]. Employing different modes of liquid chromatography one can separate polymers selectively with respect to molar mass (or rather hydrodynamic volume), chemical composition or functionality. By combining these techniques with one another, together with a selective detector, an all-encompassing understanding of the polymeric system in question will be obtained.

In this section the main chromatography modes of polymers will be discussed: size exclusion chromatography, SEC, liquid adsorption chromatography, LAC and liquid chromatography at the critical point, LCCC (Figure 2.8). In addition two dimensional chromatography, 2-D, and coupled techniques will be mentioned.

2.5.1 Size Exclusion Chromatography – SEC

SEC is the most popular and convenient method for the fractionation of polymers^[48]. This method entails the separation of polymer molecules from one another according to their molecular size in solution. SEC has by far dominated the area of molecular characterization of polymers.

The retention volume, V_r , is determined by:

$$V_r = V_0 + V_p K_d \quad [2.12]$$

K_d , the distribution coefficient or separation coefficient, is equal to the ratio of the concentrations of the analyte in the stationary and the mobile phases, which is furthermore related to the change in Gibbs free energy, ΔG :

$$\begin{aligned} \Delta G^0 &= \Delta H^0 - T\Delta S^0 = RT \ln K_d \\ K_d &= e^{\frac{-\Delta G}{RT}} \end{aligned} \quad [2.13]$$

For SEC, in the absolute ideal scenario, separation is only directed by conformational changes of the macromolecules by means of a thermodynamically good solvent for the polymer, suppressing any enthalpic interactions with the stationary phase. Hence:

$$K_{SEC} = e^{\Delta S / RT}, \quad 0 < K_{SEC} \leq 1 \quad [2.14]$$

$$\Delta H \ll T\Delta S$$

K_{SEC} varies between zero and one. When K_{SEC} equals zero, it implies that the molecules are too large to penetrate the pores, resulting in total exclusion. On the other hand, when K_{SEC} equals one, the maximum value, all the pores are accessible to the analyte molecules. This holds true for small molecules which can enter the pores. As a result, retention decreases with an increase in molar mass^[45-49].

SEC is, therefore, an entropy governed separation technique, which mainly responds to the differences in molecular size which is dominated by chain length or molar mass providing

information of the MMD of the polymeric system. When SEC is coupled to more than one detector, information on the average chemical composition as a function of molar mass (or rather hydrodynamic volume) can be obtained. Basically the number of detectors should equal the number of different chemical components of chemical heterogeneous polymers which should respond differently to those components^[46].

This technique however, should be employed very cautiously when analyzing heterogeneous polymers, such as graft copolymers. The mass distribution of these types of systems can only be correlated within one heterogeneity type^[47]. The chromatogram obtained by means of this technique, represents the distribution of molecules having a different functionality. This implies that the molecular weight distribution cannot be ascribed to a specific functionality type as the sizes of macromolecules in solution depend on the various different molecular characteristics, making this technique only semi-quantitative for complex polymer systems^[49].

2.5.2 Liquid Adsorption Chromatography – LAC

Liquid adsorption chromatography (LAC) entails the separation of macromolecules according to their chemical composition^[49]. This technique basically implies that macromolecules interact with the stationary phase as the polymer system is injected in an adsorli into the column. Interactions include: adsorption, hydrophobic interaction and critical point phenomena^[47]. Various authors^[49] have successfully employed LAC for the discrimination of polymer blends, statistical and graft copolymers as well as separation according to tacticity.

As the thermodynamic quality of the solvent decreases, adsorptive interactions become the dominating factor to the total retention volume. It has been reported^[46] that the interactions are exponentially related to the degree of polymerization owing to more monomeric units available for interactions with the stationary phase (Martin's rule)^[46, 49]. This implies that the retention volumes in LAC will increase exponentially with an increase in molar mass. With this said, one has to conclude that it is impossible to obtain all retention volumes for oligomers and polymers in an isocratic elution system.

In the *ideal* case of LAC the retention can be described by the enthalpic term only:

$$K_{LAC} = e^{-\Delta H / RT}, \quad K_{LAC} \geq 1 \quad [2.15]$$

$$T\Delta S \ll \Delta H$$

Hence LAC is an enthalpy governed process. It should be stressed that entropic interactions cannot be totally ignored, as only a fraction of the pores of the stationary phase are accessible.

Whilst SEC is an isocratic separation method, chromatography under adsorption conditions requires the use of a gradient profile, hence the use of adsorli, desorli solvents. In short a gradient profile for gradient elution chromatography, GE-LC, will start with eluent that is weak. This will

cause the polymer to precipitate. As one increases the strength of the solvent the polymer will steadily start to desorb and elute. Molar mass and chemical composition plays a role in elution, hence a situation must be reached where the polymer is completely dissolved and at critical conditions the high molar mass fraction elutes independently of the molar mass, i.e. $\Phi_{cr} > \Phi_{sol}$ (Φ_{cr} : fraction of strong solvent at the critical point; Φ_{sol} : fraction at the point of complete solubility). When $\Phi_{cr} < \Phi_{sol}$, incomplete dissolution occurs owing to the inadequate affinity that the eluent has towards the polymer. Consequently remaining high molar fractions will elute at a later stage at a higher solvent strength. In this case one cannot assume molar mass independence of the system. Only when $\Phi_{cr} > \Phi_{sol}$, elution will solely depend on the chemical composition of the polymer^[46].

It must, therefore, be made unambiguous that LAC is governed by exclusion, solubility effects as well as adsorption, which is either dominated by precipitation/redissolution or adsorption phenomena. The main objective of employing LAC to characterize the CCD of the polymer system under question should be to have as little molecular mass resolution interference as possible.

C. Schunk and T. Long^[50] successfully characterized PMMA-g-PDMS, an inorganic-organic polymer system by employing GE-LC followed by SEC characterization. This approach of analysis allowed for the investigation of the number of PDMS side chains incorporated into the PMMA backbone. Similarly, Graef *et al.*^[51] focussed on the analysis of the graft copolymer system, styrene-methyl methacrylate grafted onto epoxidized natural rubber. GE-LC was successfully performed to gather information concerning the grafting efficiency of the emulsion reaction.

Although GE-LC has proven to be a powerful tool, LCCC is a more viable technique as it is independent of any molar mass considerations, whereas it is not the case with GE-LC. This statement will be discussed further in the next section.

2.5.3 Liquid Chromatography at the Critical Point – LCCC

The third mode of chromatography, liquid adsorption chromatography at the critical adsorption point, LCCC (also termed LC-PEAT; liquid chromatography at the point of exclusion-adsorption transition or LC-CAP; liquid chromatography at the critical point of adsorption^[52, 53]), entails no enthalpy or entropy contributions: enthalpic and entropic contributions balance each other out, thus the free energy vanishes. Practically this implies that separation of polymers at the critical condition (or condition of entropy-enthalpy compensation, CEEC^[54]) will allow for the elution of homopolymers, hence polymers with the same repeat unit, elutes at exactly the same elution volume regardless of their molecular mass on a porous separation phase by making use of a composition/mixed mobile phase^[55].

One can interpret this type of chromatography behaviour mathematically by considering a block copolymer, AB, under such conditions^[47]:

$$\Delta G_{AB} = \sum n_A \Delta G_A + n_B \Delta G_B \quad [2.16]$$

The above equation simply states that the Gibbs free energy is the summation of the contributions from block A and block B, ΔG_A and ΔG_B . At the critical condition, as mentioned before, the entropy and enthalpy conditions balances out, and the free energy almost equals to zero:

$$\begin{aligned} \Delta H &= T\Delta S \\ \Delta G &\approx 0 \\ K_d &= 1 \\ V_R &= V_p + V_0 = V_m \end{aligned} \quad [2.17]$$

V_m is the total volume of liquid within the column. If experimentally we get the critical point of homopolymer A, the block segment A in AB, will be regarded as chromatographic invisible. In effect elution of the block copolymer AB will exclusively take place with respect to block B in the copolymer:

$$\begin{aligned} \Delta G_A &= 0 \\ \Delta G_{AB} &= n_B \Delta G_B \\ K_d^{AB} &= K_d^B \end{aligned} \quad [2.18]$$

In such a block- or graft copolymer system, the one kind of polymer will elute either according to LAC or SEC. The latter is more common for high polymers. Figure 2.9 is a schematic representation of AB copolymers subjected to LCCC. Segments B, in block AB, determine the SEC elution profile, regardless of segments A, whilst homo segments A, will elute at exactly the same retention time, regardless of their M_w .

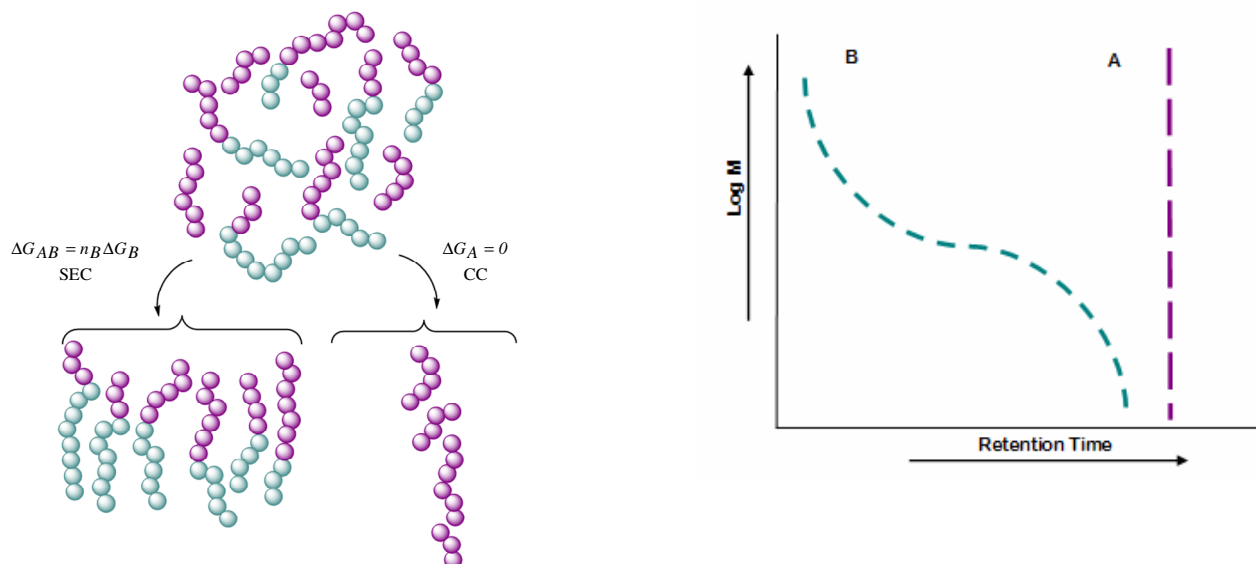


Figure 2.9: Schematic illustration of block-copolymer *AB* under critical conditions.

LCCC can further be subdivided into LC-LCA: liquid chromatography of macromolecules under limiting conditions of adsorption, and LC-LCD: liquid chromatography of macromolecules under limiting conditions^[46, 49, 52]. LC-LCA is based on a combination of exclusion and adsorption mechanisms. Macromolecules will elute under limiting conditions of adsorption, hence macromolecules will elute irrespective of their hydrodynamic volume. The mobile phase promotes adsorption of the macromolecules only slightly whilst the solvent of the sample suppresses the adsorption of the macromolecules – hence a desorli. In the case of LC-LCD, the eluent promotes desorption, thus the opposite from LC-LCA, and the sample solvent promotes adsorption.

Although LCCC is powerful and seems mathematically simple, it suffers from serious drawbacks experimentally. This was reported by D. Berek^[49] and has also been experimentally observed in this study.

Minute changes can be observed of the critical point, as this point is very sensitive toward temperature, moisture, change in eluent composition (thus inconsistent pressure differences), and variations in the physical structure of macromolecules, column packing, etc. This of course compromises the reproducibility of results to a great extent. Furthermore, Beaudoin *et al.*^[56] studied the sample recovery in LCCC, concluding that there is indeed a loss in a material, or otherwise said, some of the sample is trapped in the column. D. Berek found similar results and concluded that this can be due to precipitation when using a solvent/non-solvent eluent as the mobile phase. To overcome most of these problems, careful considerations should be taken when deciding upon one's chromatography variables. Hence adsorli and desorli thermodynamically good solvents should be selected appropriately. T. Macko and D Hunkeler^[54] compiled a comprehensive survey of data of conditions that can be employed for certain polymeric systems.

Regardless of LCCC's drawbacks, it remains a useful technique to analyse complex polymers (such as the graft-copolymers synthesised in this study) and to obtain certain information of the polymeric system. Capek *et al.*^[57] utilized LCCC to gather information about the molecular weight of the backbone of polystyrene-*g*-polyethylene oxide. They showed that not only does LCCC give information regarding the functionality type distribution of macromonomers and molecular weight distribution of blocks in block copolymer systems, but it can also provide reliable information regarding the molecular weight of the grafts.

2.5.4 Two-Dimensional Chromatography – 2-D

To reiterate, graft copolymer systems are multifaceted owing to their architectural structure as well as the synthetic route which is used for the development of such polymers. Necessarily this leads to the requirement of a multidimensional separation technique which can evaluate the different

distribution function in more than one direction, i.e. a technique where the chemical composition and molecular mass information can be obtained as well as correlated with one another (Figure 2.10). Logically then, if one requires two sets of information about the system, one needs two sets of equations to determine the number of unknowns. Practically speaking; two different separation techniques need to be employed.

Kilz^[58] developed a fully automated 2-D chromatographic system which consisted of two chromatographs. This was revolutionary as the major disadvantage of previous coupled techniques was that they occurred in an off-line/stop-flow mode. A storage loop system was employed to transfer fractions from the first dimension to the second dimension of separation, hence a fully automated on-line system.

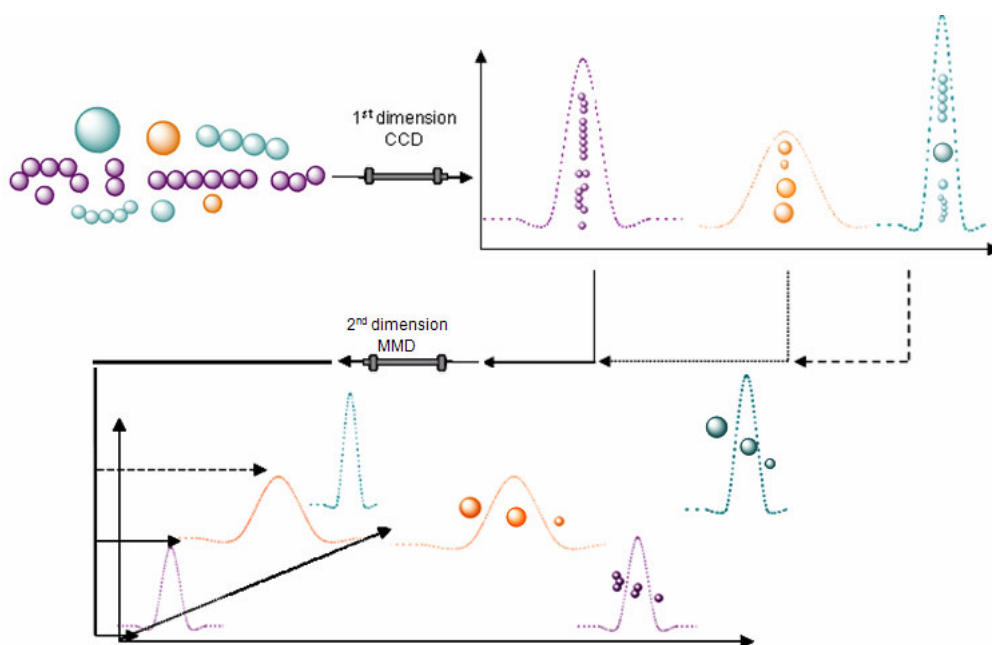


Figure 2.10: Schematic illustration for the analysis of a complex polymer system (redrawn from reference^[59]).

It is of utmost importance to decide upon the sequence of separation in order to gain as much information as possible. It has been reported that one should apply the method which will result in the highest selectivity for one property, thus selectivity towards only one structural feature and none towards other properties in the first dimension^[45, 46]. LCCC and GE-LC are normally employed in the first dimension in a 2-D chromatography setup, allowing one to obtain chemical homogenous fractions. When this is followed by SEC in the second dimension, the MMD can be obtained for the individual components in the polymeric system. The choice of eluents is dependent on the polymeric species under question. Careful consideration needs to be taken in choosing a proper eluent system for efficient separation. ELSD as a detector in the second dimension, when using

THF as a solvent, is extremely useful and powerful to obtain the information under question. More than one detector (a detector in the first as well as the second dimension) will provide more information about the polymeric system under question.

To accentuate the power of 2-D chromatography, A.H Muller *et al.*^[60] showed how one can evaluate the grafting efficiency via 2-D. In their study, they synthesised PnBuA-*g*-PMMA, poly(*n*-butylacrylate-*g*-methylmethacrylate) by means of conventional, controlled radical as well as anionic copolymerizations. Graft copolymers necessarily lead to formation of different species, wanted and unwanted: graft copolymer, unreacted macromonomer, ungrafted backbone and star polymers (a backbone with only one graft). In the first dimension, separation was accomplished under LCCC for PnBuA, implying that PnBuA will elute independently of its molecular weight. The products which were separated according to their CCD, was immediately thereafter injected into a SEC column (by means of a storage loop). Utilising 2-D it became evident that the three different graft copolymers obtained by the various techniques varied significantly structurally and had significant different molecular weight distributions. Unlike block copolymers under critical conditions, the graft copolymer product eluted prior to that of the homo-polymer (in this case PMMA) which does not elute at the critical point.

2.5.5 Coupling techniques with chromatography

Coupling liquid chromatography with another interface: LC-MS (liquid chromatography coupled to a mass spectrometer) or LC-FTIR (liquid chromatography coupled to a Fourier-transform infrared spectrometer), is a very powerful tool for a comprehensive study of the polymers in question^[61]. LC-MS, which normally have electro spray ionization, ESI, or atmospheric pressure chemical ionization, APCI, interfaces, is a very limited technique when it comes to the analysis of polymers. It cannot differentiate between structural isomers; chemical composition information is unnoticed owing to the complexity of the spectra and functional-groups are difficult to recognize etc.

FTIR on the other hand, is an important complementary technique as variation in structural detail between molecules can be characterized when coupled to SEC. This allows one to obtain structural information as a function of molecular mass. Furthermore; FTIR is superior to conventional detectors: differential refractive index (dRI), evaporative light scattering detection (ELSD), and ultra-violet (UV). ELSD and dRI detectors are non-specific, ELSD detectors are largely dependent on the chemical nature, molar mass, chemical composition, eluent composition, viscosity and surface tension^[48]; UV-Vis detectors are more selective, but the main problem with this detector is that many polymers do not show any UV activity, making it a non-suitable detector for general polymer-composition analysis^[62].

There exist mainly two methods when coupling LC to FTIR: on-line or a solvent elimination approach. In this study the solvent elimination approach was utilized by making use of a heated nebulizer. S.J Kok *et al.*^[63] did a comparative study between on-line flow-cell and off-line solvent-elimination interfaces making use of two model polymer systems. Although they concluded that flow-cell interfaces provide dependable chemical composition data across the molecular mass distribution, complete spectral information without solvent interference is still best obtained with the solvent-elimination approach, as most LC solvents show strong IR absorption bands. The solvent-elimination approach basically implies an off-line coupling of FTIR to a HPLC system: hence a collection module and an optic module (Figure 2.11). The coupling of HPLC to FTIR is made possible by using an LC-transform unit. This interface, which was introduced by Lab Connection Inc. based on Work that Gagel and Biemann^[61] did, splits the effluent of the LC column with a fraction directed to a heated nebulizer nozzle located above a rotating sample collection disc. The nozzle evaporates the mobile phase rapidly whilst depositing a tightly focused track of the solute on the collection disc. This collection disc is made of germanium which is optically transparent in the range of 6000-450 cm^{-1} ^[59]. When a full chromatogram has been collected it is transferred to the optics module in a FTIR spectrometer to obtain a full FTIR spectrum for each position on the disc. From this spray deposition a chemigram can be constructed from the series of spectra that was obtained from the sample fraction. A chemigram can be constructed from plotting the absorbance at a specific wavenumber/range of wavenumbers as a function of the elution volume from the chromatogram. The information that one principally obtains, is a concentration profile of a specific functional group^[64].

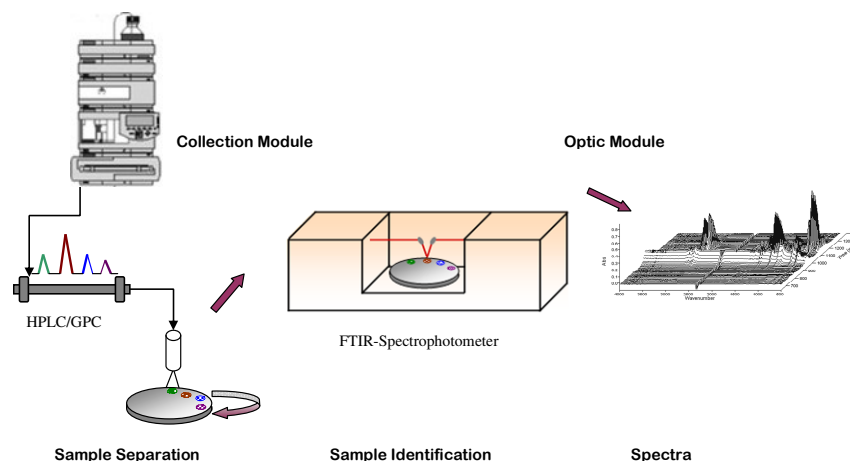


Figure 2.11: Schematic illustration of liquid chromatography coupled to FTIR spectroscopy^[45, 59].

Adrian *et al.*^[58], did a comprehensive analytical study of poly(styrene-*b*-butadiene-*g*-butyl acrylate). The different products in the graft polymeric system were separated by making use of LCCC. This was further coupled to SEC, obtaining information of molar mass distribution of the

different chemical compositions present. Besides obtaining a 2-D chromatogram for the polymer system, they also combined a semi on-line infrared detection device. By employing such a route, absolute chemical compositions of the different fractions were obtained as individual spectra are quantified by making use of appropriate calibration curves.

Needless to say, to fully comprehend the chemical as well as molecular structure, of graft copolymers, coupling LC with FTIR is inevitable.

This concludes the literature and historical review of this study. The study of experimental and analytical procedures used in this study will follow in the next chapter.

2.6 References

- [1] G. Kickelbick, *Hybrid Materials. Synthesis, Characterization and Application* (Wiley-VCH Verlag GmbH & Co, Germany, 2007), pp.
- [2] H. Shinoda, P. J. Miller, K. Matyjaszewski, *Macromolecules* **34**, 3186 **2001**.
- [3] V. Castelvetro, C. De Vita, *Advances in Colloid and Interface Science* **108-109**, 167 **2004**.
- [4] J. Pyun, Matyjaszewski, K., *Chemistry of Materials* **13**, 3436 **2001**.
- [5] D. Berek, *Macromolecules* **37**, 6096 **2004**.
- [6] Matyjaszewski K., *Statistical, Gradient, Block and Graft Copolymers by Controlled/Living Radical Polymerizations* (Springer-Verlag Berlin Heidelberg, New York, 2002), pp.
- [7] F. Xu, T. Li, J. Xia, F. Qiu, Y. Yang, *Polymer* **48**, 1428 **2007**.
- [8] S. Peleshanko, V. V. Tsukruk, *Progress in Polymer Science* **33**, 523 **2008**.
- [9] Y. You, C. Hong, P. Wang, W. Wang, W. Lu, C. Pan, *Polymer* **45**, 4647 **2004**.
- [10] Y. Cai, M. Hartenstein, A. H. E. Muller, *Macromolecules* **37**, 7484 **2004**.
- [11] I. V. Dimitrov, I. V. Berlinova, N. G. Vladimirov, *Macromolecules* **39**, 2423 **2006**.
- [12] E. H. I. J. Brandrup, *Polymer Handbook* (John Wiley & Sons Inc, New York, ed. second edition, 1975), pp.
- [13] S. D. Smith, J. M. DeSimone, H. Huang, G. York, D. W. Dwight, G. L. Wilkes, J. E. McGrath, *Macromolecules* **25**, 2575 **1992**.
- [14] M. Meincken, T. A. Berhane, P. E. Mallon, *Polymer* **46**, 203 **2005**.
- [15] H. D. Maynard, S.-P. Lyu, G. H. Fredrickson, F. Wudl, B. F. Chmelka, *Polymer* **42**, 7567 **2001**.
- [16] Y. Lee, I. Akiba, S. Akiyama, *Journal of Applied Polymer Science* **87**, 375 **2003**.
- [17] N. Wu, L. Huang, A. Zheng, H. Xiao, *Journal of Applied Polymer Science* **99**, 2936 **2006**.
- [18] Y. Lee, I. Akiba, S. Akiyama, *Journal of Applied Polymer Science* **86**, 1736 **2002**.
- [19] X. Chen, J. A. Gardella, P. L. Kumler, *Macromolecules* **26**, 3778 **1993**.
- [20] A. Schluter, R. W. Cahn, P. Haasen, K. E.J., *Synthesis of Polymers* (Wiley-VCH Verlag GmbH, Weinheim, 1999), pp. 1-649.
- [21] *Encyclopedia of Polymer Science and Technology*. J. I. Kroschwitz, Ed. (John Wiley & sons, Inc, New Jersey, 2003), pp.
- [22] K. Ito, *Progress in Polymer Science* **23**, 581 **1998**.
- [23] K. Ito, S. Kawaguchi, *Advances in Polymer Science* **142**, 130 **1999**.
- [24] I. Capek, Akashi, *Journal of Macromolecular Science, Reviews in Macromolecular Chemistry and Physics* **C33(4)**, 369 **1993**.

-
- [25] D. W. Jenkins, S. M. Hudson, *Chemical Reviews* **101**, 3245 **2001**.
- [26] F. Meijs, E. Rizzardo, *Journal of Molecular Science, Reviews in Macromolecular Chemistry and Physics* **C30 (3&4)**, 305 **1990**.
- [27] K. Matyjaszewski, A. H. E. Müller, *Progress in Polymer Science* **31**, 1039 **2006**.
- [28] K. L. Ngai, G. Floudas, D. J. Plazek, A. K. Rizos, *Encyclopedia of Polymer Science and Technology*. J. I. Kroschwitz, Ed. (John Wiley & Sons, Inc., New Jersey, 2003), pp. 111-140.
- [29] W. Lee, H. Lee, J. Cha, T. Chang, K. J. Hanley, T. P. Lodge, *Macromolecules* **33**, 5111 **2000**.
- [30] H. Nikos, I. Hermis, P. Stergios, P. Marinos, *Journal of Polymer Science Part A: Polymer Chemistry* **38**, 3211 **2000**.
- [31] *Encyclopedia of Polymer Science and Technology*. J. I. Kroschwitz, Ed. (John Wiley & Sons, Inc., Publication, New Jersey, 2003), pp. 111-143.
- [32] P. M. O'Donnell, K. Brzezinska, D. Powell, K. B. Wagener, *Macromolecules* **34**, 6845 **2001**.
- [33] J. Smid, M. Van Beylen, T. E. Hogen-Esch, *Progress in Polymer Science* **31**, 1041 **2006**.
- [34] R. P. Quirk, J. Janoski, S. R. Chowdhury, *Macromolecules* **42**, 494 **2009**.
- [35] P. F. Rempp, E. Franta, *Advances in Polymer Science* **58**, 3 **1984**.
- [36] N. Hadjichristidis, M. Pitsikalis, S. Pispas, H. Iatrou, *Chemical Reviews* **101**, 3747 **2001**.
- [37] K. Matyjaszewski, J. Xia, *Chemical Reviews* **101**, 2921 **2001**.
- [38] R. C. Advincula, W. J. Brittain, K. C. Caster, J. Ruhe, *Polymer Brushes* (WILEY-VCH Verlag GmbH & Co. KGaA, Weinheim, 2004), pp.
- [39] D. Gromadzki, R. Makuska, M. Netopilík, P. Holler, J. Lokaj, M. Janata, P. Stepánek, *European Polymer Journal* **44**, 59 **2008**.
- [40] *Encyclopedia of Polymer Science and Technology*. J. I. Kroschwitz, Ed. (John Wiley & sons, Inc., New Jersey, 2003), pp. 348-375.
- [41] S. S. Sheiko, B. S. Sumerlin, K. Matyjaszewski, *Progress in Polymer Science* **33**, 759 **2008**.
- [42] M. Pitsikalis, S. Pispas, J. W. Mays, N. Hadjichristidas, *Advances in Polymer Science* **135**, 2 **1998**.
- [43] *Encyclopedia of Chemical Technology*. J. I. Knowlton, M. Howe-Grant, Eds., Copolymers (John Wiley and Sons, New York), pp. 349.
- [44] C. J. Hawker, A. W. Bosman, E. Harth, *Chemical Reviews* **101**, 3661 **2001**.
- [45] D. Held, Kilz, P., *Macromolecular Symposia* **231**, 145–165 **2006**.
- [46] H. J. A. Philipsen, *Journal of Chromatography A* **1037**, 329 **2004**.
- [47] H. Pasch, *Advances in Polymer Science* **128**, 2 **1997**.
- [48] *Encyclopedia of Polymer Science and Technology*. J. I. Kroschwitz, Ed. (John Wiley & sons, Inc, New Jersey, 2003), pp. 598-634.
- [49] D. Berek, *Progress in Polymer Science* **25**, 873 **2000**.
-

-
- [50] T. C. Schunk, T. E. Long, *Journal of Chromatography A* **692**, 221 **1995**.
- [51] S. M. Graef, A. V. Zyl, R. D. Sanderson, B. Klumperman, H. Pasch, *Journal of Applied Polymer Science* **88**, 2530 **2003**.
- [52] T. Chang, *Advances in Polymer Science* **163**, 4 **2003**.
- [53] W. Lee, D. Cho, T. Chang, K. J. Hanley, T. P. Lodge, *Macromolecules* **34**, 2353 **2001**.
- [54] T. Macko, D. Hunkeler, *Advances in Polymer Science* **163**, 61 **2003**.
- [55] J. Falkenhagen, H. Much, W. Stauf, A. H. E. Muller, *Macromolecules* **33**, 3687 **2000**.
- [56] E. Beaudoin, A. Favier, C. Galindo, A. Lapp, C. Petit, D. Gigmes, S. Marque, D. Bertin, *European Polymer Journal* **44**, 514 **2008**.
- [57] I. Capek, R. Murgascaronová, D. Berek, *Polymer International* **44**, 174 **1997**.
- [58] J. Adrian, E. Esser, G. Hellmann, H. Pasch, *Polymer* **41**, 2439 **2000**.
- [59] P. Harold, *Macromolecular Symposia* **178**, 25 **2002**.
- [60] S. G. Roos, B. Schmitt, A. H. E. Muller, *Polymer Preprints (ACS, Div. Polym. Chem.)* **40**, 984 **1999**.
- [61] H. Pasch, *Advances in Polymer Science*, **150**, 1 **2000**.
- [62] S. J. Kok, N. C. Arentsen, P. J. C. H. Cools, T. Hankemeier, P. J. Schoenmakers, *Journal of Chromatography A* **948**, 257 **2002**.
- [63] S. J. Kok, C. A. Wold, T. Hankemeier, P. J. Schoenmakers, *Journal of Chromatography A* **1017**, 83 **2003**.
- [64] P. Harald, A. Martina, R. Frank, B. Stefan, *Macromolecular Rapid Communications* **26**, 438 **2005**.

Chapter 3

Experimental

Scientific thought, then, is not momentary; it is not a static instance; it is a process – Jean Piaget.

3.1 Synthesis

This chapter will give a general overview of the experimental procedures used for the synthesis of the graft copolymers as well as the analytical instrumentation conditions and sample preparation used.

3.1.1 Materials

All glassware (reaction vessels and syringes) were dried after thorough cleaning in an oven at 120 °C. The following chemicals were used for the synthetic part of this project:

- The following chemicals were used as received without any further purification:

KOH: Associated Chemical Enterprises, 85%, Argon: Afrox Scientific UHP Cyl 17.4 kg N5.0, 99.999%, Nitrogen: Afrox Scientific UHP Cyl 11 kg N5.0, 99.999%. Allyl-chlorodimethylsilane, ACDMS, 98%; Chlorodimethylsilane, CDMS, 98%; Allyl-2-bromo-2-methyl-propionate, ABMP, 98%; 4,4'-dinonyl-2,2'-bipyridyl, dNbipy, 97%; Butyllithium, BuLi: 15 % in hexane; Platinum(0)-1,3-divinyl-1,1,3,3-tetramethyl- disiloxane complex: Karstedt Catalyst, 1 M in xylene; Benzophenone, BP, 99% ; Bromobenzene, 98%, Sodium metal, CuCl, Copper(I)chloride 99.995% all purchased from Sigma-Aldrich. 1,4-Dioxane, 95% and MgSO₄, 95% both from Saarchem. Sulphuric acid, H₂SO₄, 95% from Merck; deuterated chloroform, CDCl₃ from Cambridge Isotope Laboratories and methanol, MeOH, Sasol, Class 3. The following polydimethylsiloxanes were purchased from Gelest, Inc: vinylmethylsiloxane – dimethylsiloxane copolymers, trimethylsiloxy terminated (VDT); methylhydrosiloxane – dimethylsiloxane copolymers, trimethylsiloxy terminated (HMS) and mono-methacryloxypropyl terminated polydimethylsiloxanes – asymmetric (MCR).

- The following chemicals were further purified:

Styrene, technical grade from Plascon; Toluene, 99.8% from Kimix. 2,2'-azobis(isobutyronitrile), AIBN, 98% from Delta Scientific was recrystallized from methanol.

- The following solvents were used as received for chromatography analysis: Tetrahydrofuran, THF, HPLC grade and n-Hexane, HPLC grade, both from Sigma-Aldrich.

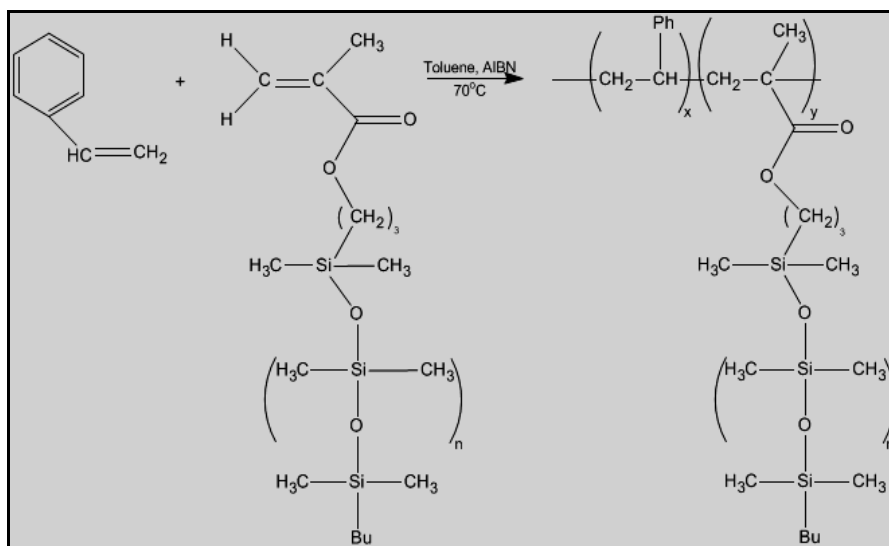
3.1.2 Purification of solvents

Toluene had to be purified and dried from impurities such as water which could have a severe affect on some of the highly sensitive reactions used (anionic polymerization). A solvent still apparatus^[1] was used where distillation could be carried out under an argon atmosphere. Finely sliced sodium metal pieces together with benzophenone was added to the toluene^[2]. Upon heating the solvent turned into a deep blue colour due to the formation of benzophenone ketyl which indicates that the solvent is dry. The solvent was allowed to reflux for 2 hours before collection.

3.1.3 Purification of monomers

Styrene was washed with 0.3 M potassium hydroxide (KOH) three times in a 1:1 volume ratio by means of a separating funnel to ensure removal of all the hydroquinone inhibitor as well as any other impurities. The resultant yellow styrene monomer was decanted into a round bottom flask together with glass beads and molecular sieves. Distillation was carried out under reduced pressure^[1] at 35 °C to avoid thermal auto-polymerization of the styrene monomer. The first fraction was collected and discarded. The collection of the clean purified fraction was redistilled again to achieve ultra high pure monomer. The final purified fraction was dried over anhydrous magnesium sulphate and flushed with argon gas for 10 min to ensure a completely dry monomer. The distilled styrene was then stored over molecular sieves at -8 °C prior to use.

3.1.4 Synthesis of PSty-g-PDMS – Grafting through



Scheme 3.1: Synthesis of PSty-g-PDMS; free radical polymerization of styrene monomer with PDMS macromonomer.

Polystyrene-*graft*-polydimethylsiloxane was synthesised via a free radical copolymerization process (Scheme 3.1). Commercial mono-methacryloxypropyl terminated polydimethylsiloxanes with three different molecular weights, M_n : 1000, 5000, 10 000, were reacted with styrene monomer, varying the weight ratios of PDMS macromonomer to styrene, where the percentage solids constituted of 20 wt% and toluene 80 wt% of the reaction. AIBN was added as initiator at 0.1 wt% based on styrene monomer added to the reaction. The reaction was allowed to proceed for 48 hours at 70 °C. The product was precipitated in ice cold methanol with a few drops of concentrated sulphuric acid. The

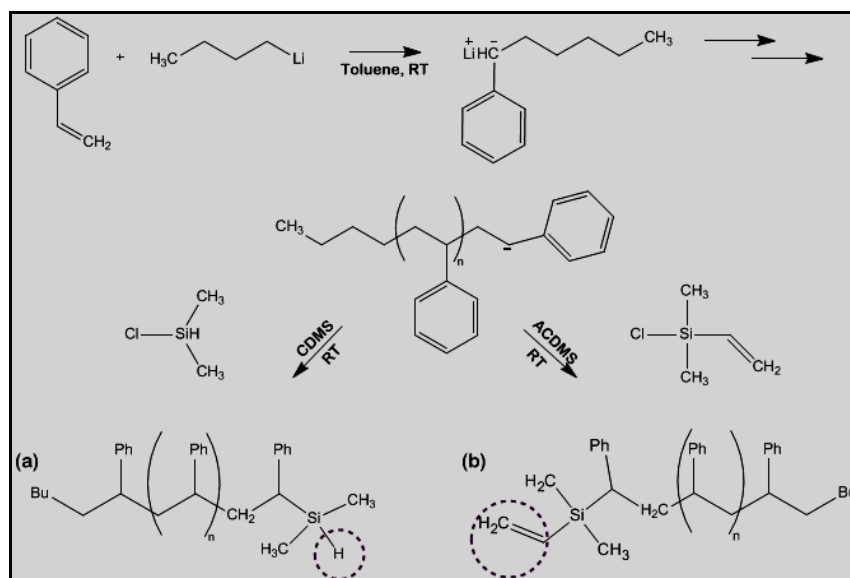
precipitate was filtered and dried under vacuum for 12 hours at 50 °C to remove any unreacted monomer.

3.1.5 Synthesis of PDMS-*g*-PSty – Grafting onto

The following section will describe the synthetic procedures used to obtain polydimethylsiloxane-*graft*-polystyrene. Two synthetic approaches were used, namely anionic polymerization (grafting onto) and ATRP (grafting from).

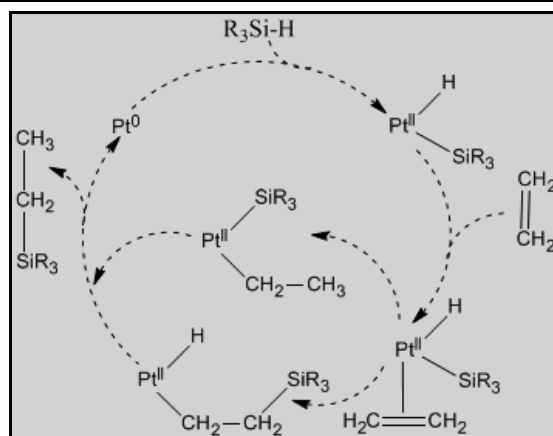
3.1.5.1 Anionic polymerization of polystyrene

Styrene macromonomer was polymerised by means of anionic polymerization (see Scheme 3.2). This allowed for control over the molecular weight, polydispersity as well as the termination with specific end-groups^[3], thus functionalisation of the styrene macromonomer. Owing to the sensitivity of the reaction towards water and oxygen, reactions were performed in an argon atmosphere glove box. All equipment were thoroughly cleaned and dried over night at 120 °C. Only stainless steel needles and glass syringes were used to avoid possible contamination from plastic dissolution. These were purged with argon before usage.



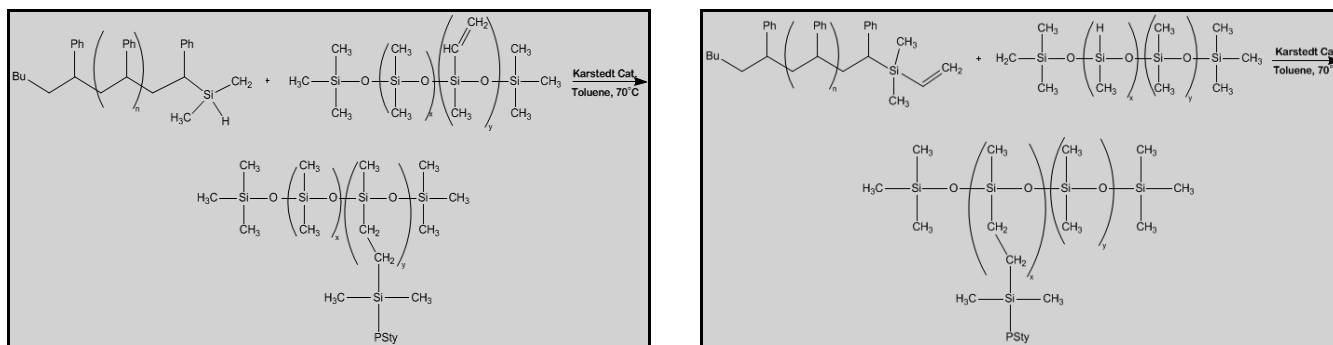
Scheme 3.2: Anionic polymerization and termination of functionalised polystyrene.

The procedure was as follows. A schlenk tube which served as the reaction vessel was flushed with argon. Styrene monomer and toluene were added in a 1:10 ratio to the schlenk tube in the glove box. The vessel was sealed and freeze-thaw cycles were performed 3 times on the reaction vessel to ensure the complete removal of oxygen. After the freeze-thaw cycles were completed, the reaction



Scheme 3.4: Modified Chalk-Harrod mechanism^[7].

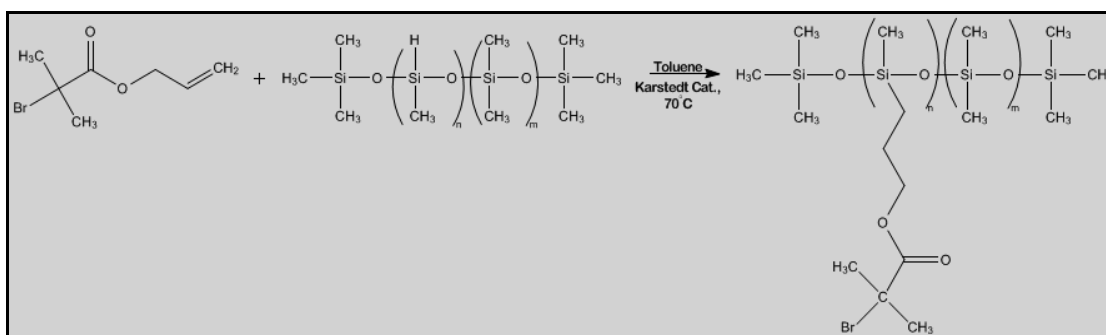
Commercial polydimethylsiloxanes were used for the grafting reaction. In the case of the silane functional polystyrenes, vinylmethylsiloxane – dimethylsiloxane copolymers, trimethylsiloxy terminated (VDT) were used; and for the vinyl functional polystyrenes methylhydrosiloxane – dimethylsiloxane copolymers, trimethylsiloxy terminated (HMS) were used. Grafting of the macromonomer functional polystyrenes and polydimethylsiloxane proceeded as follows. A round bottomed flask was charged with the functional PSty and PDMS prepolymers in a 1:1 mol ratio relative to the backbone functional content. Toluene was added in a 10:1 (toluene:solids) weight ratio. The reaction flask was tightly sealed with a rubber septum and purged with argon for 10 min. After purging the Karstedt's catalyst was added in a 1 to 100 ratio with regards to the mol polystyrene prepolymer added (catalyst: PSty prepolymer). The reaction flask was submerged in an oil bath at 70 °C for 24 hours, where after the product was precipitated in ice cold rapidly stirring methanol together with a few drops of H₂SO₄. The precipitate was filtered and dried under vacuum at room temperature for 12 hours.



Scheme 3.5: Two different routes using hydrosilylation coupling reaction to synthesize graft copolymers.

3.1.6 PDMS-*g*-PSty – Grafting from

3.1.6.1 ATRP macroinitiator method

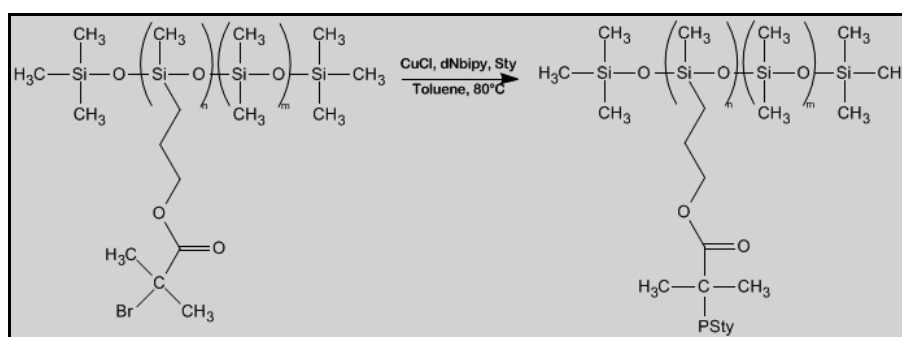


Scheme 3.6: Modification of silane terminal PDMS to ATRP macroinitiator.

This synthetic route was employed to synthesise a PDMS macroinitiator (Scheme 3.6) which was in turn used to initiate the ATRP polymerization of styrene using a CuCl catalyst and dNbipy as ligand^[8]. The commercial PDMS, HMS (methylhydrosiloxane) was used where the silane functional group could be modified to produce the bromoisobutyrate-macroinitiator for the ATRP reaction. This was achieved by adding PDMS and toluene into a round bottomed flask, where toluene was added in a 2:1 (toluene:PDMS) weight ratio. The flask was sealed and purged for 10 min where after the ABMP compound was injected with a stainless steel needle in a 50% molar excess to the mol silane functional groups present. The flask was purged again for 10 min. After final purging the Karstedt's catalyst was added in a 1% mol ratio with regards to the mol silane functional groups present. The flask was placed in an oil bath at 70 °C for 12 hours. When the reaction was completed, a rotary evaporator was used to remove all solvents. The final product was placed in a vacuum oven at 50 °C for the removal of solvent that might be present as well as unreacted ABMP. Scheme 3.6 presents the reaction pathway for the synthesis of the macroinitiator.

The ATRP procedure, illustrated in Scheme 3.7, was used for the grafting from reaction to obtain the desired graft copolymer, PDMS-*g*-PSty. The transfer of reagents all took place in a dry-box which was under Ar. A schlenk tube was charged with the bromoisobutyrate-functionalised PDMS macroinitiator, together with the desired amount of styrene monomer and toluene. Toluene was added in a 2:1 (toluene: sty monomer) weight ratio whilst the amount of styrene was added according to equation 3.1. After the desired amount of styrene was added, freeze-thaw vacuum cycles were employed to remove any oxygen present. The ratio of CuCl:dNbipy was 1:2 and added to the reaction in a 1:100 mol ratio with regards to the amount of bromine functional groups present. To ease the transfer of the metal ligand catalyst to the reaction vessel, it was first dissolved in 1.5 ml toluene in a 50 ml volumetric flask. After three freeze-thaw cycles, the metal ligand catalyst

was added in the reaction mixture (transfer took place in the dry-box) whilst stirring. The reaction flask was placed in an oil bath at 80 °C for 48 hours. A lower temperature was used to avoid possible thermal initiation of the styrene monomer which can lead to undesired species. After the reaction proceeded, the solvent was removed by means of a rotary evaporator. The resultant product was placed in a vacuum oven at 50 °C for 12 hours to remove any excess monomer and solvent which may still be present. The Cu⁺ ions were removed as follows. A 1 inch alumina column was used which was flushed with THF. The product was redissolved in THF and placed through the column for the removal of the Cu⁺ ions. This was repeated several times. The final collected fraction was placed in a rotary evaporator for the removal of the THF and placed in a vacuum oven for 12 hours for the complete removal of solvent.



Scheme 3.7: Polymerization of PDMS-g-PSty by means of ATRP with PDMS as macroinitiator.

3.1.7 Extraction of homo-polymers

Various methods were employed for the extraction of homo-PDMS and homo-PSty, but proved to be unsuccessful. The following routes were employed:

PDMS homo polymers were first removed via hexane extraction as reported in literature. This route, however, did not work as the siloxane content was too low^[9]. Thereafter the following was attempted. PDMS were removed by dissolving the polymer in Br-benzene at a concentration of 0.05 g/ml^[10]. The solution was then allowed to be cooled to 0 °C. When this temperature was reached the solution was centrifuged at 2000 rpm for 30 minutes. Essentially after centrifuging the homo-PDMS floats on the surface of the solution and can be separated from the graft-copolymer. However this proved to be very difficult as the graft copolymer and PDMS homo-polymer never formed a distinct separate layer.

Homo-polystyrene proved to be even more tedious and difficult to remove. The polymer was dissolved in dioxane containing 0.1% BHT to give a 1.3% solution. Titration with a 50:50 mixture of MeOH and water was used until the solution became milky. This milky precipitate is that of the graft copolymer^[9]. However, if one does not take extreme care the homo-polystyrene will also precipitate out if too much MeOH/water is added.

3.2 Characterization of polymers synthesised

3.2.1 Chromatographic analysis

Chromatographic analysis formed a crucial part of the analysis for the polymers synthesised under owing to the fact that incomplete separation of the homo-polymers from the graft-copolymer via synthetic routes occurred. Employing the correct chromatographic mode, one can separate the homo species from the graft copolymer. One can furthermore couple chromatography off-line or on-line for further analysis of the different components in the final product.

3.2.1.1 Size Exclusion Chromatography – SEC

One of the most routine analyses of polymers is size exclusion chromatography for the determination of the molecular weight, or rather the hydrodynamic volume, of the polymer as separation is based according to their size in solution^[11]. Hence the chain length can be directly correlated to the molar mass by means of a calibration curve obtained from standards or from molar mass sensitive detectors^[12]. In this study a calibration curve was derived from polystyrene standards by means of a dRI detector.

SEC analysis was carried out on a Waters instrument consisting of the following units:

- Waters 1515 isocratic HPLC pump
- Waters 717 plus Autosampler
- Waters 2487 Dual λ Absorbance detector
- Waters 2414 Refractive index (RI) at 30 °C

The following column set was used for separation:

- Two PLgel 5 μ m mixed-C, 300 \times 7.5 mm from Polymer Laboratories
- PLgel 5 μ m guard 50 \times 7.5 mm from Polymer Laboratories

The PLgel columns were connected in series together with the guard column at 30 °C. The stationary phase is made out of a highly crosslinked porous polystyrene/divinylbenzene matrix. The following conditions were used for the run of the sample:

- Eluent: THF Chromasovle HPLC grade, stabilized with 0.125% BHT, sparged with IR-grade helium
- Flow rate: 1 mL/min

- Sample concentration: 5mg/mL, dissolved in stabilized THF
- Injection volume: 100 μ L
- Runtime: 30 min

The system was calibrated by means of narrow polystyrene standards from Polymer Laboratories (PSty standards). Data was acquired from the Breeze Version 3.30 SPA (Waters) software. It must be highlighted at this point that PDMS used in this study has a very similar refractive index to that of THF. The implication of this was that the chromatograms obtained from the RI detector were not suitable for the material which contained PDMS segments

3.2.1.2 SEC for material with PDMS segments

SEC analysis for the material which contained PDMS was acquired on the following instrument consisting out of the following components:

- Waters 2690 Separations module (Alliance)
- Detector: PL-ELS 10000 Evaporative light scattering detector (ELSD) from Polymer Laboratories

The following column set was used for separation:

- PLgel 5 μ m MIXED-C, 300x7.5mm

The stationary phase is made out of a highly crosslinked porous polystyrene/divinylbenzene matrix. The following conditions were used for the run of the sample:

- Column temperature: 30 $^{\circ}$ C
- Solvent: THF Chromasolve HPLC grade
- Flow rate: 1 mL/min
- Sample concentration: 5mg/mL, dissolved in THF (unstabilized)
- Injection volume: 100 μ L
- Runtime: 12 min

The system was calibrated by means of narrow polystyrene standards from Polymer Laboratories (PS standards) ranging from 2590 to 38640 M_n . Data was recorded and processed on PSS WinGPC unity (Build 2019) software.

3.2.1.3 Liquid Chromatography at Critical Conditions – LCCC

As highlighted before, the extraction of the homo- components in the polymeric system proved to be challenging and somewhat impossible. This leads to one of the main objectives of this project: the development of a chromatographic method for the separation of the different components. To achieve this, the critical point of polystyrene for PSty-*g*-PDMS and PDMS-*g*-PSty was developed. What this essentially implies, is that elution of the polystyrene chains takes place independently of their molecular mass or hydrodynamic volume^[11, 13, 14]. Thus the graft copolymer will elute solely according to the molecular weight of the PDMS segments as the polystyrene will elute at a constant elution volume regardless of their molecular mass in the case of block copolymers. This technique was performed on a Waters Alliance system consisting of the following components:

- Detectors: Agilent 1100 series variable wavelength and PL-ELS 1000 detector (ELSD)
- Column: Supelco Nucleosil silica, 100 Å, 5 µm, 250 x 46(ID) mm (a polar column).
- Column temperature: 23 °C
- Flow rate: 1 mL/min
- Solvent system: THF (desorli): Hexane (adsorli); 41:59 (this composition value varied however between 41:59 and 42:58 as conditions changed over time)^[13]
- Sample composition: 5 mg/ml prepared in the same solvent composition as the mobile phase
- Injection volume: 25 µL
- Data processing: PSS WinGPC unity (Build 2019) software.

3.2.1.4 Two-dimensional chromatography – 2-D

Graft copolymers are complex materials which are molecular heterogeneously distributed in more than one direction. For a full comprehensive study of the chemical as well as the molecular heterogeneity of the graft copolymer, two-dimensional chromatography was utilized. The 2-D chromatograms will provide a wealth of information of the graft copolymers which is not easily recognizable in one dimensional chromatography studies. Thus 2-D is a complementary technique to other modes of chromatography such as SEC^[15].

For this particular study separation in the first dimension was based on chemical composition whilst the second dimension was based on molecular weight. LCCC was used for the separation according to chemical composition where after these fractions were on-line (automatically) transferred to the second dimension by means of an on-line storage loop system. Separation in the second dimension was based on molecular weight or rather hydrodynamic volume (SEC mode).

The two dimensional chromatography equipment used were as follows:

- Chromatograph 1: Waters 2690 Separation module (Alliance)
- Chromatograph 2: Waters 515 HPLC pump

The chromatographic system was connected via an electrically driven eight-port valve (Valco) with two storage loops. PSS WinGPC (Build 2019) software was used for data acquisition.

The experimental conditions for the first and second dimension respectively were as follows:

First dimension – LCCC

- Column: Supelco Nucleosil silica, 100 Å, 5 µm, 250 x 46(ID) mm
- Column temperature: 23 °C
- Solvent system: THF (desorli): Hexane (adsorli); 41:59 (this composition value varied however between 41:59 and 42:58 as conditions changed over time)
- Sample composition: 5 mg/mL prepared in the same solvent composition as the mobile phase
- Flow rate: 0.03 mL/min
- Injection volume: 25 µL
- Detector: Agilent 1100 series variable wavelength

Second dimension

- Column: PLgel 5µm MIXED-C, 300x7.5mm
- Column temperature: 30 °C
- Eluent/Mobile phase: THF
- Loop volume: 100 µL
- Flow rate: 1.5 mL/min
- Detector: PL-ELS 1000 detector (ELSD)

The second dimension was calibrated by means of narrow polystyrene standards from Polymer Laboratories (PSty standards) ranging from 2590 to 38640 M_n .

3.2.2 Off-line coupling of chromatography

3.2.2.1 Off-line coupling of chromatography to FT-IR

This method provides an off-line connection between a chromatographic and spectroscopic technique. Essentially from this one can obtain the infra-red (IR) spectra of the individual components separated chromatographically. An LC-transform instrument acts as the interface between the HPLC and FT-IR instruments^[15]. Principally the polymer is separated into different fractions by means of LCCC and then the fractionated samples are transferred to the LC-Transform unit. The LC-FTIR interface was used parallel with an ELSD detector (PL-ELS 1000) via a flow splitter. This interface evaporates the solvent and leaves behind a deposition on a germanium disc where after an IR spectrum can be obtained from the deposition on the disc.

The equipment and conditions were as follow:

- Chromatography – LCCC: same as for **section 3.2.1.3**

The interface used consisted of the following:

- LC-transform Model 303, Lab Connections, series 300
- Nozzle: fixed distance of 8mm from above collection surface
- Nebulizer nozzle temperature: 28 °C
- Rotating stage: 80 °C at 10°.min⁻¹ or 20°.min⁻¹, where the disc movement was controlled by a motor
- Vacuum chamber: pressure was maintained at 10 torr using a vacuum pump together with a liquid nitrogen trap to remove all solvent vapours
- Collection disc: rear-surface-aluminized germanium disc, 60 x 2 mm

After deposition was completed, the collection disc was placed onto a LC-transform FT-IR unit, inside the FT-IR instrument (Perkin Elmer, FT-IR spectrometer, Paragon 1000 PC) sample chamber. The unit was scanned at the same rotation as was used for the collection. This ensured a compatible run time with the chromatographic run and a FT-IR spectrum could be obtained for each fraction. The scan resolution was varied between 8 cm⁻¹ to 32 cm⁻¹. From this two-dimensional information was acquired having elution time versus IR spectra. This led to the development of Gram-Schmidt plots which provided information regarding the chemical composition of the different separated fractions. Spectrum TimeBase Version 2.0 software was used for all data processing.

3.2.2.2 Off-line coupling of chromatography to TEM

TEM, transmission electron microscopy, imaging was done at the University of Cape Town's Physics Department at the electron microscopy unit. A JEOL 1200 EX11 instrument was used. Essentially TEM imaging will allow for the morphological study of the sample as it has a very high resolution and magnification ability. The differences in electron densities of the sample are detected, where after an enlargement of the image is developed on the area which is focused on. Polystyrene and PDMS has such different electron densities, that no staining of the material is required for viewing. Samples were prepared by making use of the following method. The LC-transform interface was used for the depositions of the different fractions, separated chromatographically in the LCCC mode, onto a germanium disc. Rotation proceeded at $20^{\circ}.\text{min}^{-1}$ on the heated stage (as describe in the previous section). From this the chromatographic spray could be mapped. Silica chips were carefully placed onto the deposition track. Deposition of the sample was allowed to spray twice or sometimes thrice over the silica chips at a concentration of 10 mg/mL with an injection volume of 30 μL . The silica chips were removed from the germanium disk and transferred to a 2 mL vial where THF was used to rinse the fraction (spray of). A syringe was used to transfer the sample solution drop wise to a 250 mL beaker filled with distilled water. As the polymeric material is hydrophobic in nature it should form a thin film on the layer of the water, whilst the THF solvent diffuses rapidly into the water. Tweezers were used to "scoop" the thin material onto a copper grid (Cu, 3 mm, SPI 200 mesh regular grid, SPI supplies, West Chester, USA). The supporting grids containing the film were transferred to a vacuum oven for annealing at 120 $^{\circ}\text{C}$ for 48 hours. Figure 3.1 illustrates this procedure. TEM images were afterwards obtained from these grids, and allowed for the direct morphological study of the different fractions separated via chromatographic techniques.

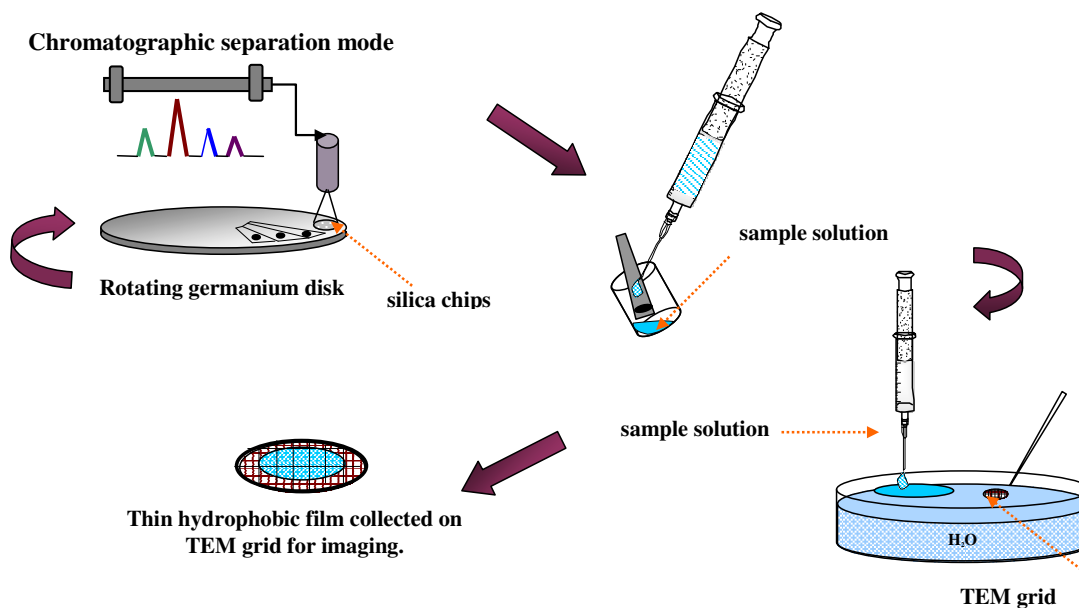


Figure 3.1: Graphic illustration of the indirect deposition of the polymeric fraction onto a TEM grid.

3.2.3. Nuclear Magnetic Resonance – NMR

Proton NMR analyses were performed on a Varian VXR, 300 MHz, Spectrometer at the University of Stellenbosch for routine ^1H -NMR analysis for the determination of molecular structure. The Varian *Unity* Inova, 400 MHz (using 128 scans) or 600 MHz were used for the precise integration of data (mainly for the determination of termination efficiency). Between 30-60 mg of sample was weighed and dissolved in deuterated chloroform (d-chloroform) in an NMR borosilicate tube to a 5 mm height mark^[16].

This concludes the experimental chapter. The following chapter will discuss the results obtained from this study.

3.3 References

- [1] L. M. Harwood, C. J. Moody, J. M. Percy, *Experimental Organic Chemistry, Standard and Microscale* (Blackwell Science, 1999), pp. 143-154.
- [2] A. Schwartz, *Chemical and Engineering News* 24, 88, **1978**.
- [3] R. P. Quirk, J. Janoski, S. R. Chowdhury, *Macromolecules* 42, 494, **2009**.
- [4] A. Schluter, R. W. Cahn, P. Haasen, K. E.J., *Synthesis of Polymers* (Wiley-VCH Verlag GmbH, Weinheim, 1999), pp. 1-649.
- [5] L. N. Lewis, J. Stein, Y. Gao, R. E. Colborn, G. Hutchins, *Platinum Metals Reviews* 41, 66, **1997**.
- [6] V. V. Anti, Cacute, M. P. Anti, Cacute, M. N. Govedarica, P. R. Dvorni, Cacute, *Journal of Polymer Science Part A: Polymer Chemistry* 45, 2246, **2007**.
- [7] S. Sakaki, N. Mizoe, M. Sugimoto, *Organometallics* 17, 2510, **1998**.
- [8] K. Matyjaszewski, J. Xia, *Chemical Reviews* 101, 2921, **2001**.
- [9] J. G. Zilliox, J. E. L. Roovers, S. Bywater, *Macromolecules* 8, 573, **1975**.
- [10] J. C. Saam, D. J. Gordon, S. Lindsey, *Macromolecules* 3, 1, **1970**.
- [11] H. J. A. Philipsen, *Journal of Chromatography A* 1037, 329, **2004**.
- [12] H. Pasch, *Advances in Polymer Science* 150, 1, **2000**.
- [13] T. Macko, D. Hunkeler, *Advances in Polymer Science* 163, 61, **2003**.
- [14] P. Harold, *Macromolecular Symposia* 178, 25, **2002**.
- [15] D. Held, Kilz, P., *Macromolecular Symposia* 231, 145–165, **2006**.
- [16] L. M. Harwood, C. J. Moody, J. M. Percy, *Experimental Organic Chemistry, Standard and Microscale* (Blackwell Science, 1999), pp. 306-341.

Chapter 4

Results and Discussion

If something happens once, it won't happen again. If something happens twice, it will surely happen a third – Paulo Coelho, The Alchemist

4 Introduction

Graft copolymers are readily made by the copolymerization of macromonomers with low molecular weight monomers (such as styrene). Conventional polymerization, i.e. FRP, has been employed extensively for the polymerization of graft copolymers. In this study conventional FRP, as well as controlled polymerization techniques, were used for the copolymerization of styrene and macromonomer-PDMS. PSty-*g*-PDMS was synthesised via a FRP, whilst PDMS-*g*-PSty was synthesised using two different controlled synthetic techniques, anionic polymerization and ATRP^[1].

It is to be expected that during copolymerization the grafting reaction of the polymer can take place, but homopolymerization of the homo-macromonomer (PDMS) can also take place leading to the formation of a polymacromonomer as well as the formation of polystyrene^[2].

It is therefore necessary to have a greater understanding of the complex multi-component material as some of the species can contribute to product failure.

4.1 Grafting through – Psty-*g*-PDMS

The synthesis and characterization of the copolymerization of PDMS macromonomer with styrene monomer will be discussed in this section. As mentioned previously the grafting through approach was utilized to synthesise PSty-*g*-PDMS polymers via conventional free radical polymerization.

Commercial PDMS-macromonomers with different lengths (and viscosities) were used in the copolymerization. In addition, the graft copolymer composition was altered by varying the PSty to PDMS macromonomer ratios. Table 4.1 gives a summary of copolymers synthesised and the ratios used for the formation of the graft product.

Table 4.1: Formulation of reactions performed – PSty-*g*-PDMS.

Sample code	Feed					
	Mono-Methacryloxypropyl Terminated PDMS				Styrene monomer	AIBN
	M_n^a (g/mol)	Viscosity ^a (Pa.s)	(g)	(wt%)	(g)	(mg)
Short 10	1000	10	0.2	10	1.8	1.8
Short 25			0.5	25	1.5	1.5
Short 35			0.7	35	1.3	1.3
Medium 10	5000	70 - 80	0.2	10	1.8	1.8
Medium 25			0.5	25	1.5	1.5
Medium 35			0.7	35	1.3	1.3
Long 10	10 000	150 - 200	0.2	10	1.8	1.8
Long 25			0.5	25	1.5	1.5
Long 35			0.7	35	1.3	1.3

^aObtained from Gelest, Inc. catalogue

The terms short, medium and long will be used from this point further denoting the lengths (M_n values) of the PDMS-macromonomers, 1000, 5000, and 10 000 respectively.

4.1.1 NMR results of the grafting reactions

Figure 4.1(a) shows the ¹H-NMR obtained for the short PDMS macromonomer used, Figure 4.1(b) for the graft product and Figure 4.1(c) for the styrene monomer used after distillation.

From Figure 4.1(b) it is clear that there is a definite broadening in the peaks between the regions of 1-2 and 6-7 ppm. The peaks assigned (a) and (b) are the two protons respectively from the vinyl group present in the macromonomer-PDMS. Peaks (m) and (l) are significant to that of the protons from the vinyl group present in the styrene monomer. It can be seen in Figure 4.1(b) that there is a clear diminishing of the peaks at δ 6.096 ppm (a), δ 5.25 ppm (b), δ 6.547 ppm (m), and δ 5.997 ppm (l) (indicated by the dotted box).

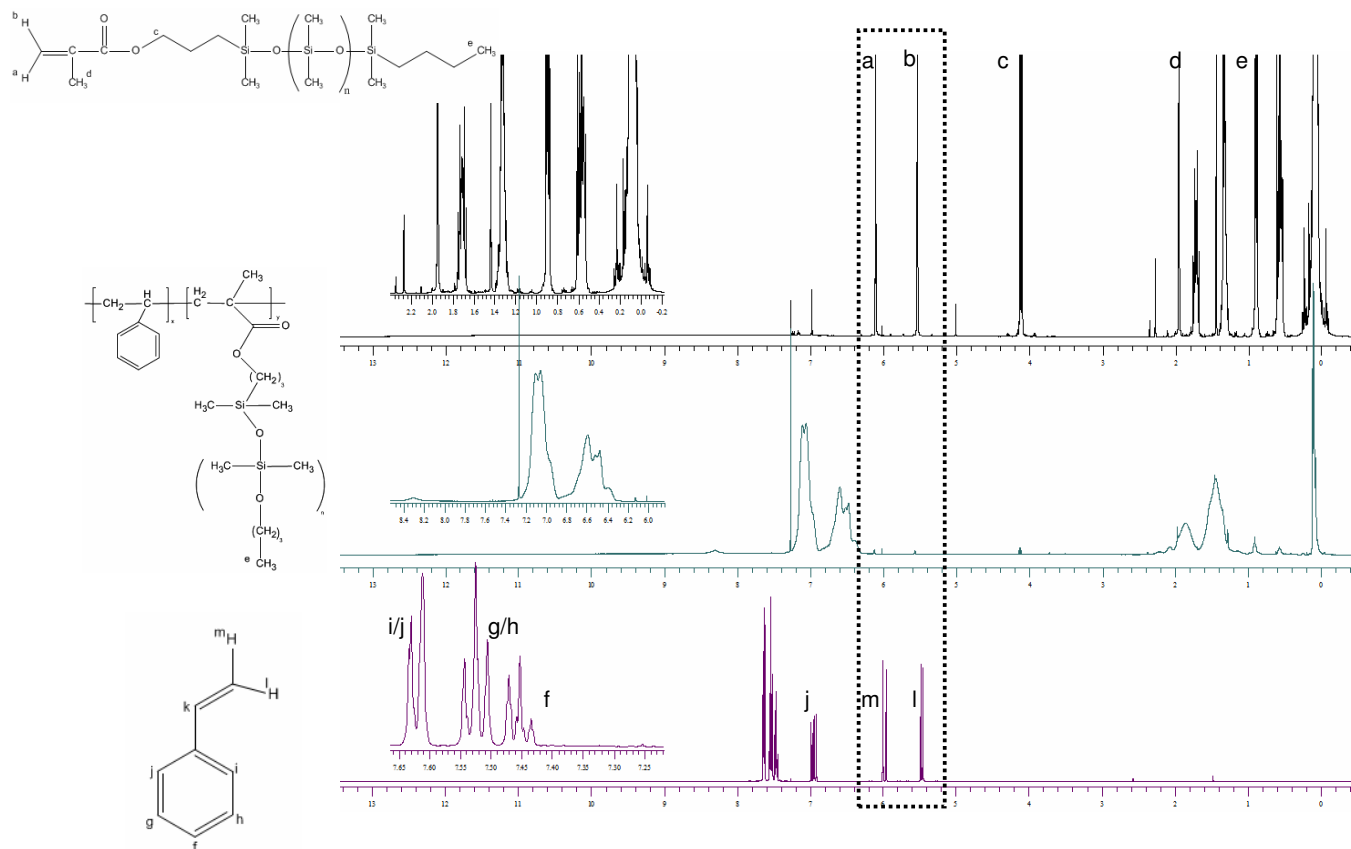


Figure 4.1 (a), (b), (c): $^1\text{H-NMR}$ spectra obtained for mono-methacryloxypropyl PDMS, PSty-*g*-PDMS, and styrene monomer respectively.

4.1.2 SEC results of the grafting reactions before extraction – RI detector

Initially the products obtained were analyzed by means of size exclusion chromatography using a dual RI and UV detector. However, M_n , M_w and PDI's values were not obtained as the PDMS-macromonomer used in this study has very similar refractive indexes to that of THF: 1.411, 1.406, and 1.405 respectively for the short, medium and long commercial macromonomers; which is very close to that of THF solvent, 1.407^[3] used as mobile phase in the SEC experiments. The implication of this is that contributions of homo-PDMS present will be excluded in the data. With this said, it is still worthwhile to discuss the chromatograms obtained from these detectors. The use of the UV detector at 254 nm played a vital role as PDMS species will not show any UV absorbance, whilst any styrene molecules present will exhibit a very strong, clear UV absorbance at this wavelength.

As mentioned elsewhere, using conventional free radical polymerization will necessarily give rise to a heterogeneously branched copolymer due to the random inclusion of the macromonomers in the polymer chains^[4]. Furthermore, it is also to be expected that the

different branch length macromonomers bearing different viscosities and reactivity ratios to styrene monomer, will give rise to different chemical compositions, i.e. graft-copolymer, homo-PDMS, and homo-PSty.

Figures 4.2 and 4.3 are the chromatograms obtained using the short PDMS macromonomer. Figure 4.2 shows the RI and UV response for short 25 and Figure 4.3 illustrates the different chromatograms obtained by using short PDMS macromonomer varying with feed ratios.

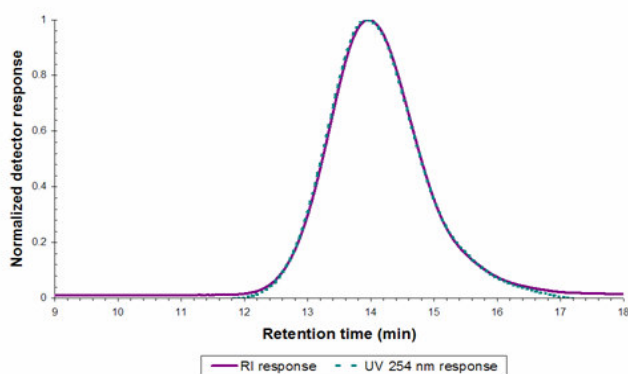


Figure 4.2: SEC graph obtained for short 25.

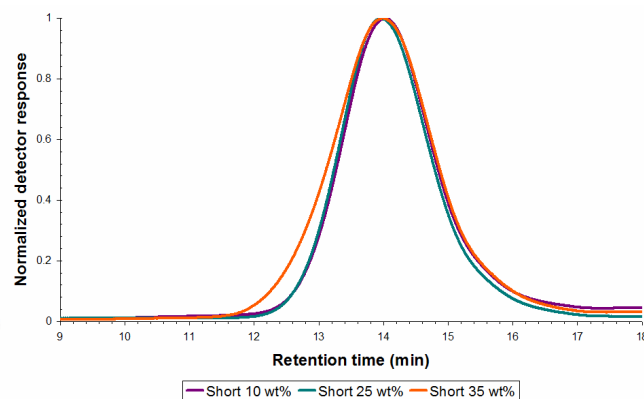


Figure 4.3: Short SEC graphs overlaid, RI response.

Figure 4.2 shows a gaussian distribution for the RI and UV response obtained for short 25. Similar results (see Figure 4.3) were obtained for short 10 and short 35. This shows that the PSty is present across the entire distribution in all three reactions (varying the feed ratio of PDMS-macromonomer to styrene monomer) with the short macromonomer.

Figure 4.4 shows a bimodal distribution in the molar mass as do all the distributions in the medium series. The UV response is weak on the smaller distribution at large retention times. In Figure 4.5 it is apparent that the intensity of the shoulder increases along the series with an increase in the PDMS feed ratio.

Figures 4.6 and 4.7 show the SEC results for the long macromonomer series. Once again a shoulder is seen at longer retention times, but is not as distinct as for the medium series. The RI and UV 254 nm response for Figure 4.7 (long 25), shows similar intensities along the distribution of the chromatogram obtained.

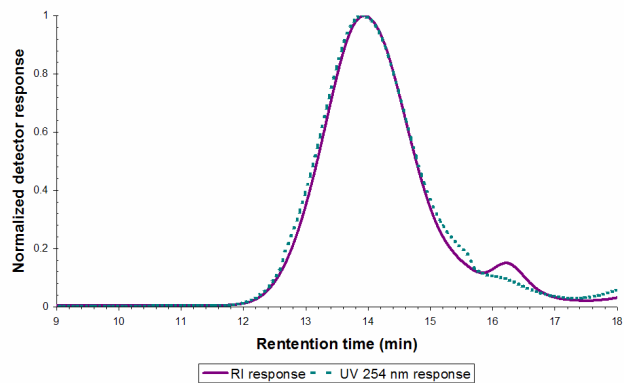


Figure 4.4: SEC graphs obtained for medium 25.

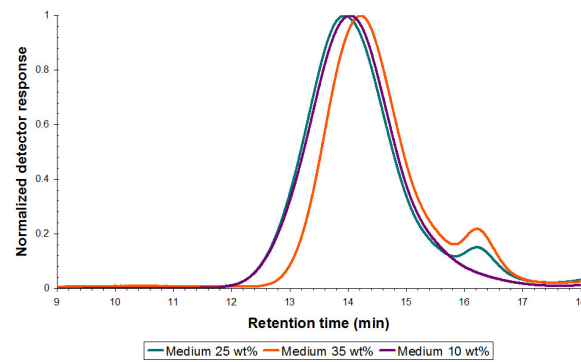


Figure 4.5: Medium SEC graphs overlaid, RI response.

It is clear from these results that different distributions are obtained by different branch length of the macromonomer in use. Furthermore, it seems that by varying the feed ratio of the macromonomer, with a certain branch length, will not lead to great deviations as the M_n , M_w and PDI's values remained fairly constant in a series. Figure 4.8 and 4.9 shows the SEC chromatograms (RI and UV responses respectively) for the graft copolymers synthesised with PDMS-macromonomers with different branch length (short, medium, long) in a 25 wt% ratio. It is also apparent that there remains a UV absorbance along the chromatogram.

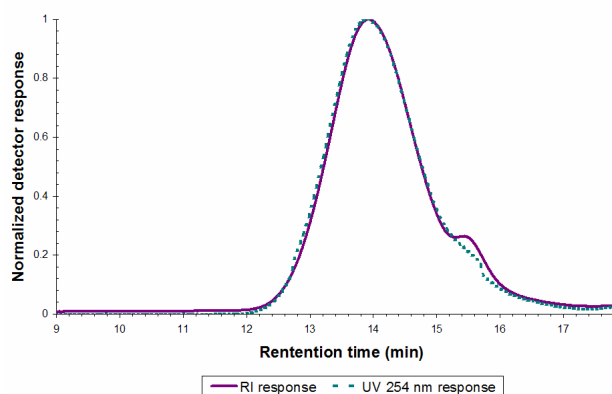


Figure 4.6: SEC graph obtained for long 25.

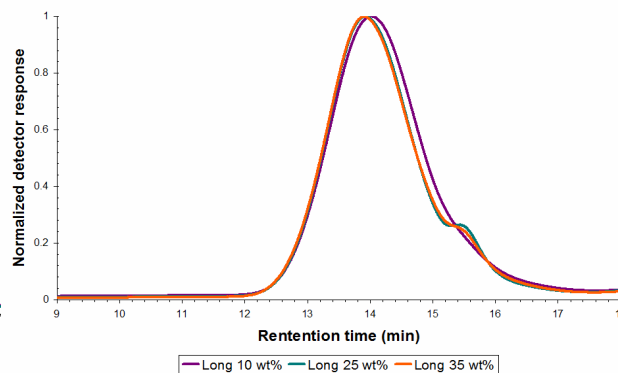


Figure 4.7: Long SEC graphs overlaid, RI response.

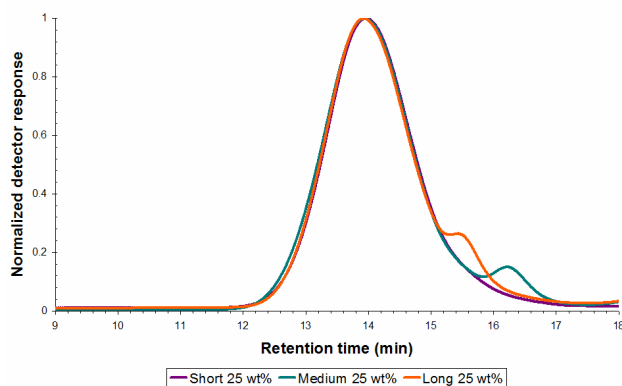


Figure 4.8: 25 wt%, SEC graphs overlaid, RI response.

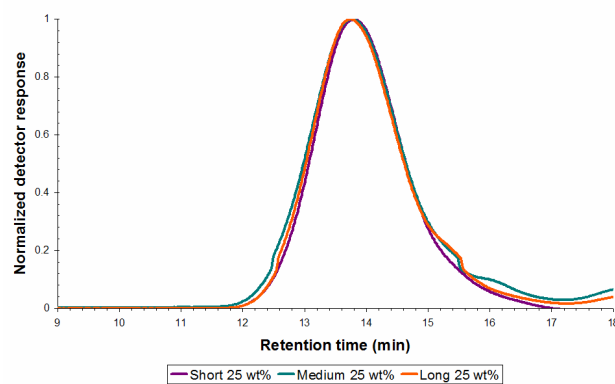


Figure 4.9: 25 wt% SEC graphs overlaid, UV response.

4.1.3 SEC results for the grafting reactions before extraction – ELSD detector

It has been mentioned that the refractive indexes for PDMS and THF are very similar and therefore the detection of homo-PDMS will be excluded from data obtained from the RI detector. However, the use of an ELSD detector allows for the detection of all species present in the system as the solvent is evaporated before detection. Table 4.2 shows a summary of the M_n , M_w , and PDI's obtained using the ELSD calibrated with polystyrene standards. Hence, all values indicated are relative to that of polystyrene. To avoid repetition, the feed ratios were excluded in Table 4.2 (see Table 4.1).

Table 4.2: Experimentally obtained molecular weights of the graft copolymers – ELSD detector.

Sample code	Mono-Methacryloxypropyl Terminated PDMS		M_n^a (g/mol)	M_w^a (g/mol)	PDI ^a
	M_n^b (g/mol)	Viscosity (Pa.s)			
Short 10	1000	10	59650	87660	1.47
Short 25			61340	91430	1.49
Short 35			59950	96220	1.61
Medium 10	5000	70-80	38030	82350	2.17
Medium 25			69330	96010	1.39
Medium 35			53880	69500	1.29
Long 10	10 000	150-200	48220	85150	1.77
Long 25			77770	100400	1.29
Long 35			77640	98760	1.27

^aDetermined via SEC using PSty standards for calibration, PL Mixed C, ELSD detector

^bObtained from Gelest, Inc. catalogue

It should be made unambiguous that the M_n and M_w values obtained are relative to that of the PSty standards used for calibration. The data summarized in Table 4.1 obtained for the different polymers, are before extraction of homo-polymers that may have formed during polymerization.

Figures 4.10 and 4.11 show the SEC traces for the ELSD and UV responses respectively for the short series. The short series SEC chromatograms show a similar gaussian distribution as was obtained from the RI detector, showing a fairly homogenous product was formed in this series.

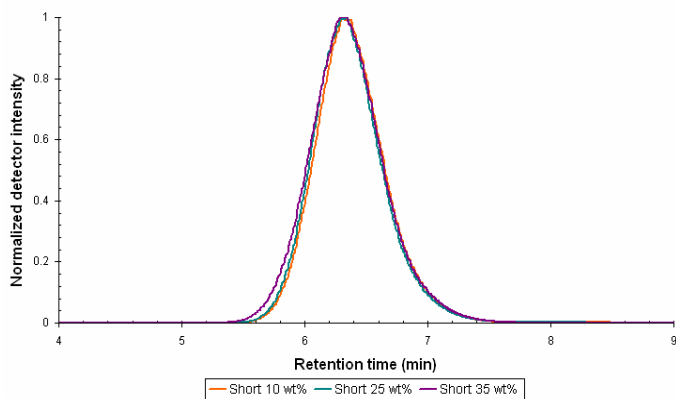


Figure 4.10: Short series, graphs overlaid – ELSD response.

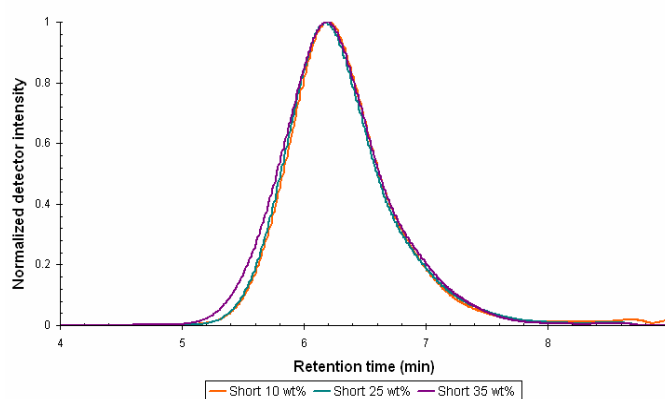


Figure 4.11: Short series, graphs overlaid – UV response.

The medium series shows a very apparent bimodal distribution, Figure 4.12, with an increase in macromonomer feed. The UV response intensity, Figure 4.13, remained analogous with the variation of the macromonomer in the specific series.

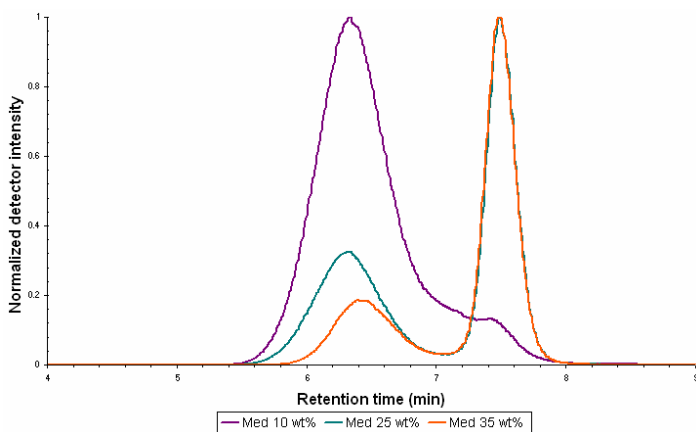


Figure 4.12: Medium series graphs overlaid, ELSD response.

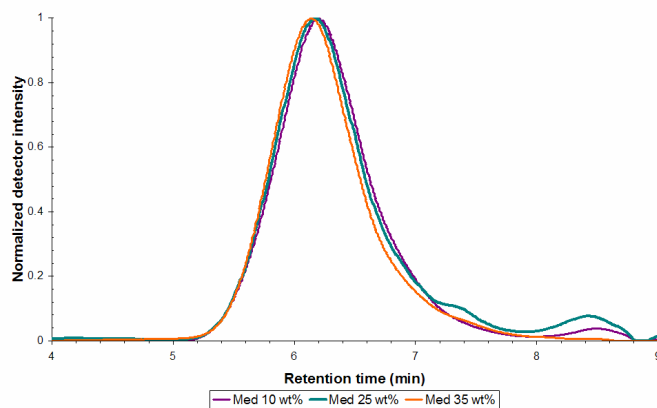


Figure 4.13: Medium series graphs overlaid, UV response.

Comparable results were obtained for the long series as for the medium series. It is very apparent in Figure 4.14 that a heterogeneously distributed product was formed. Figure 4.15 shows the UV response for the long series.

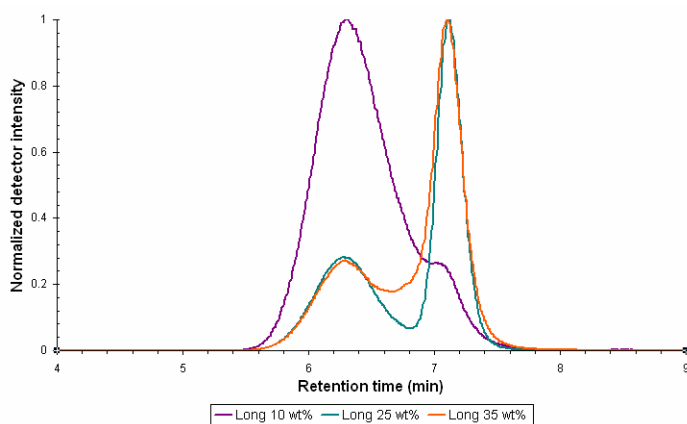


Figure 4.14: Long series graphs overlaid, ELSD response.

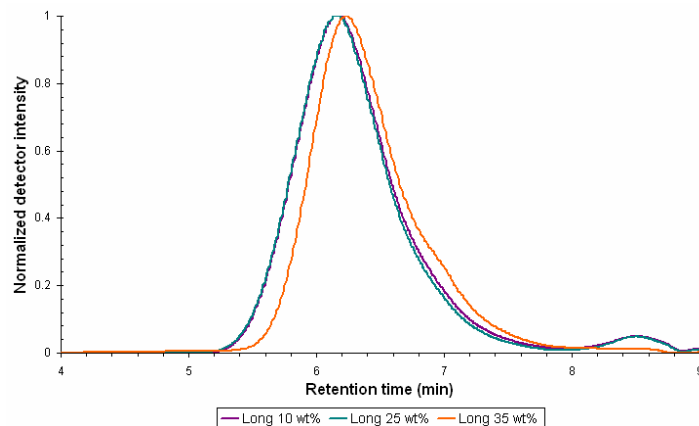


Figure 4.15: Long series graphs overlaid, UV response.

Figures 4.14 and 4.15 show the ELSD response for the medium series and long macromonomer series. Unlike the RI response shown in Figure 4.4 and 4.6 (medium and long respectively), the intensity of the second peak is far greater. This is indicative of the fact that a large amount of unreacted PDMS macromonomer remains after the copolymerization reaction.

It is to be expected that a non-uniform (non-gaussian) distribution will arise in the molecular weight distribution of the graft copolymers. This can be attributed to the reactivity of the macromonomers relative to the styrene monomer; the incompatibility of the branches and the backbone^[5-7] and viscosity effects that will necessarily influence the degree of polymerization as an increase in the viscosity will result in an increase in diffusion effects^[6]. The latter mentioned, viscosity effects, played a very definite role in the formation of heterogeneously formed products. The reason for this is that the segment density around the propagation radical site of the formed copolymer becomes relatively large, and results in a decrease in polymerization as the radical site becomes more hindered making insertion of the macromonomer extremely difficult.

4.1.4 SEC results of the grafting reactions after extraction – ELSD detector

Extraction of homo-polymers; homo-PDMS and homo-PSty were performed as explained in section 3.1.7. The extraction of homo-PSty and homo-PDMS proved to be extremely difficult and laborious with little or no success. This can be ascribed to the polarities of the homo-polymers which are very similar to that of the formed graft product, making it extremely difficult to find a proper solvent-nonsolvent system for the removal of homo-polymers. It has been reported that

homo-PDMS are easily removed only for copolymers which contain up to 70% siloxane content^[8]. As homo-polystyrene was not present in great excess, the removal of this homo-polymer was completely unsuccessful and, in most cases, led to product loss.

Figures 4.16 and Figure 4.17 show the unsuccessful removal of homo-PDMS. In Figure 4.16, the SEC chromatogram for the unextracted long 25 sample and the extracted long 25 sample clearly shows the presence of homo-PDMS (the shoulder which does not exhibit a UV response at 254 nm) in both samples. Figure 4.17, which is the LCCC chromatogram of the unextracted and extracted medium 25, confirms the presence of homo-PDMS (the peak that distinctly shows no UV response at 254 nm) after attempts for the removal of PDMS homo-macromonomer and homo-polymer.

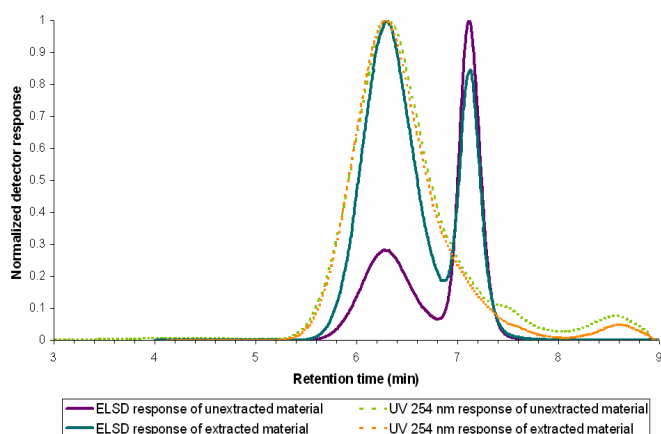


Figure 4.16: SEC chromatogram of long 25, showing the unsuccessful removal of homo-PDMS.

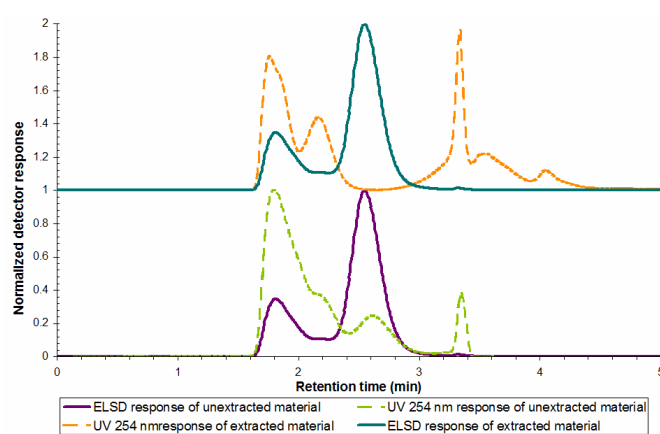


Figure 4.17: LCCC chromatogram of medium 25, showing the unsuccessful removal of homo-PDMS.

This removal of the homo-polymers (homo-polystyrene and homo-PDMS) via laborious extraction method routes proved to be futile, and necessarily led to the development of chromatographic techniques for the chemical separation of the different species present. In this study chemical composition separation were obtained by means of employing LCCC for polystyrene. The background of LCCC has been explained extensively in **section 2.5.3**.

4.1.5 HPLC analysis

In this section the development of an LCCC and 2-D system suited for the graft copolymers in this study will be discussed. LCCC at the critical point of PSty was chosen to allow for the chemical composition separation analysis for the graft copolymer.

4.1.5.1 Liquid chromatography at the critical point of styrene

Critical liquid chromatography has been discussed in depth in **section 2.5.3**. The power of this technique for the separation and consequent analysis of the product formed, lies in the fact that one can separate the species into their chemical compositions. Hence, the elucidation of the chemical heterogeneity can be made known which is not apparent in techniques such as SEC. It has to be mentioned at this point that great consideration must be taken for the determination of the critical point, as minute changes are a possibility^[9].

As mentioned before the critical point of polystyrene was determined using THF, a desorli solvent for polystyrene, and hexane, an adsorli solvent for polystyrene. Consequently PSty will elute at the same elution time irrespective of the molecular weight of the polystyrene chains at the critical point. Finding the critical conditions proved to be quite time consuming and a lot of drift in the data occurred. This can be ascribed to numerous possibilities, where inconsistent pump pressure is the most likely of them all.

The initial conditions for the critical point were a Nucleosil 300 Si column at 30 °C as the stationary phase, and the mobile phase set at 43:57 (THF: *n*-Hexane). This condition showed a lot of drifts in the data obtained, with minute changes occurring frequently. The conditions were changed to a Supelco Nucleosil silica, 100 Å, 5 µm, 250 x 46 (ID) mm column as stationary phase with the THF:*n*-Hexane set at a 48:52, desorli: adsorli ratio. These conditions proved stable for the critical point and have also been reported in a detailed review in which a survey of experimental critical conditions systems for synthetic polymers was probed by T. Macko and D. Hunkeler^[10]. Figure 4.18 shows an example of determining the critical conditions by varying the mobile solvent phase. This figure shows unequivocally that at 42:58 (THF:*n*-Hexane) critical conditions for styrene are achieved. To avoid possible sample solvent interference, samples were dissolved in a 41:59 (THF:*n*-Hexane) solvent composition. These conditions remained stable and did not give discrepancies in data.

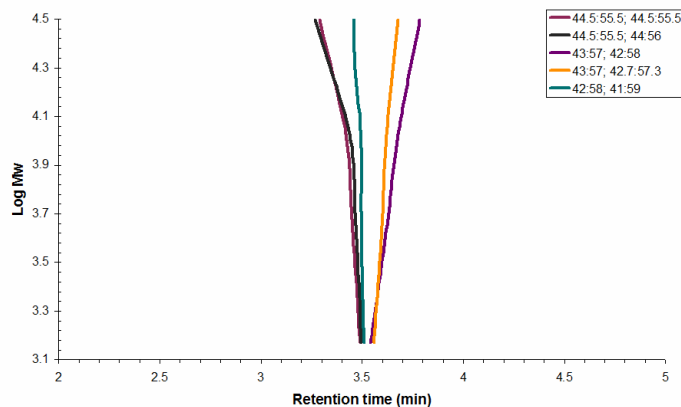


Figure 4.18: An example of the determination of the critical point by varying the mobile phase composition.

Dual detectors were employed during analysis; an ELSD and UV detector. The UV detector was set at 254 nm. At this wavelength styrene molecules will show a strong UV absorption. Employing these two detectors, a wealth of information can be obtained from the chromatograms as the ELSD will detect all of the species present, as this detector is not restricted by solvent interference as for the dRI detector, and the UV detector will only detect species which contain styrene molecules.

Figures 4.19, 4.20, and 4.21 are the chromatograms obtained for 10, 25 and 35 wt % short macromonomers series, respectively. The blue dotted chromatogram is an overlay of the homo-PDMS macromonomer used, and the orange dotted chromatogram is that of a polystyrene standard that has a molecular weight in the range of that of the polymer.

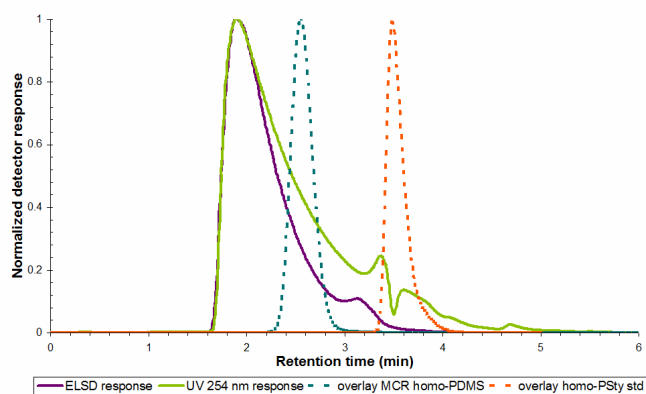


Figure 4.19: Chromatogram of short 10.

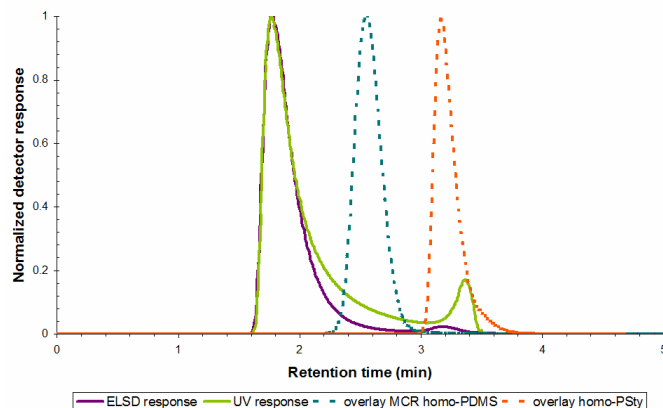


Figure 4.20: Chromatogram of short 25.

The short 10 sample shows a broad chemical distribution with a slight shoulder. This shoulder could be due to the formation of graft consisting of a backbone with only one graft (also known as a one arm star polymer)^[1]. No apparent unreacted homo-PDMS macromonomer or poly(macromonomer) are visible nor is there any homo-PSty evident. The former mentioned might be obscured as elution takes place under the critical conditions of styrene and hence homo-PDMS

will most likely co-elute with the graft copolymer. Figure 4.20 shows a distinct peak at the elution volume of polystyrene at the critical point. An UV absorbance is also apparent, indicating that this sample contains a small amount of homo-PSty. Similar results for the short 35 (Figure 4.21) were obtained. Figure 4.22 represents an overlay of this series indicating that a narrower chemical distribution occurs with an increase in the feed ratio of the macromonomer in the system.

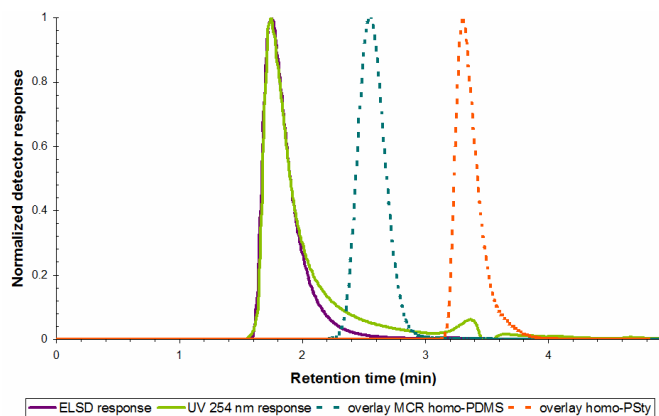


Figure 4.21: Chromatogram of short 35.

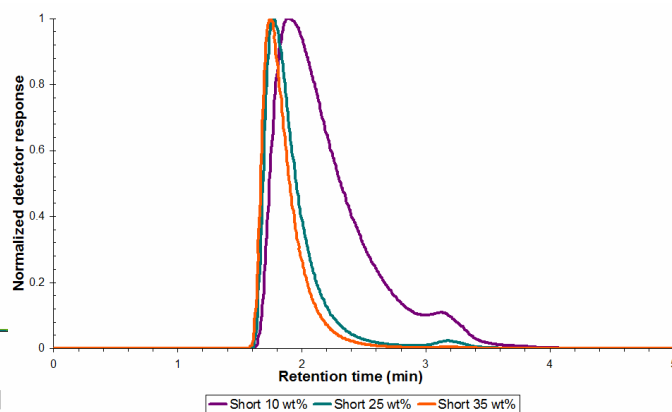


Figure 4.22: Overlaid chromatograms, short series ELSD response.

The medium series shows a great deal more chemical heterogeneity than that of the short series. Three very distinct peaks for all samples of the series were detected. The first peak shows a somewhat bimodal distribution. From Figures 4.23, 4.24 and 4.25 it is evident that a fair amount of homo-PSty is present as the UV detector shows a clear response at the critical point of homo-PSty. Homo-PDMS is also present throughout the series, however it seems to co-elute to some extent with the graft material. An increase in the feed ratio of the macromonomer gives a distinct increase in the ELSD and UV response for the graft material (which elutes first), and more apparent peaks for the homo-species present in the material.

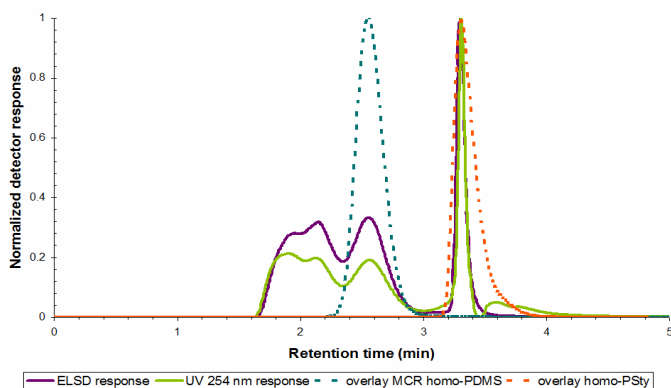


Figure 4.23: Chromatogram of medium 10.

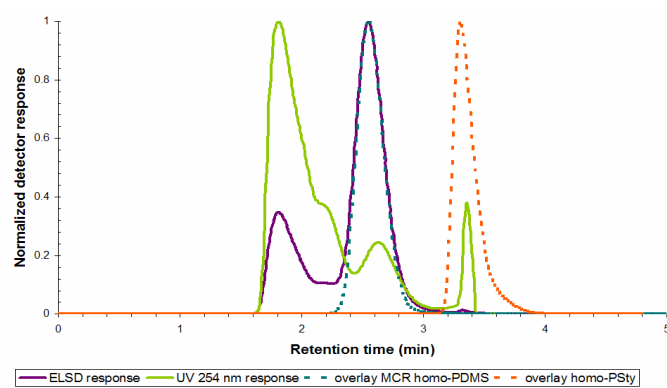


Figure 4.24: Chromatogram of medium 25.

Figure 4.26 clearly shows that there is a decrease in homo-PSty, an increase in homo-PDMS and an increase in graft formation with an increase in feed ratio of the macromonomer.

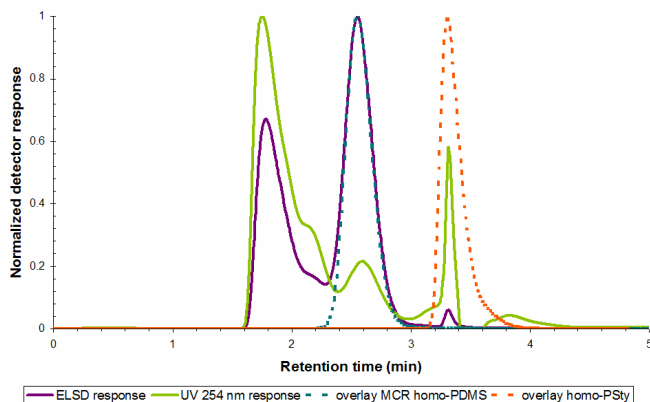


Figure 4.25: Chromatogram of medium 35.

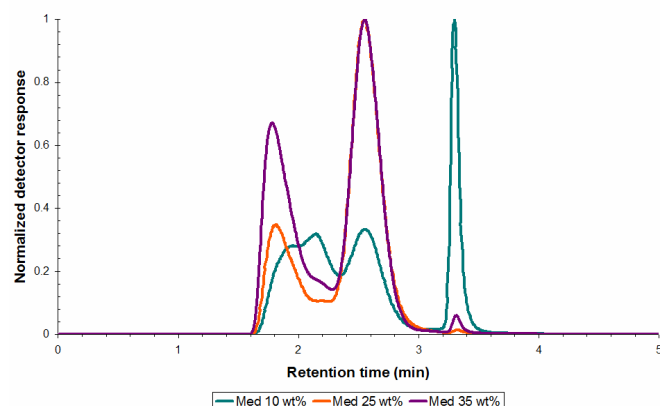


Figure 4.26: Overlaid chromatograms, medium series, ELSD response.

As can be seen in Figures 4.27, 4.28 and 4.29 (long 10, long 25 and long 35), the long series shows similar results to that of the medium series.

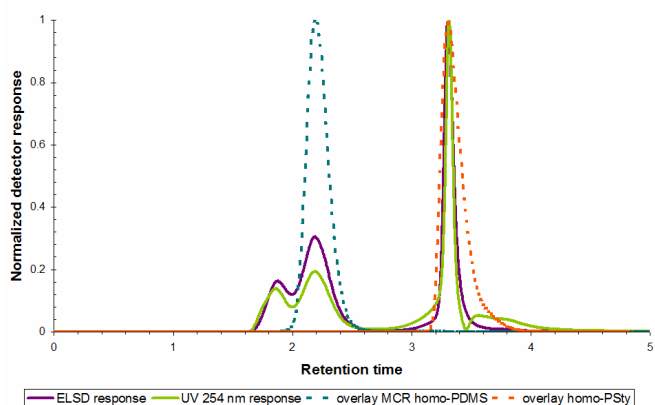


Figure 4.27: Chromatogram of long 10.

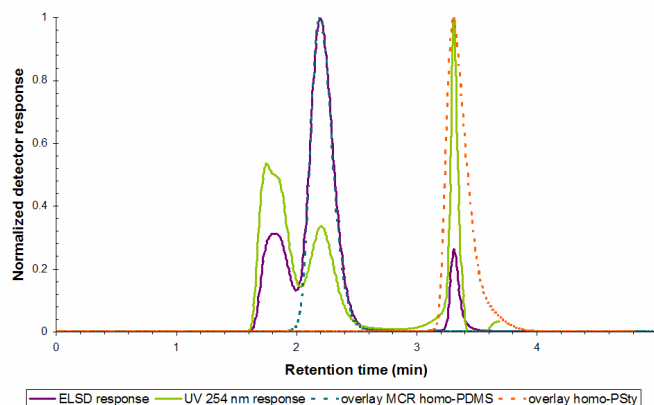


Figure 4.28: Chromatogram of long 25.

A very strong ELSD response for homo-PSty can be seen in the long 10 series that gradually diminishes with an increase in the macromonomer feed ratio. Figure 4.30 shows an overlay of the chromatograms obtained from the ELSD detector. The unreacted macromonomer, somewhat co-elutes with the graft product. The results for the series are summarized in Figure 4.31 and Figure 4.32. These results manifest the significant role that viscosity and chain mobility of the macromonomer plays in the formation of the graft material using the grafting through technique. From these one-dimensional results one can conclude that the short series shows the greatest

chemical uniformity, hence inclusion of the PDMS graft, whilst there is lesser inclusion in the medium and long series.

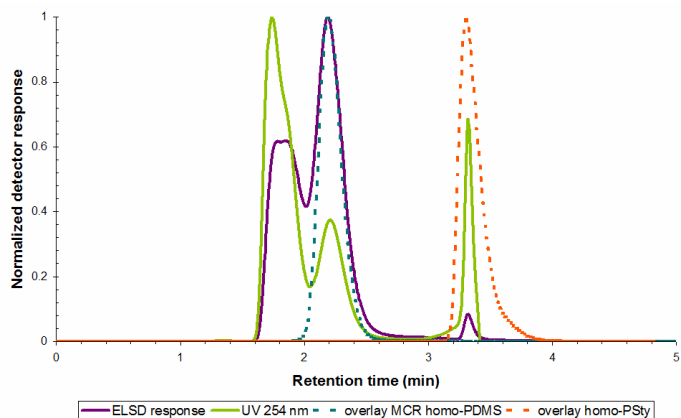


Figure 4.29: Chromatogram of long 35.

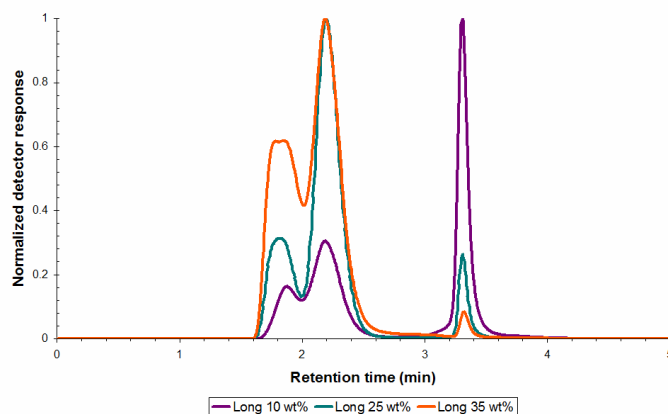


Figure 4.30: Overlaid chromatograms long series, ELSD response.

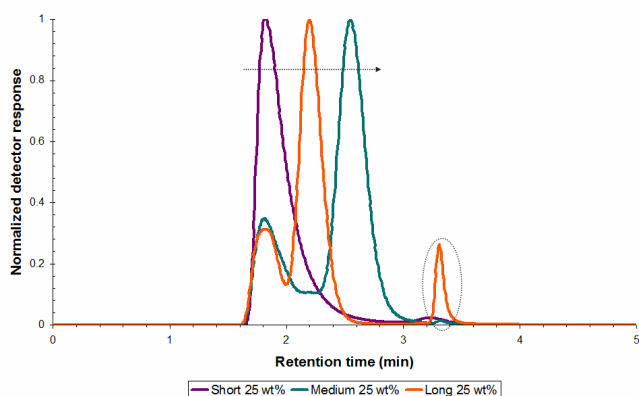


Figure 4.31: 25 wt% series graphs overlaid, ELSD response.

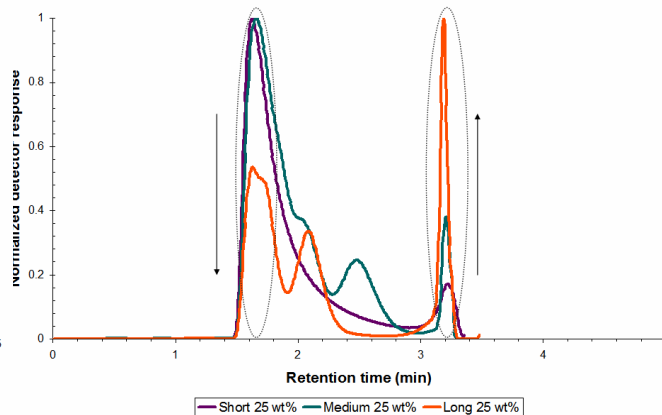


Figure 4.32: 25 wt% series graphs overlaid, UV response.

The LCCC results show that homo-PSty elutes in one chromatographic peak, and hence was successfully separated from the graft copolymer. From one-dimensional observation it seems as if the graft copolymer elutes at a lower retention time than that of the unreacted macromonomer (the blue dotted graph is that of the initial macromonomer overlaid with the graph obtained). These LCCC results are quite interesting as the PSty-*g*-PDMS separates very differently to that of its block counterpart, PSty-*b*-PDMS under the critical conditions of PSty. For PSty-*b*-PDMS under critical conditions of PSty, the graft copolymer will coelute together with the unreacted homo-PDMS. The reason for this is that the styrene segments in the block polymer are made completely chromatographic “invisible” and thus only the PDMS segments in the block copolymer will contribute to the separation. This, however, does not seem to be the case for the graft copolymer. The reason for this is that the graft product will possess a very different hydrodynamic volume to

that of the poly-macromonomer (PDMS) which is linear in nature. Although the contributions from styrene is made chromatographically “invisible” it will *still* contribute to the hydrodynamic nature of the graft copolymer, and therefore the unreacted PDMS macromonomer and homo-PDMS will elute at a higher retention volume than that of the graft material as these materials will separate in SEC (separation of the species which contains PDMS elutes under SEC conditions when PSty elutes at critical conditions).

Employing critical conditions of polystyrene as a means to separate the product into its chemical components has proven to be very successful. Information which is not apparent from the SEC results was revealed in the LCCC mode. The employment of dual detectors was very informative as PDMS does not have a UV absorbance at 254 nm. Hence, the peaks were easily distinguishable between that of the graft product, unreacted macromonomer PDMS, and polystyrene.

Although the chemical heterogeneity of the product was elucidated in the results, one further characterization is required to understand the multi-dimensional distribution of the polymer. Such a method is 2-D chromatography, which is a very powerful tool as it is selective towards different distributions, i.e. selective toward CCD and MMD. Coupling a chromatographic technique to FT-IR spectroscopy, better insight in the chemical micro-structure will become evident^[11].

In the next section the 25 wt% series were characterized with 2-D, LCCC-FTIR, and LCCC-TEM to give complete information on the graft material and the grafting reaction

4.1.5.2 Two-dimensional chromatography results

Heterogeneous species that formed during the polymerization reaction were separated according to their chemical composition in the first dimension via LCCC (according to PSty) and SEC in the second dimension. The second dimension calls for a powerful detector, thus an ELSD detector was employed which is extremely effective when THF (an organic solvent) is used. Employing this technique the heterogeneous nature of the polymer can be better understood as the species are firstly separated according to their chemical composition and then these different chemical species are separated according to their molecular weights or rather hydrodynamic volume.

2-D chromatograms were obtained for short 25, medium 25 and long 25. The reason for analyzing these three different products is that a correlation between the lengths of the macromonomer needs to be established i.e. how the macromonomer length influences the grafting reaction.

4.1.5.2.1 PSty-*g*-PDMS: Short 25

The result of the two-dimensional separation of the short 25 sample is illustrated in Figure 4.33 where the abscissa of the figure represents the molar mass distribution of the product. The chemical heterogeneity is presented in the ordinate of Figure 4.33.

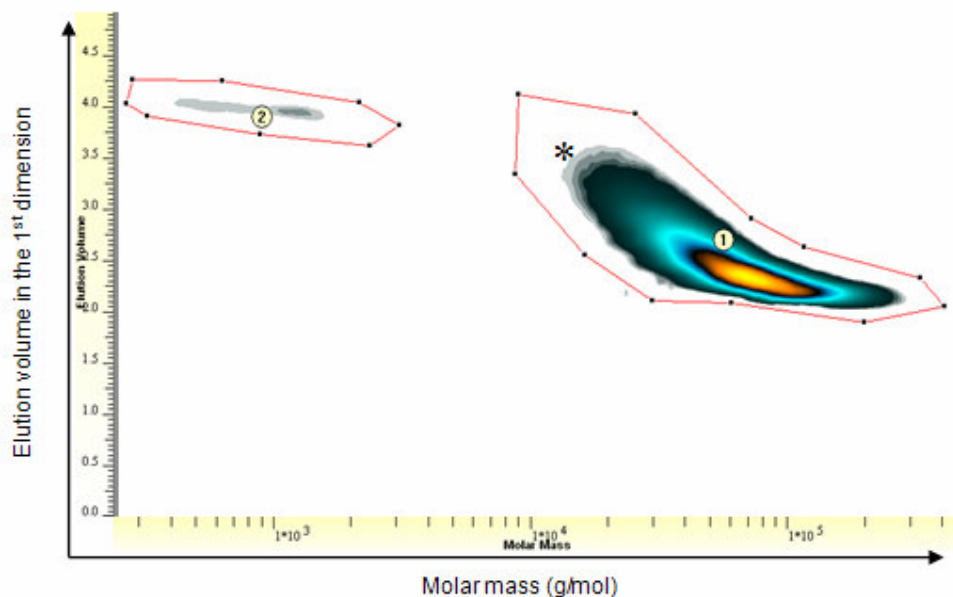


Figure 4.33: 2-D chromatogram for short 25.

Figure 4.33 shows two distinct chemically dissimilar products. Product 2 (assigned in Figure 4.33) is that of homo-PSty eluting at critical conditions and it has a very low molar mass. Product 1, the graft copolymer, exhibits a unique shape. This irregular shape of product 1 suggests that the graft

product contains heterogeneously distributed branches which are expected from a free radical polymerization^[12]. The “tail” of product 1 which elutes at a higher elution volume, suggests that it is richer in styrene units while the more densely grafted polymer elutes at a shorter retention time and has a higher molar mass.

The integration of the peaks allows for the quantitative determination of the composition. The results are summarized in Table 4.3.

Table 4.3: Molecular weights obtained for the different products for short 25.

No	Area %	Volume %	M_n (g/mol)	M_w (g/mol)	PDI
1	9.777	93.34	45574	63420	1.4
2	2.516	2.48	665	924	1.4

From the two-dimensional information obtained it is apparent that the short 25 sample contains a very high percentage of graft material with little homo-PSty and no apparent homo-PDMS macromonomer. This indicates that the grafting reaction was extremely successful using the short macromonomer.

4.1.5.2.2 PSty-g-PDMS: Medium 25

The first dimensional results already suggested that this product was chemically heterogeneously distributed. The SEC results also showed a bimodal distribution. It is therefore expected that this product will be highly distributed along the ordinate and abscissa direction.

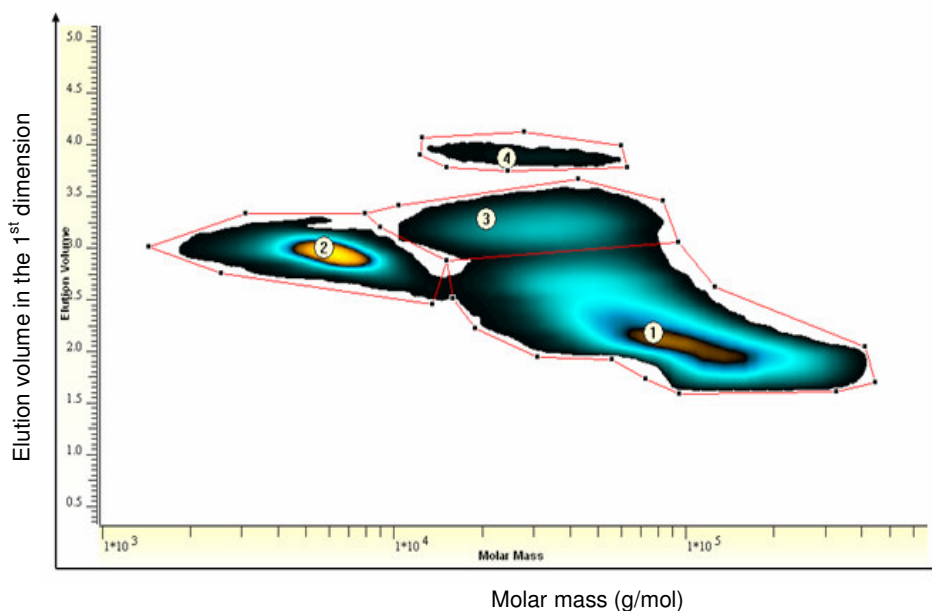


Figure 4.34: 2-D chromatogram for medium 25.

There are 4 chemically different products distinguishable in Figure 4.34. This figure further shows that these 4 products are further distributed in molar masses. The results for these products are summarized in Table 4.4.

Table 4.4: Molecular weights obtained for the different products for medium 25.

No	Area %	Volume %	M_n (g/mol)	M_w (g/mol)	PDI
1	9.282	67.73	68156.8	93850.8	1.38
2	3.818	21.34	5371.2	5768.26	1.07
3	3.1915	9.113	27706.4	32056.7	1.16
4	1.468	0.345	24349.2	28135.6	1.16

Product 4 can easily be assigned to that of homo-Psty as it elutes at the critical elution volume of that of homo-Psty in the first dimension. Product 2, which has a distinctly different elution volume along the abscissa, can be assigned to PDMS homo-macromonomer. Products 1 and 3 are not as easily assigned. As shown on the ordinate product 1 and 3 differ chemically from each other. Furthermore, product 3 shows a similar elution volume along the abscissa to that of homo-PSty (assigned no 4). However, on the ordinate product 2 (homo-macromonomer PDMS) and product 3 exhibit very similar elution volumes. It is therefore reasonable to conclude from this that product 3 is rich in styrene *but* contains at least some PDMS segments (or segment). Product 1 is the more advanced product of 3, implying that product 1 consists of a higher amount of grafted PDMS and a higher molar mass. With this said, it can be concluded that product 1 is that of the graft material and product 3 is most likely a backbone with exactly one side chain (star polymer)^[1].

Figure 4.35 shows a three dimensional view of the 2-D graph in Figure 4.34. From this illustration it is apparent that the product is still very rich in homo-macromonomer PDMS. This can be seen from the intensity scale. The graft product, product 1, exhibits a higher intensity than that of product 3. Thus, the graft product is present in a higher amount than that of the “star” polymer/the lower content PDMS polymer.

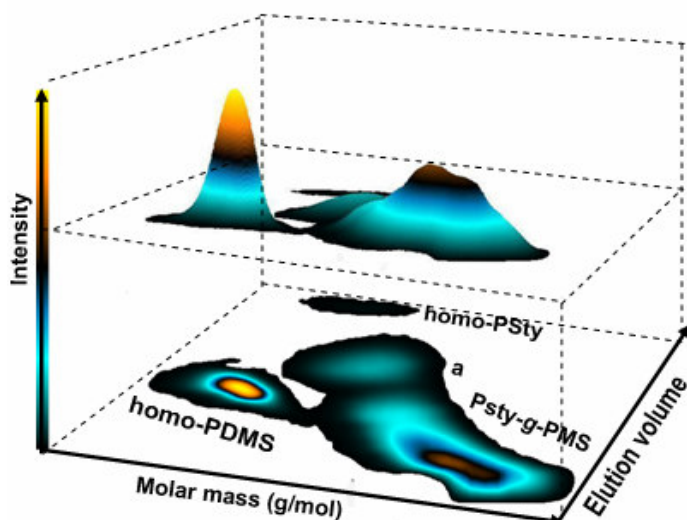


Figure 4.35: Three dimensional view of medium 25's 2-D plot.

Figure 4.36 shows the 2-D chromatogram of the short 25 sample overlaid with that of the medium 25 sample. The 2-D chromatogram for short 25 is represented by isolines, whilst medium 25 is represented by a solid figure. This figure illustrates the role chain mobility (graft length) plays in the polymerization reaction. The short PDMS-macromonomer is more effectively incorporated in the polymer chain during the formation of the copolymer, whilst there is a lesser inclusion of the medium PDMS-macromonomer and a greater heterogeneity. The product is distributed in the chemical-, molar mass- and branching direction.

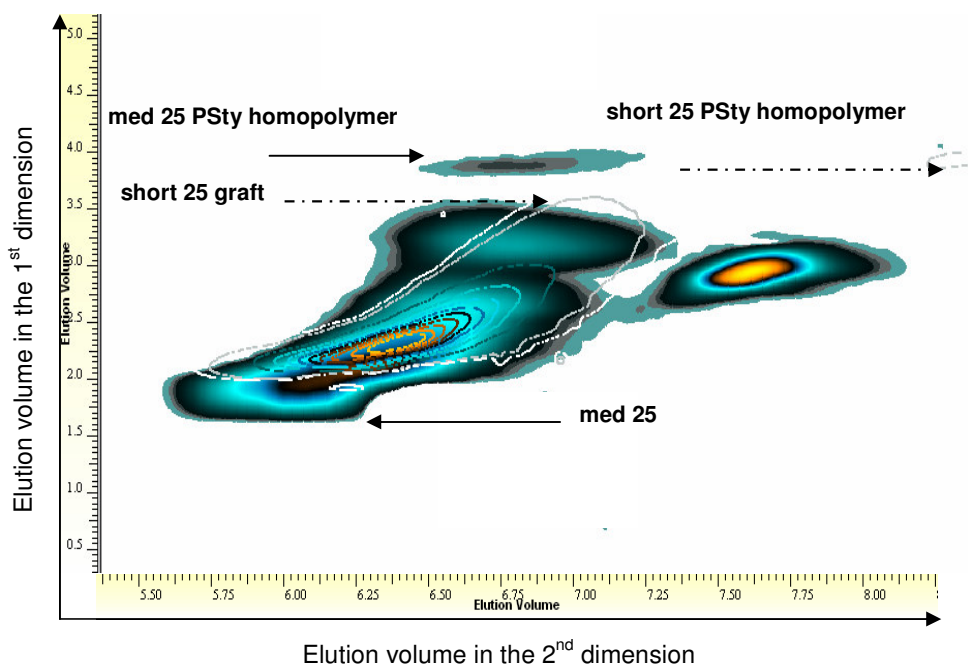


Figure 4.36: 2-D chromatograms overlaid: short 25 and medium 25.

4.1.5.2.3 PSty-g-PDMS: Long 25

The two dimensional results (Figure 4.37) for the long 25 product exhibited similar results to that of the medium 25 sample. Four chemically different products are distinguishable on the ordinate of Figure 4.37.

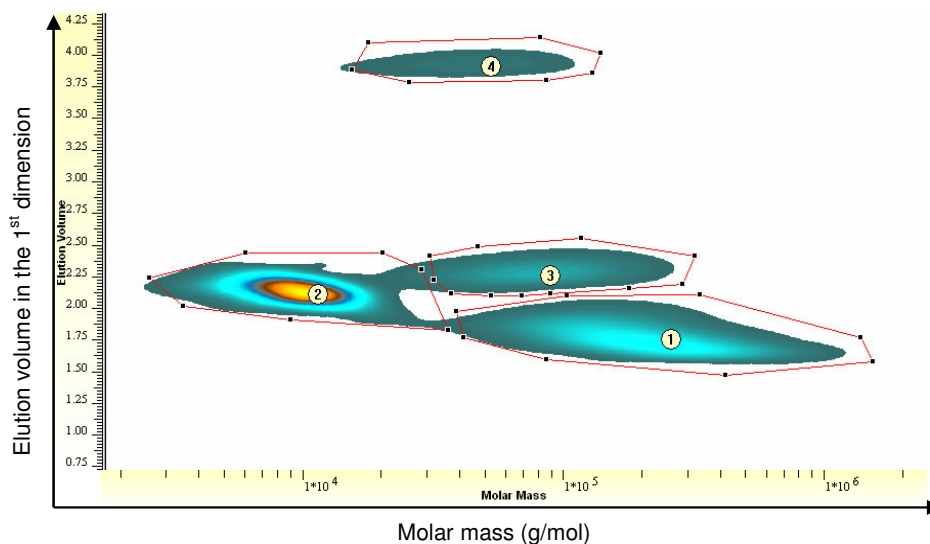


Figure 4.37: 2-D chromatogram for long 25.

Product 1 can be assigned to the graft polymer as it overlaps with the homo-macromonomer in the direction of the ordinate, but elutes at a much lower retention time as indicated along the abscissa. Product 2, that of the homo-macromonomer PDMS, is present in a large volume % (see Table 4.5) indicating that the formation of the graft copolymer was not as successful as for the short series. Yet again, as was seen for the medium series (see Figure 4.34), product 3 is most likely a one-arm star polymer owing to the fact that this product has a similar elution volume on the abscissa direction of that of the homo-PSty and on the ordinate the product has a similar elution volume to that of the the homo-macromonomer. The M_n , M_w and PDI values are summarized in Table 4.5.

Table 4.5: Molecular weights obtained for the different products for long 25.

No	Area %	Volume %	M_n (g/mol)	M_w (g/mol)	PDI
1	6.070	25.72	158563	228497	1.19
2	4.260	65.20	8532	9506	1.05
3	3.025	6.335	70339	87589	1.12
4	2.348	1.418	37738	48232	1.10

Since macromonomers are less reactive than their corresponding low molecular weight monomers, it was not unexpected to see as much residual macromonomer. From the 2-D results it became very apparent that chain mobility and chain length plays a vital role in the formation of the graft copolymer. The short 25 product shows the greatest formation of the desired graft product, whilst the long 25 product exhibits the least amount of graft material (see Table 4.6).

Table 4.6: Summary of the effect of chain length on the formation of the graft co-product.

	M_n of macromonomer (g/mol)	Volume % of graft material	Volume % of the unreacted homo-macromonomer PDMS
Short 25	800 – 1000	93.34	0
Medium 25	5000	67.73	21.34
Long 25	10 000	25.22	65.20

Although the one-dimensional results gave a better understanding of the chemical heterogeneity of the product, it did not give a comprehensive understanding of the material. Information from the 2-D contour plots was obtained, which was not at all apparent from the one dimensional (SEC and LCCC) results. It must be further noted that the separation of the graft material under critical conditions are different to that of its block counterpart.

LCCC of block copolymers allows for the determination of the block length, B, if block A is not separated according to the size of the block. Hence, block A elutes under critical conditions where the enthalpic and entropic effects balance each other out. In the case of graft copolymers, however, separation will occur according to the amount of branches/arms present *if* the backbone is made chromatographic “invisible”. S. Roos *et al.*^[13] showed similar results where graft copolymers with exactly one arm are separated from residual macromonomers. One also has to take hydrodynamic volume effects into account as a one arm polymer (star polymer) will necessarily behave differently to that of its linear counterpart. It is clear that in the case of graft copolymer separation under critical conditions, separation is more complex and difficult to interpret than in the case of block-copolymers.

From literature^[13] and the results obtained in this study^[13], it is clear that the graft material will have a lower retention time than the homo-macromonomer if the backbone is made chromatographically invisible. This allows for a complete CCD and MMD of solely the graft material.

4.1.6 Coupling of LCCC to FT-IR

Further detailed analyses of the different components in the product were necessary, and consequently a more selective detector was required. Evaporative light scattering detectors and RI detectors are non-specific whereas FT-IR spectroscopy can provide detailed analyte information and thus detailed chemical micro-structure information can be obtained^[11, 14]. Combining liquid chromatography (LC) with FT-IR spectroscopy can provide a wealth of information. When LC is coupled to FT-IR the differences in composition along the LC chromatogram will become apparent giving better insight into the product.

The basic coupling technique of LC-FT-IR has been explained in **section 2.5.5**. FT-IR spectra were obtained at regular intervals along the polymer elution volume. The micro-chemical structure of the graft material (separating by means of LCCC) became apparent across the distribution range. Figure 4.38 shows the typical data obtained when coupling LCCC to FT-IR.

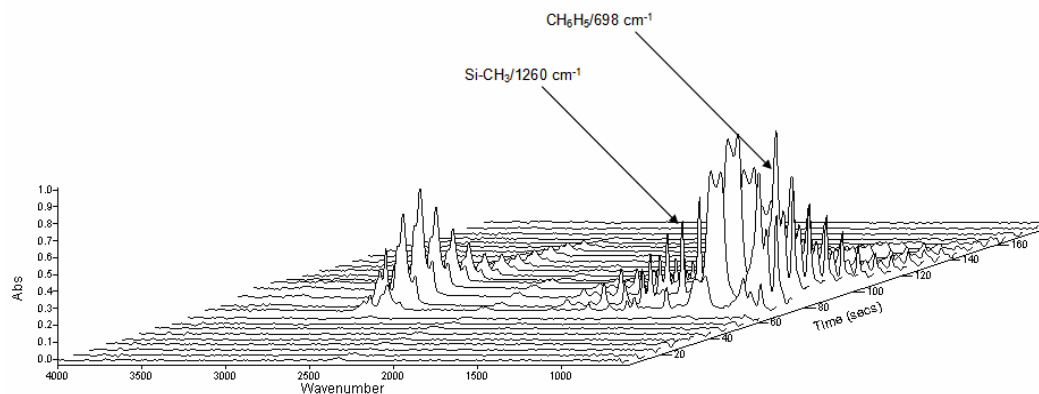


Figure 4.38: Stacked waterfall plot for short 25. The absorption bands indicated by the arrows were used for the determination of the PSty-*g*-PDMS chain composition.

A chemigram was constructed by choosing a functional group IR band and plotting the peak height against another fixed peak height. The ratio between the 1260 cm^{-1} band (indicative of Si-CH₃) and 698 cm^{-1} band (indicative of C₆H₆) was determined. This will allow one to observe where the graft material is richer in PDMS than PSty or *vice versa* as the Si-CH₃ at 1260 cm^{-1} is representative of the PDMS functional groups and the C₆H₆ at 698 cm^{-1} is representative of PSty functional groups.

The ratio of Si-CH₃/ C₆H₆ was plotted against time and overlaid with the initial chromatogram. Figure 4.39 (short 25) indicates that the graft material has a fairly uniform distribution of PDMS and PSty segments at lower retention times. This uniform distribution of PDMS/PSty is followed by an increase in the ratio. The reason for this is that the material eluting at a shorter retention time

has a higher amount of PDMS, indicating the more densely grafted polymer. This is followed by a sharp increase. This sharp increase can be ascribed to the homo-macromonomer co-eluting.

From this a conclusion can be drawn that at lower retention times a uniform distribution is seen, which is followed by an unvarying distribution. This essentially implies that the material becomes richer in PDMS segments, hence more densely grafted. These results concur with the 2-D result (refer back to Figure 4.33) obtained and give better insight in the microstructure for the short 25 sample.

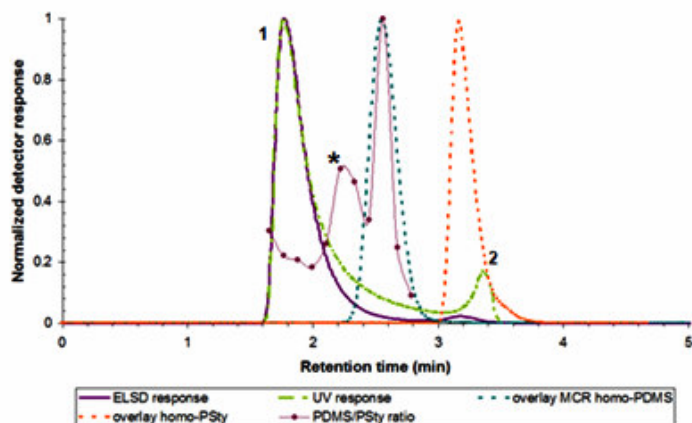


Figure 4.39: Ratio of PDMS/PSty overlaid with LCCC chromatogram: short 25.

The chemigram of medium 25 gave a wealth of information (see Figure 4.40). Initially from the one dimensional results two very distinct peaks were observed together with a lower intensity peak indicative of homo-PSty from the ELSD detector. The UV response showed a sharp intensity at lower retention time, followed by two drops and a sharp increase at the retention time of homo-PSty. The 2-D results showed that the product may contain 4 different products. The chemigram confirms this. Initially a relatively uniform distribution of PDMS/PSty is observed, followed by a sharp increase exactly where the UV response drops. After this increase, yet another increase is observed in the ratio of PDMS/PSty. This shows that the advanced graft material, which elutes at lower retention volumes, is uniformly distributed in PDMS and PSty segments. The second peak (assigned “3”) of the chemigram shows a higher ratio of PDMS/PSty. Furthermore, this peak overlaps with the shoulder of the first peak from the LCCC chromatogram. This ratio of PDMS/PSty concurs with the 2-D result (see Figure 4.34) as this is most likely a one-arm star polymer. The third sharp increase in the chemigram is indicative of the homo-macromonomer PDMS.

Figure 4.41 shows the distribution of PDMS/PSty segments overlaid with the LCCC chromatogram of the long 25 product. The ratio of PDMS/PSty does not show any regularity

implying that this graft material contains a great deal of heterogeneously distributed branches along the backbone. As was seen for the medium 25 sample, three different ratios (three different peaks) of PDMS/PSty are observed in the chemigram, the first having a lower ratio of PDMS/PSty than the second ratio. The first ratio overlaps with that of the graft copolymer, and the second with that of the one-arm star polymer with a high PDMS content (assigned “3”). The third sharp increase is exactly observed where one would expect homo-macromonomer PDMS to elute. The peak assigned “4” clearly shows no PDMS/PSty ratio as this peak is indicative of the homo-PSty eluting under critical conditions.

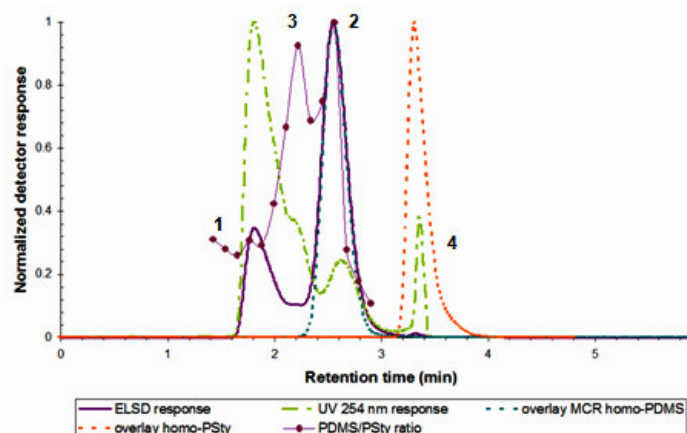


Figure 4.40: Ratio of PDMS/PSty overlaid with LCCC chromatogram: medium 25.

The chemigrams (indicated by the dotted plot) complimented the one- and two- dimensional results which were obtained. From these results a better understanding of the micro-structure of the material prevailed, one that was not that apparent from the initial chromatographic results.

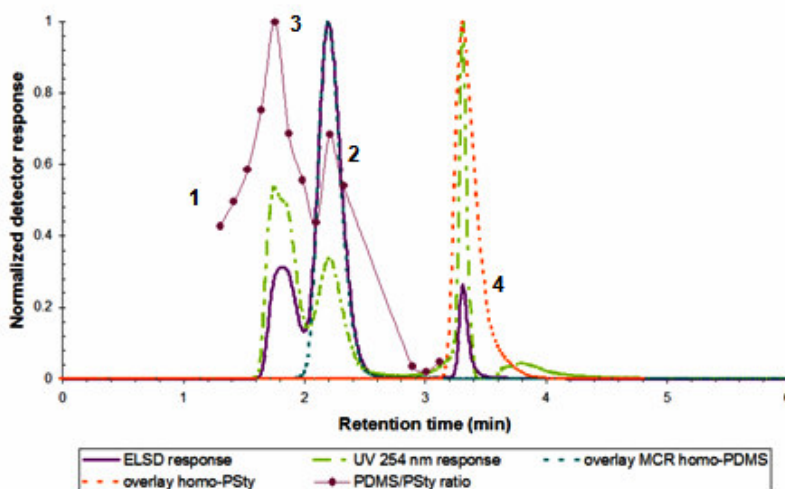


Figure 4.41: Ratio of PDMS/PSty overlaid with LCCC chromatogram: long 25.

4.1.7. Morphological analysis

It is to be expected that the graft polymers synthesised, will exhibit interesting morphologies owing to the fact that the polymers are an inorganic-organic material where the constituent segments are highly incompatible. TEM is undoubtedly an extremely powerful analytical technique to gain information about the morphology of the copolymers. Bulk TEM sample preparation, however, will not elucidate the true morphological nature of the polymer as interference from homo-polymers will certainly obscure these results.

With this said, a technique had to be used where the homo-polymers will not obscure the true morphology of the graft material. In addition the technique must also allow for the separation of thin films which are suitable for TEM analysis since conventional microtoming is not practical. Such a technique, which was developed in our group, is LCCC coupled to TEM.

4.1.7.1 LCCC coupled to TEM via indirect deposition

The method behind LCCC-TEM offline has been described previously in **section 3.2.2.2**. The offline coupling of liquid chromatography to TEM is made possible by means of an LC-transform interface (see **section 2.5.5**). LCCC-TEM will allow for the study of the morphology of PSty-g-PDMS with different branching lengths and densities in the absence of homopolymer which are difficult to remove. Essentially the information obtained will give insight to the morphological changes as a function of chemical composition distribution (CCD)

The hydrophobic nature of the material was exploited to obtain sufficient samples for TEM analysis. This was achieved by dropping the material, which was dissolved in THF after deposition on the silica chips, in a beaker filled with water. The THF solvent will rapidly dissolve into the water, whilst the polymer will stretch on the surface of the water and form a thin film suitable for TEM analysis.

Figure 4.42, shows the short 25 TEM images of the two fractions obtained as indicated on the chromatogram. The first fraction of the graft material shows wormlike/spaghetti like nanophases of polystyrene (lighter areas) in a black continuous phase of PDMS^[15]. This fraction further shows a somewhat uniform spacing with areas which are more PDMS rich than others. The second fraction clearly shows the greater present of PDMS enriched inclusions. This coincides with the 2-D chromatogram, which showed that there is an enrichment in PDMS at higher retention times (Figure 4.33), and the chemigram (Figure 4.39) for the short 25 sample, where it was observed that the unreacted PDMS-macromonomer co-elutes with the graft material at lower retention times.

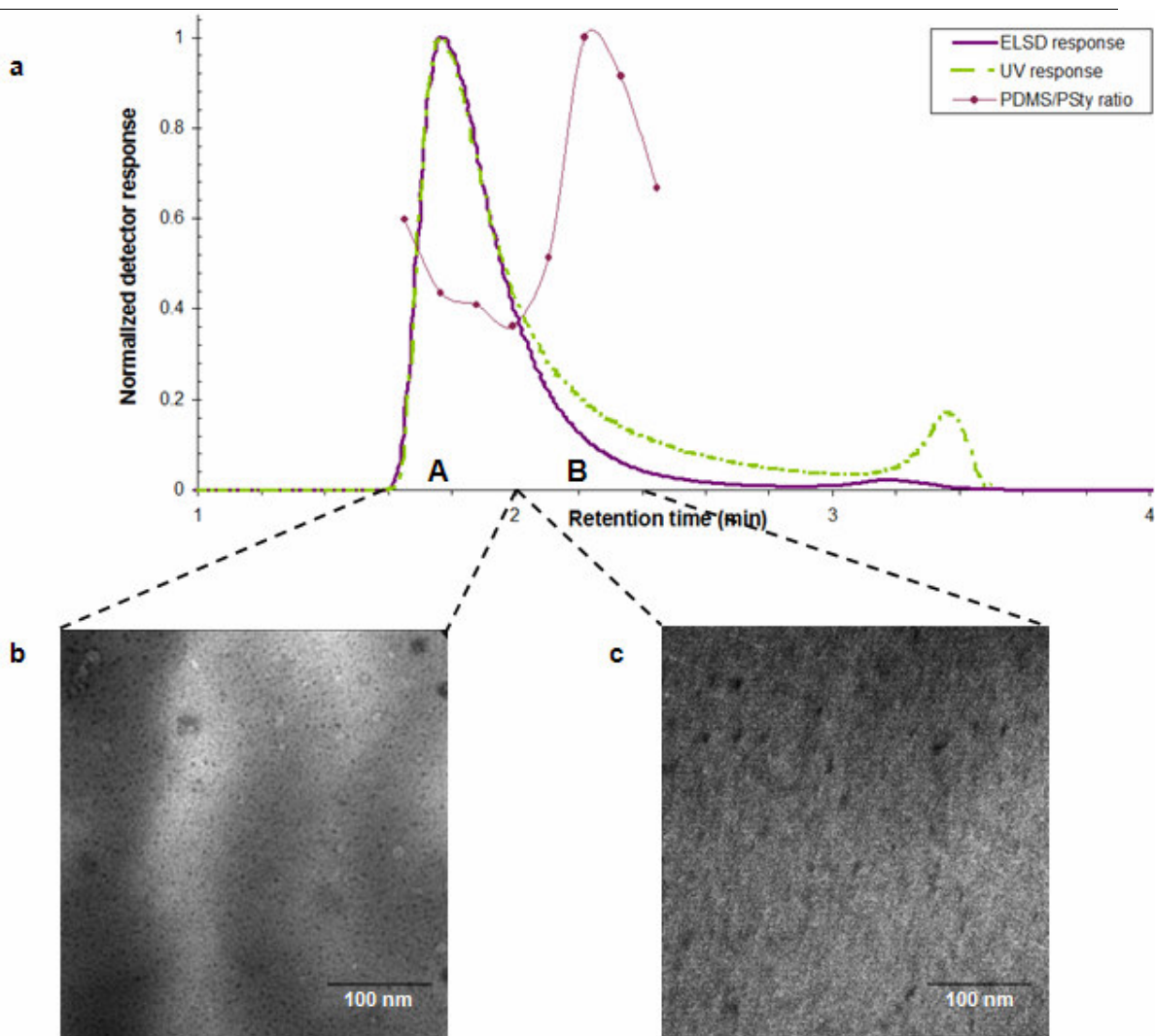


Figure 4.42 (a), (b), (c): LCCC chromatogram (a) of short 25 with chemigram overlay, TEM image of the material in region A (b) and region B (c).

The analysis of the morphology of the graft material for the medium 25 sample is shown in Figure 4.43. This material shows a significant change in morphology ordering to that of the short 25 sample. The first fraction exhibits an ordered cylindrical structure with no apparent disruption of PDMS inclusions^[16, 17]. The second fraction exhibits the same type of ordered structure as was apparent in the first fraction, although this fraction is more enriched with PDMS. Furthermore, numerous “black” inclusions are observed in this fraction as well. This is most likely homo-PDMS macromonomer, which can co-elute with the graft material at lower retention times.

The short 25 sample shows a completely different phase morphology ordering to that of the medium 25 sample. It is apparent that the degree of phase separation (as seen in Figure 4.43) becomes greater with an increase in PDMS molar mass. S.D Smith *et al.*^[16] obtained similar results.

Coupling LCCC-TEM offline proved to be very useful as the graft materials' morphology could be successfully studied without the requirement of the removal of homo-contaminants or laborious sample preparation such as cryo-microtoming.

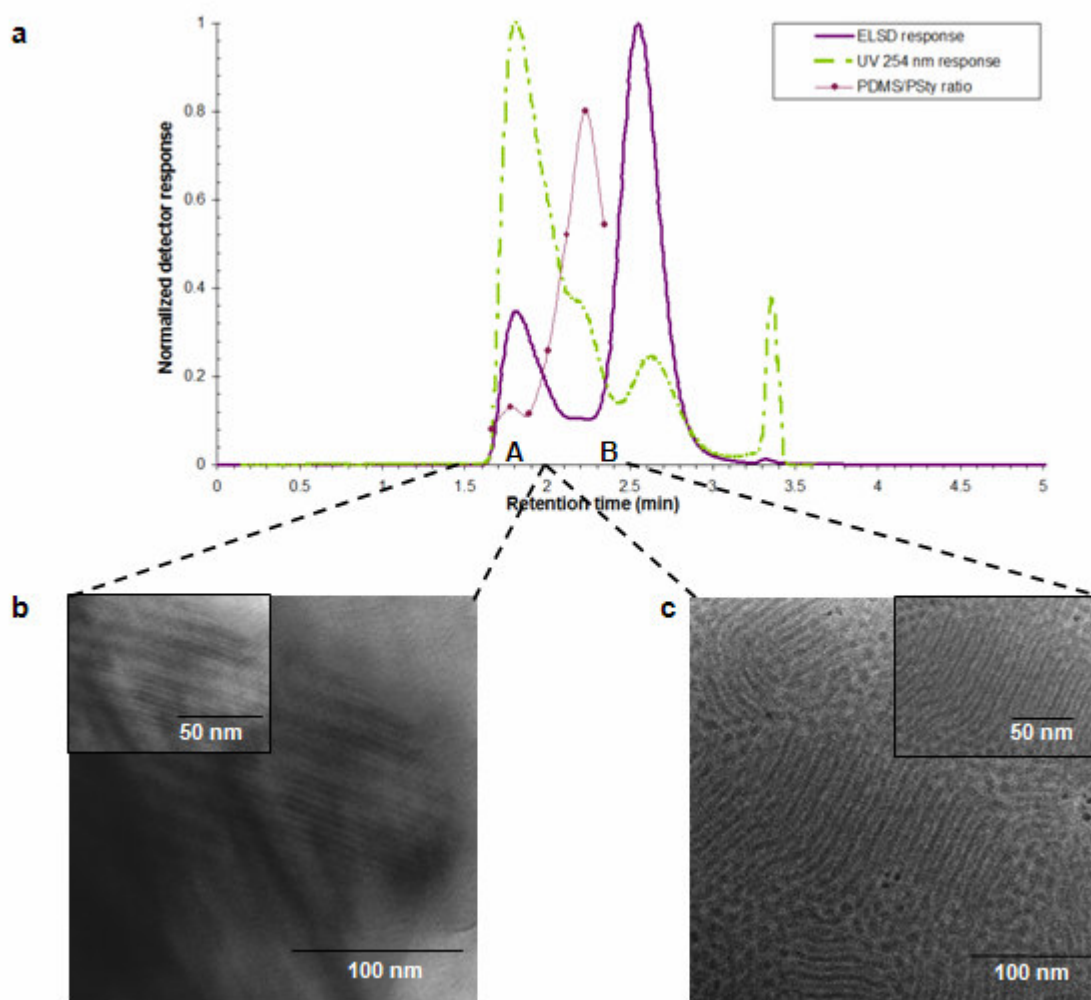


Figure 4.43 (a), (b), (c): LCCC chromatogram (a) of medium 25 with chemigram overlay, TEM image of the material in region A (b) and region B (c).

Results obtained showed that the coupling of a chromatographic technique proved to be an effective way of determining the morphology of the hybrid material as a function of chemical composition distribution (CCD). Although the morphology with regards to a change in chemical composition was studied in this project, this technique of course leaves open the possibility to study the morphology with a change in molar mass distribution (MMD) employing SEC as the LC separation mode.

This concludes section 4.1 which dealt with the synthesis and analysis of PSty-*g*-PDMS. In the next sections the synthesis and analysis of PDMS-*g*-PSty will be discussed.

4.2 Grafting onto – PDMS-*g*-PSty

The grafting onto technique was employed as one of the techniques to synthesise PDMS-*g*-PSty. This is essentially the “reverse” of the graft copolymer discussed in the previous section. In this case the backbone of the polymer consists of PDMS and the side chains PSty. This was achieved by the synthesis of a PSty prepolymer anionically and terminated with either an allyl or silane functional group. The PDMS prepolymers used were commercially obtained from Gelest, Inc. Coupling was achieved via a hydrosilylation reaction by means of a platinum catalyst (Karstedt catalyst). The synthesis of the PSty prepolymers, the coupling reaction and the analysis of the final product will be discussed in this section.

4.2.1.1 Synthesis and analysis of PSty prepolymer – Allyl functionality

PSty with varying molecular weights were synthesised by means of living anionic polymerization as this synthetic route allows one to control the molecular weight and produce polymer of controlled functionality. Previous studies conducted by our group showed that PSty reached an optimum conversion at 30 minutes and hence was terminated with either ACDMS, allylchlorodimethylsilane, or CDMS, chlorodimethylsilane (see **section 3.1.5.1**). The reason for using chlorosilane (Si-Cl) terminating agents lies in the fact that these bonds are highly reactive towards nucleophiles, more so than their C-Cl counterparts. This will result in more efficient and quantitative termination of the living PSty system.

The feed ratio for the formation of the PSty prepolymer, which were terminated with ACDMS, together with the M_n , M_w and PDI's are summarized in the Table 4.7.

Table 4.7: Feed ratio and molecular weights obtained for PSty prepolymer terminated with ACDMS.

M_w aimed for	Sample Code	PSty added mmol	BuLi mmol	M_w^a (g/mol)	M_n^a (g/mol)	PDI
30 000	Psty_vs_3_30	87.4	0.606	26825	28501	1.06
20 000	PSty_vn_3_20	87.4	0.910	26496	20977	1.26
10 000	PSty_vs_1_10	87.4	1.817	13149	10744	1.22
5000	PSty_vn_2_5	87.4	3.634	7133	5577	1.27

^aDetermined via SEC using PSty standards for calibration, PL Mixed C, ELSD detector

As mentioned before, commercial PDMS prepolymers which contain MeHSiO groups along the backbone in different mole percentages were used. Table 4.8 gives a summary of the different PDMS prepolymers used.

Table 4.8: Summary of the PDMS prepolymers with MeHSiO functional groups.

Sample Code	Viscosity (Pa.s)	M _w (g/mol)	Mole % MeHSiO
HMS-013	5000-8000	45 000 - 60 000	0.5-1
HMS-031	25-35	1900 -2000	3-4
HMS-071	25-35	1900 -2000	6-7
HMS-301	25-35	1900 -2000	25-30

It was of utmost importance to determine the termination efficiency of the PSty prepolymer as this will influence the amount of PDMS prepolymer as well as catalyst that needed to be added for the coupling reaction. Therefore the Varian ^{Unity}Inova, 600 MHz were used to obtain ¹H-NMR spectra to determine the silane or allyl end group termination efficiency.

Figure 4.44 shows a typical ¹H-NMR spectrum obtained for the allyl terminal PSty. The termination efficiency was determined by integrating the peak at a chemical shift of 0.8 ppm (indicated by d in Figure 4.44) indicative of the terminal group, to that of the allyl proton (c in Figure 4.44) indicative of the methyl group protons of the initiator fragment.

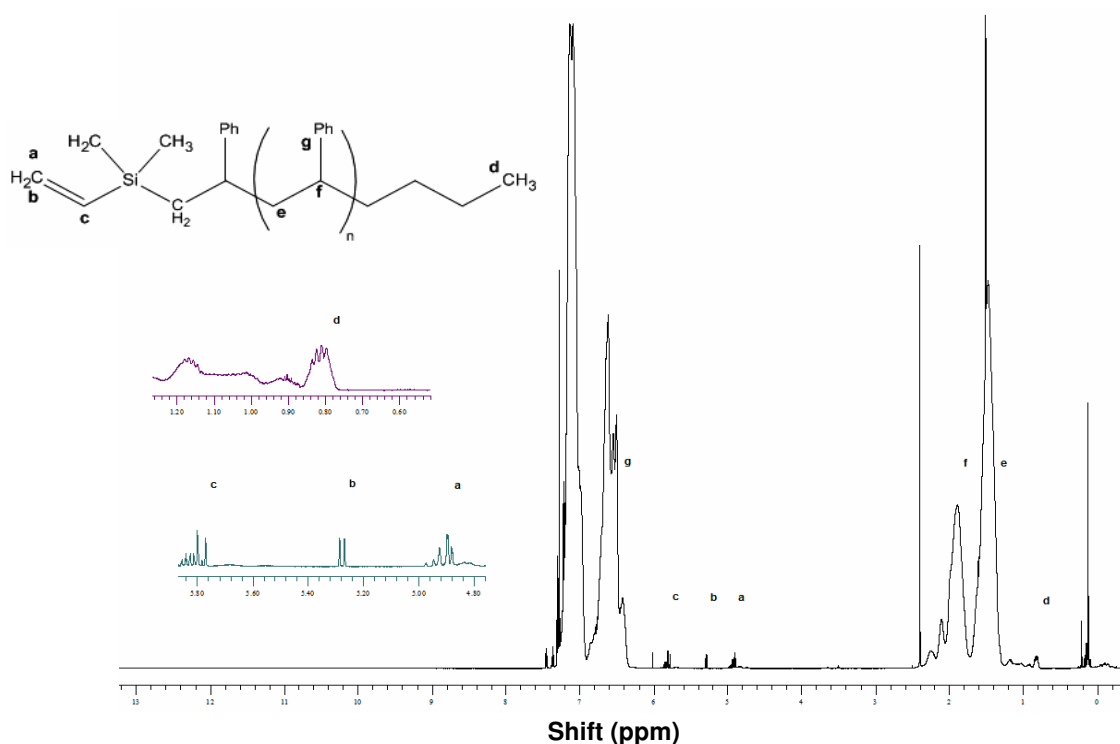
**Figure 4.44:** Typical ¹H-NMR spectrum for PSty with an allyl endgroup.

Table 4.9 shows the termination efficiency of the PSty-allyl functionality which were used for the coupling reaction with the PDMS-silane functionality. These PSty prepolymers were chosen as they showed very narrow PDI's, hence each branch length is more or less the same length, and

exhibited good terminating efficiency. Each of the four different PSty prepolymers with molecular weights in the range of 30 000, 20 000, 10 000 and 5000 were reacted with the four different PDMS prepolymers which contain different MeHSiO mole percentages along the backbone.

In the next section the coupling of the PSty prepolymers to the PDMS prepolymers via a hydrosilylation reaction will be discussed.

Table 4.9: Termination efficiency of PSty allyl functional prepolymers calculated from $^1\text{H-NMR}$.

PSty allyl functionality (-C=CH ₂)		
Code	M _n (g/mol)	Termination efficiency
Psty_vs_3_30	28501	83%
Psty_vn_3_20	20977	93%
Psty_vs_1_10	10744	93%
Psty_vn_2_5	5577	80%

4.2.1.2 Hydrosilylation – PDMS-g-PSty

A hydrosilylation reaction (as explained in **section 3.1.5.2**) was employed for the coupling of the silane functional species (PDMS prepolymer) with allyl functional species (PSty prepolymer). The so-called Karstedt catalyst, which is a divinyl-platinum complex catalyst, has been proven in literature to work well in this type of coupling reactions where one of the products contains a silane group^[18]. As for the PSty-g-PDMS series, removal of the homopolymers proved to be very problematic, laborious and unsuccessful. Hence, chromatographic techniques were required to fully comprehend the nature of the material which formed after the grafting reaction. These chromatographic techniques were employed to obtain information about the molecular mass distribution (MMD) of the polymers as well as the chemical composition distribution (CCD).

The four different polystyrene prepolymers with M_n values close to 30 000, 20 000, 10 000 and 5000 were reacted with the four different commercial polydimethylsiloxanes with different molecular weights and more importantly different mol percentages of the MeHSiO groups. This resulted in 16 different polymers which would give insight into the effect that the polystyrene length has on the grafting reaction, as well as how the viscosity *and* the different mole percentages of the functional group on the PDMS backbone will affect the grafting efficiency.

4.2.1.2.1 SEC results for the grafting reactions – ELSD detector

SEC results using the dual detector system, ELSD and UV detectors, were used to determine the molecular mass distribution. Furthermore, before any chemical composition analysis of the various PDMS-*g*-PSty's, the SEC results already revealed which grafting reactions were unsuccessful.

Figures 4.45 and Figure 4.46 show typical chromatograms which were obtained when the polystyrene prepolymer of a molar mass close to 30 000 were used during the grafting reactions. As one can clearly observe from the chromatogram in Figure 4.45 (HMS 071_30) no graft material formed as the signal is exactly that of the polystyrene prepolymer and the homo-PDMS. This was the case for all of the polymers which were synthesised with this long polystyrene prepolymer.

The SEC results further showed that when the PDMS prepolymer (HMS 013) which only had between 0.5 – 1% functionality groups and had an extremely high viscosity, were used for the grafting reactions, the reactions were unsuccessful regardless of the length of the polystyrene prepolymer. This is shown in Figure 4.47, where the different products have exactly the same ELSD response as that of the PDMS prepolymer. Figure 4.48 illustrates the UV 254 nm response obtained for this series. The UV response for the samples is mapping exactly that of the homo-PSty prepolymer except for HMS 013_10 where a weak UV response can be seen over the elution range. This might be an indication that some graft material formed, but with a very low grafting efficiency.

These results show that the lengths of the polystyrene prepolymers as well as the amount of functional groups present on the PDMS prepolymers backbone will greatly affect the grafting reactions.

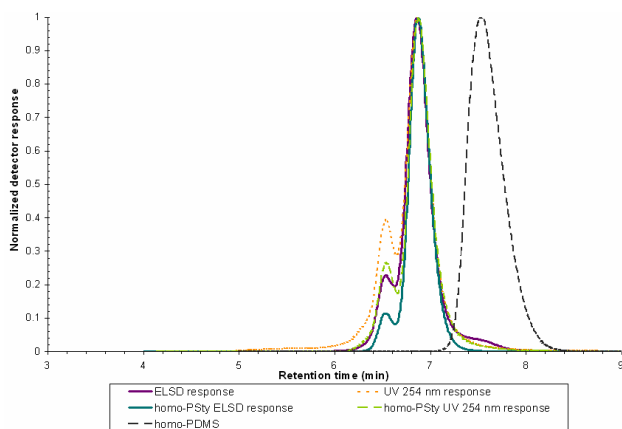


Figure 4.45: SEC chromatogram of HMS_071_30 overlaid with prepolymer PSty_vs_3_30.

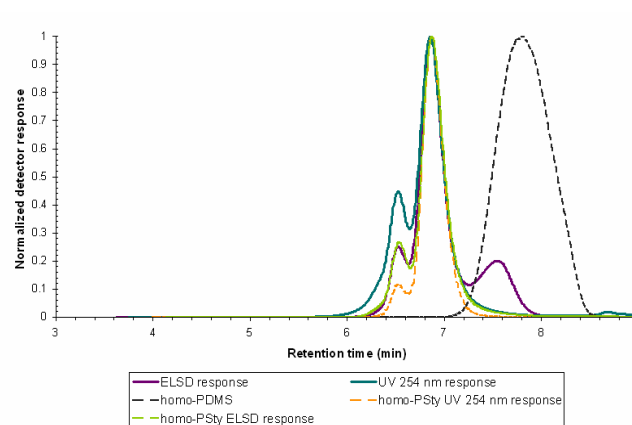


Figure 4.46: SEC chromatogram of HMS_031_30 overlaid with prepolymer PSty_vs_3_30.

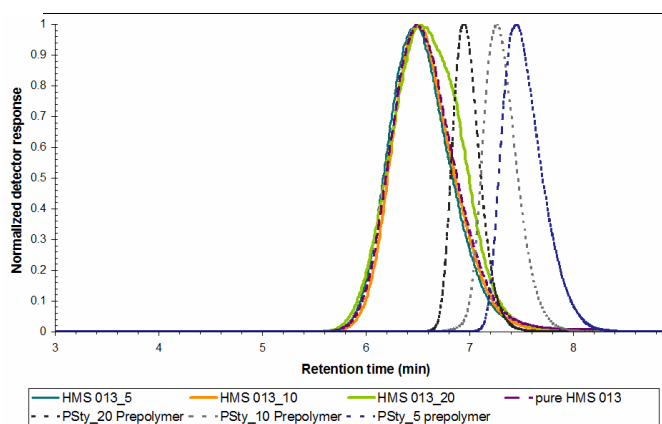


Figure 4.47: SEC chromatograms of HMS_013 series, ELSD response.

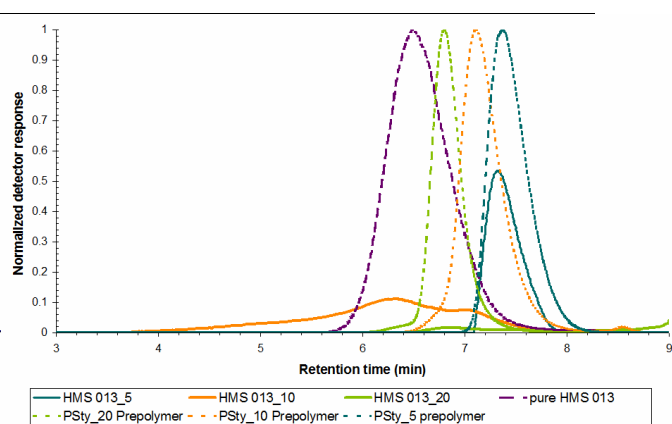


Figure 4.48: SEC chromatograms of HMS_013 series, UV 254 nm response.

Figures 4.48, 4.49 and 4.50 show the chromatograms obtained for the HMS 301 series. These reactions were successful, however the SEC chromatograms show that there is a large amount of homo-polystyrene still present regardless of the length of the polystyrene prepolymer. Two distinct peaks are observed, the first at 4.5-6 min and the latter at 6.5-8 min. The peak at a lower retention time (4.5-6 min), hence higher molar mass, shows a distinct shoulder which becomes more apparent when the polystyrene prepolymer had a lower molar mass.

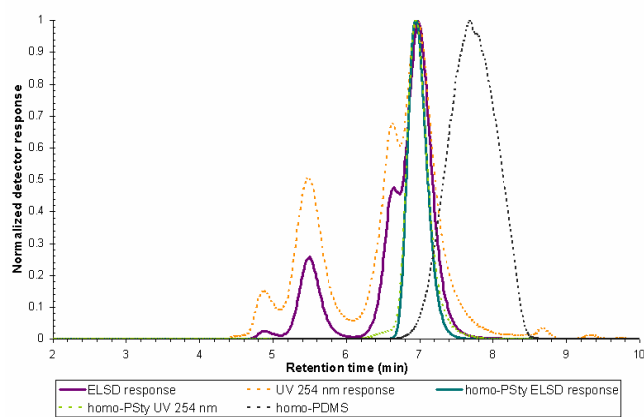


Figure 4.48: SEC chromatogram of HMS 301_20.

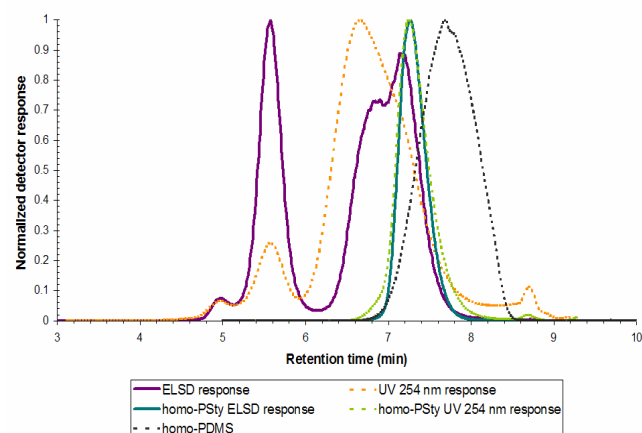


Figure 4.49: SEC chromatogram of HMS 301_10

The molar masses for the three different peaks of each of the polymers of the HMS 301 series were obtained and are summarized in Table 4.10. The last peak of each of the polymers for the HMS 301 are assigned as (a), the middle peak as (b) and the latter, hence lowest retention times, as (c). Little to no PDMS-macromonomer is observed for the high functionality PDMS-macromonomer (HMS 301), indicating that all the polymer chains have been grafted.

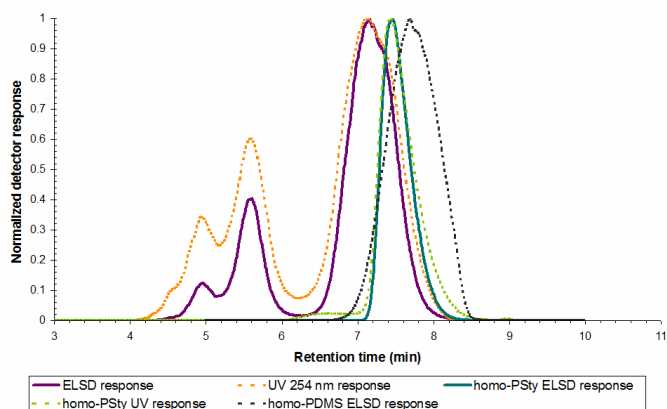


Figure 4.50: SEC chromatogram of HMS 301_5.

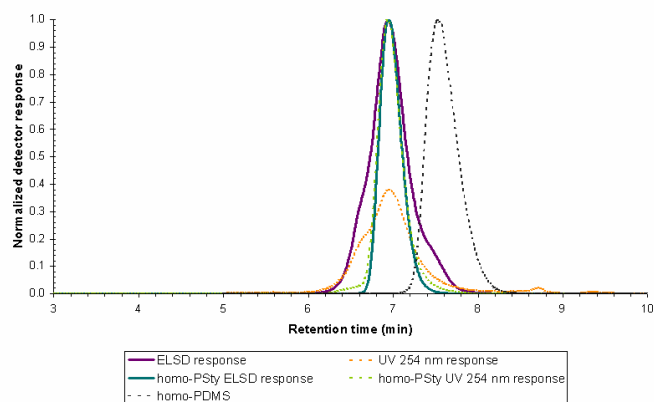


Figure 4.51: SEC chromatogram of HMS 071_20.

The HMS 071 series is illustrated in Figures 4.51, 4.52, and 4.53. The graft products (eluting at 6.5-8.5 min) co-elutes with the PDMS-macromonomer as the graft copolymers have a much lower molar mass than that of the HMS 301 series. Figure 4.51, for HMS 071_20, shows a shoulder at higher retention times (7-8 min). This shoulder can be assigned to unreacted/ungrafted macromonomer-PDMS which is co-eluting with the graft material. This shoulder is evident in the HMS 071_10 and HMS 071_5 series but not as apparent.

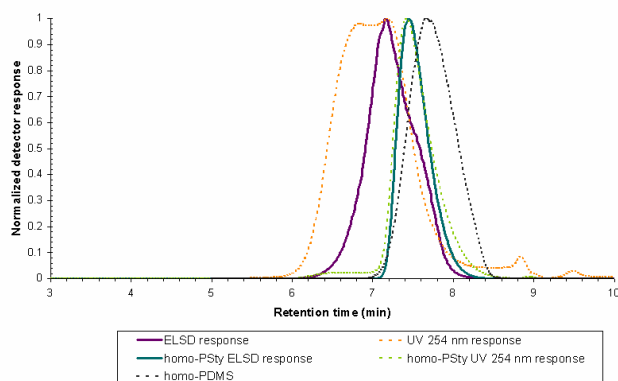


Figure 4.52: SEC chromatogram of HMS 071_10

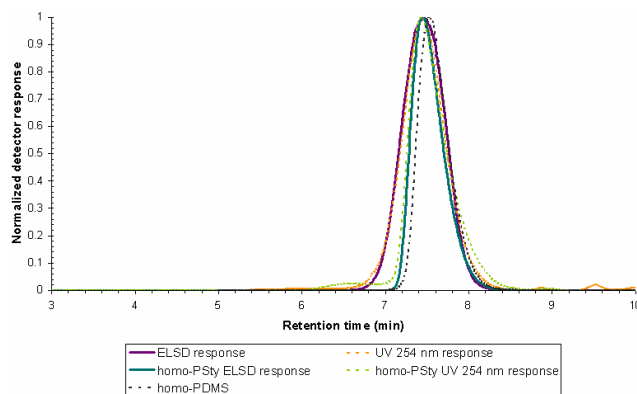


Figure 4.53: SEC chromatogram of HMS 071_5

In Figures 4.54, 4.55 and 4.56 the chromatograms obtained are illustrated for the HMS 031 series. The graft material elutes at lower retention times. It is quite possible that the unreacted prepolymers (PSty and PDMS-macromonomer) are co-eluting with the graft material.

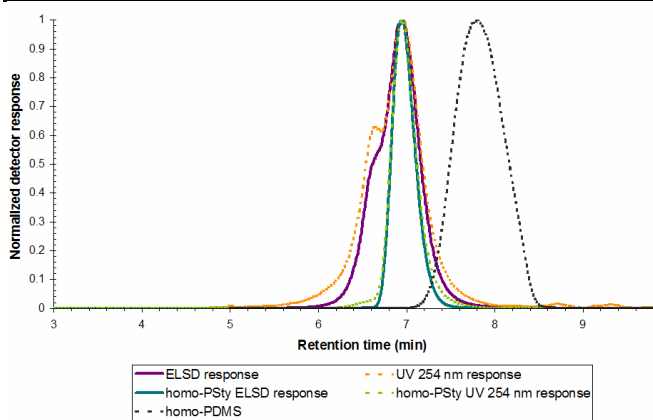


Figure 4.54: SEC chromatogram of HMS
031_20.

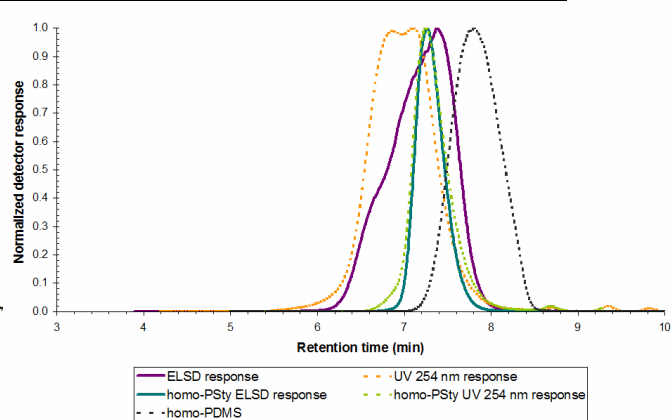


Figure 4.55: SEC chromatogram of HMS
031_10.

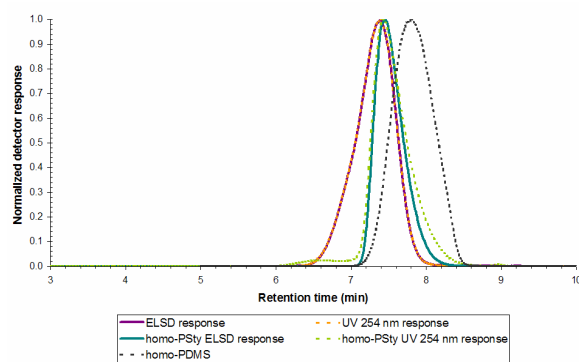


Figure 4.56: SEC chromatogram of HMS 031_5.

The SEC results were obtained by employing an ELSD detector. The M_n , M_w and PDI's values are summarized in Table 4.10:

Table 4.10: Summary of M_n , M_w , and PDI's values obtained for the coupling reaction.

Series	Code	M_n (g/mol)	M_w (g/mol)	PDI
20 000	HMS 301_20 (a)	21432	27159	1.23
	HMS 301_20 (b)	450790	490430	1.08
	HMS 301_20 (c)	1730000	1765900	1.02
	HMS 071_20	18020	25600	1.42
	HMS 031_20	19650	29700	1.51
10 000	HMS 301_10 (a)	16431	23773	1.45
	HMS 301_10 (b)	391720	422410	1.09
	HMS 301_10 (c)	1499900	1522000	1.01
	HMS 071_10	10110	15400	1.52
	HMS 031_10	7832	13540	1.73
50000	HMS 301_5 (a)	11279	15878	1.41
	HMS 301_5 (b)	383350	417820	1.10
	HMS 301_5 (c)	1613500	1655000	1.03
	HMS 071_5	6796	8828	1.23
	HMS 031_5	3504	5521	1.58

From the SEC results it was already very apparent that the products obtained after hydrosilylation were distributed in their molecular weight. To fully comprehend the nature of the material LCCC were employed yet again. The critical point for PSty was employed as with the PSty-*g*-PDMS series.

4.2.1.2.2 HPLC results of PDMS-*g*-PSty

LCCC will separate the products obtained into its different chemical heterogeneities as observed in **section 4.1.1**. The mol percentages of the MeHSiO groups along the backbone of the PDMS prepolymer are quite low, making the grafting reaction even more difficult besides other facts that have been mentioned elsewhere (incompatibility, diffusion and viscosity effects etc). It is therefore expected that the material obtained will be chemically heterogeneously distributed *but* that the graft material will exhibit narrow PDI's as controlled synthetic techniques were employed during the grafting reaction. Furthermore, greater success for the HMS 301 prepolymers are expected as these PDMS prepolymers contains the highest amount of functional groups along the backbone.

Figure 4.57 is the chromatogram obtained for the HMS 301_10 polymer and Figure 4.58 shows a summary of the polymers from the HMS 301 series. The chemical heterogeneous nature of the polymer is clearly elucidated. Three distinct peaks are observed for HMS 301_5, HMS 301_10 and HMS301_20. The first peak is that of the graft material. This peak is not observed at all for HMS

301_30 where the polystyrene prepolymer had a M_n value close to 30 000 g/mol. This result concurs with the SEC result obtained for this polymer. The chromatogram illustrated in Figure 4.58 clearly shows how the branching length of the polystyrene prepolymer affected the grafting efficiency.

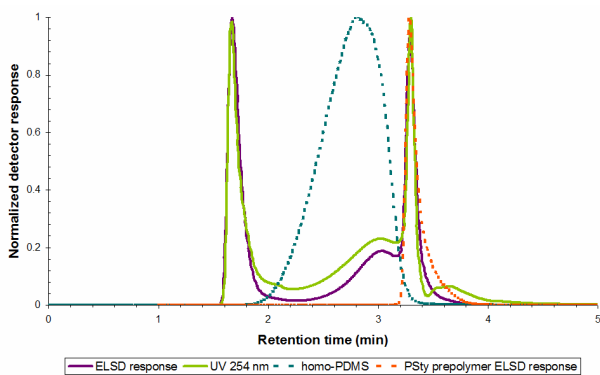


Figure 4.57: Chromatogram obtained for HMS 301_10.

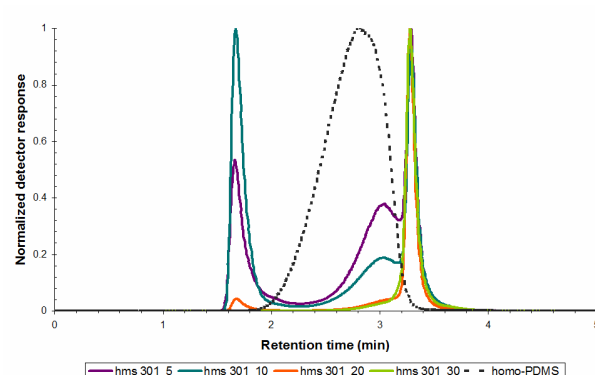


Figure 4.58: Chromatogram obtained for HMS 301 series, ELSD response.

As was expected, the grafting efficiency for the HMS 071 series (which has lower functional groups present on the backbone) was less successful in comparison to the HMS 301 series.

The results for the HMS 031 series are shown in Figure 4.61 and Figure 4.62. Similar trends as for the HMS 301 and HMS 071 are observed. Although, a very surprisingly result is that of the HMS 031_5 polymer. This polymer does not show any homo-contaminants, only a very narrow dispersed graft material.

For the HMS 301, 071 and 031 there is a UV response at 254 nm (indicative for styrene molecules) showing that there is at least some PSty grafted (see retention times between 2-3 min). This is most likely similar grafts which contain a high amount of PSty, hence high PSty grafts.

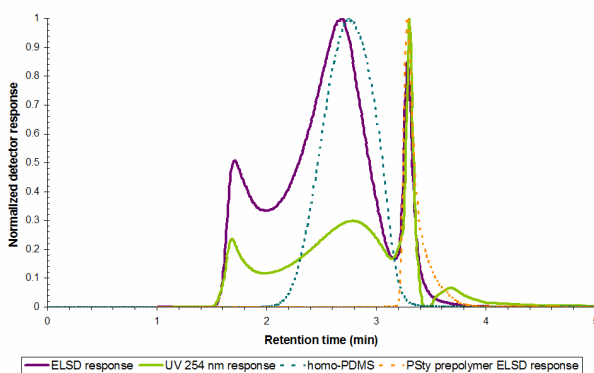


Figure 4.59: Chromatogram obtained for HMS 071_10.

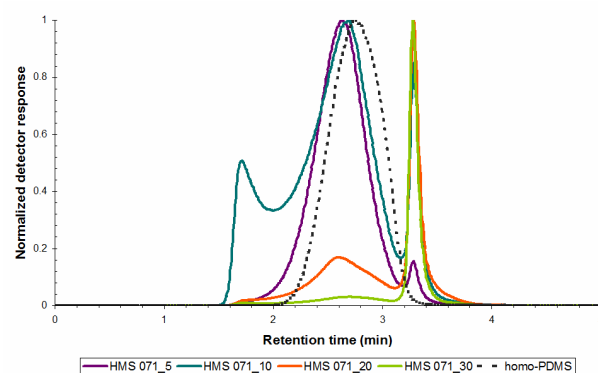


Figure 4.60: Chromatogram obtained for HMS 071 series, ELSD response.

The LCCC chromatograms gave great insight to what affects the grafting efficiency of the reactions. It became very apparent that the chain length of the polystyrene prepolymer plays a significant role during the grafting reaction as none of the reactions worked when the Psty_vs_3_30 prepolymer was used.

The grafting reactions for the HMS 013 series failed which can be ascribed to the high viscosity of the PDMS prepolymers as well as the low mol percentage functional groups which are present on the backbone of this prepolymer.

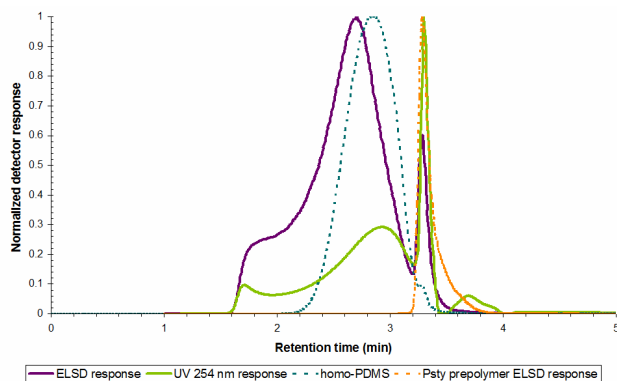


Figure 4.61: Chromatogram obtained for HMS 031_10.

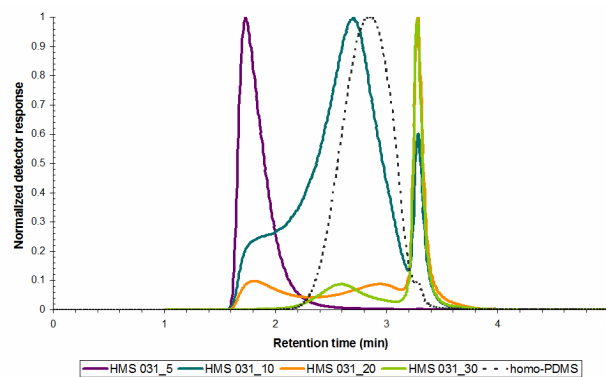


Figure 4.62: Chromatogram obtained for HMS 031 series, ELSD response.

The influence of the branch length/molecular weight of the PSty prepolymer and the influence of the mol% of functional groups on the backbone of the PDMS-macromonomer on the grafting efficiency are summarized in the Table 4.11:

Table 4.11: Influence of molecular weight of PSty prepolymer and functional groups of PDMS prepolymer on the grafting efficiency.

	PDMS-macromonomer		PSty prepolymers (M_n)			
	Functional groups	Viscosity (Pa.s)	~30 000	~20 000	~10 000	~5000
HMS 301	25-30	25-35				
HMS 071	6-7	25-35				
HMS 031	3-4	25-35				
HMS 013	0.5-1	5000-8000				

The orange blocks refer to the grafting reactions that didn't work *or* gave a very low grafting efficiency and the purple blocks to the successful grafting reactions. From this table a clear trend can be observed: the grafting efficiency only works provided that the PSty prepolymer has sufficient low enough molecular weights and if the functional groups on the PDMS-backbone are sufficiently high enough (together with a low viscosity). Furthermore, from these results it is clear that chain mobility and diffusion effects greatly influence the grafting efficiency.

4.2.1.2.3 LCCC-FTIR and two-dimensional chromatography results

The chemigrams for HMS 071_20 and HMS 071_10 are shown in Figure 4.63 and Figure 4.64. In Figure 4.63, that of HMS 071_20, the ratio of PDMS/PSty is the greatest at lower retention volumes. This confirms the formation of the graft copolymer. As was illustrated in the one-dimensional results, the polystyrene prepolymer with a M_n of close to 10 000 g/mol gave best grafting efficiencies.

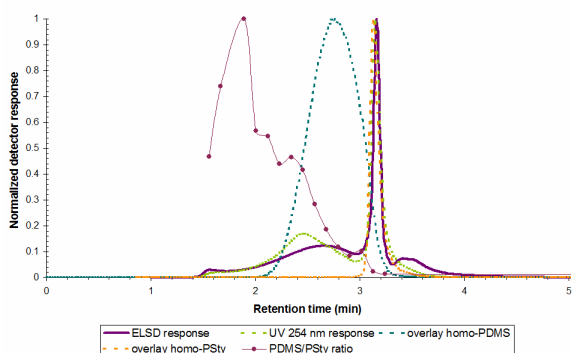


Figure 4.63: Ratio of PDMS/PSty overlaid with LCCC chromatogram: HMS 071_20.

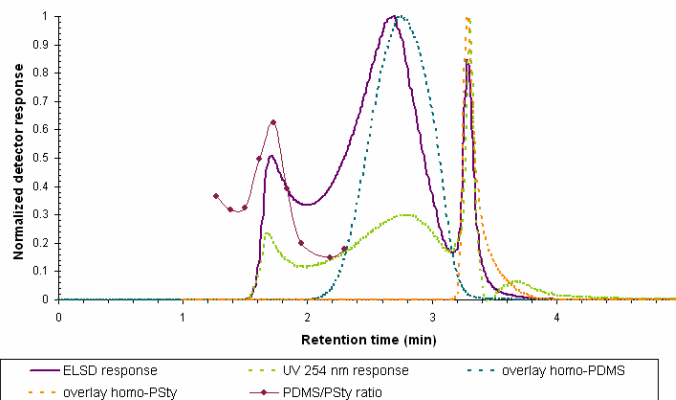


Figure 4.64: Ratio of PDMS/PSty overlaid with LCCC chromatogram: HMS 071_10.

The 2-D chromatogram for HMS 071_5 is illustrated in Figure 4.65. Only three chemically different products are observed. Along the ordinate the CCD distribution in the first dimension can be seen. Product 3 is that of homo-PSty, as PSty elutes under critical conditions. Products 1 and 2 are that of the graft material and homo-macromonomer respectively. The integration results for the products are summarized in Table 4.12.

Differently to the PSty-*g*-PDMS series which was synthesised via a conventional FRP, the graft material is not as broadly distributed on the ordinate, implying that the graft material is more homogeneous, thus branches are more homogeneously distributed along the backbone. This is not surprising as controlled techniques were used for the synthesis of PDMS-*g*-PSty. Although not as apparent as for the PSty-*g*-PDMS series, it seems that this grafting reaction also leads to the formation of a one-arm star polymer. Product 2 also contains PSty inclusions. This can be observed from one-dimensional results where a UV response at 254 nm is present over the whole elution range.

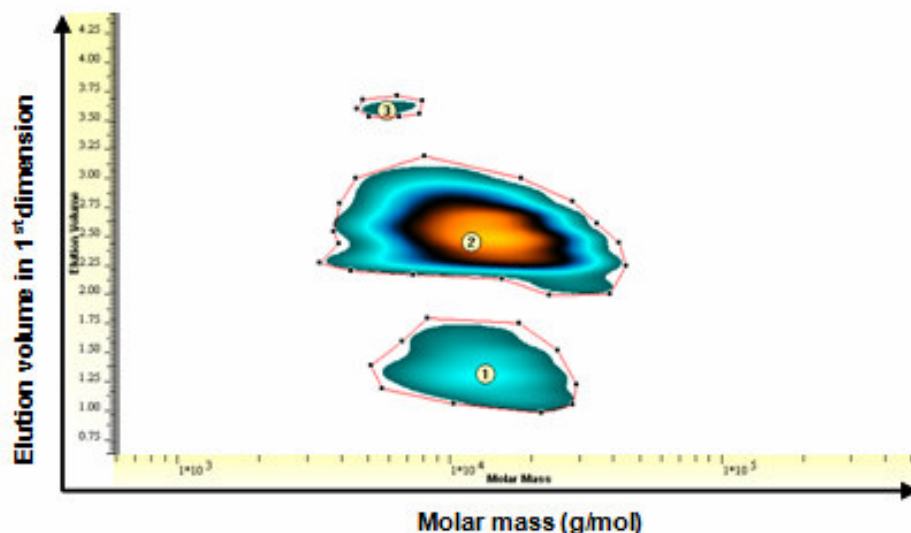


Figure 4.65: 2-D chromatogram for HMS 071_5.

Table 4.12: Molecular weights obtained for the different products for HMS 071_5.

No	Area %	Volume %	M_n (g/mol)	M_w (g/mol)	PDI
1	3.814	13.81	11354	13192	1.16
2	7.744	63.26	10374	13571	1.31
3	0.299	0.749	5665	5775	1.019

In the next section the grafting reaction of the reverse of the functional groups present on the polystyrene prepolymer (silane) and on the PDMS-macromonomer (vinyl) will be illustrated and discussed.

The one-dimensional together with the two-dimensional results shows that the grafting of these polymers does once again take place, but the efficiency is dependent greatly on the branch length of the PSty prepolymer, the functional groups present on the macromonomer as well as diffusion effects that are greatly influenced by the viscosity of the macromonomer. From these results it was determined which variations, such as branching length of the prepolymer, diffusion affects etc. play a significant role in the grafting efficiency. With this knowledge it is possible to optimize the grafting efficiency of PDMS-*g*-PSty as this controlled route is very promising as it allows for a homogeneous graft copolymer with no side reactions which can lead to product failure.

4.2.2.1 Synthesis of PSty prepolymer – Silane functionality

As was previously mentioned in **section 4.2.1.1** PSty prepolymers with varying molecular weights were synthesised by means of anionic polymerization.

The feed ratio for the formation of the PSty prepolymer, which was terminated with CDMS, together with the M_n , M_w and PDI's are summarized in the Table 4.13.

Table 4.13: Feed ratio and molecular weights obtained for PSty prepolymer terminated with CDMS.

M_w aimed for	Sample Code	PSty added (mmol)	BuLi (mmol)	M_w^a (g/mol)	M_n^a (g/mol)	PDI
20 000	PSty_hn_2_20	87.4	0.910	24424	22345	1.09
10 000	PSty_hn_2_10	87.4	1.817	12656	10915	1.15
5000	PSty_hn_1_5	87.4	3.634	7657	5884	1.30

^aDetermined via SEC using PSty standards for calibration, PL Mixed C, ELSD detector

The M_n , M_w , PDI and mole% of functional groups of the commercial PDMS macromonomer which contain vinylmethylsiloxane groups along the backbone is summarized in Table 4.14. As the M_n and M_w values were not provided these were determined via SEC using PSty standards.

Table 4.14: Summary of information of the PDMS prepolymers with vinylmethylsiloxane groups.

Sample Code	Viscosity	M_n (g/mol)	M_w (g/mol)	PDI	Mole % Vinylmethylsiloxane
VDT 131	800-1200	20606	34113	1.66	0.8-1.2
VDT 731	800-1200	22284	35378	1.59	7.0-8.0
VDT 954	300 000-500 000	88798	199130	2.24	11.0-13.0

As can be seen from Table 4.14, these PDMS-macromonomers have a very high viscosity with a low percentage of functional groups present along the backbone. This will all contribute to the difficulty of the grafting reaction.

The termination efficiency of the PSty prepolymers was determined from $^1\text{H-NMR}$ spectra (see Figure 4.66) by integrating the peak at a chemical shift of 0.18 ppm (indicated by b) indicative of the terminal group, to that of the methyl proton at a chemical shift of 0.8 (indicated by f).

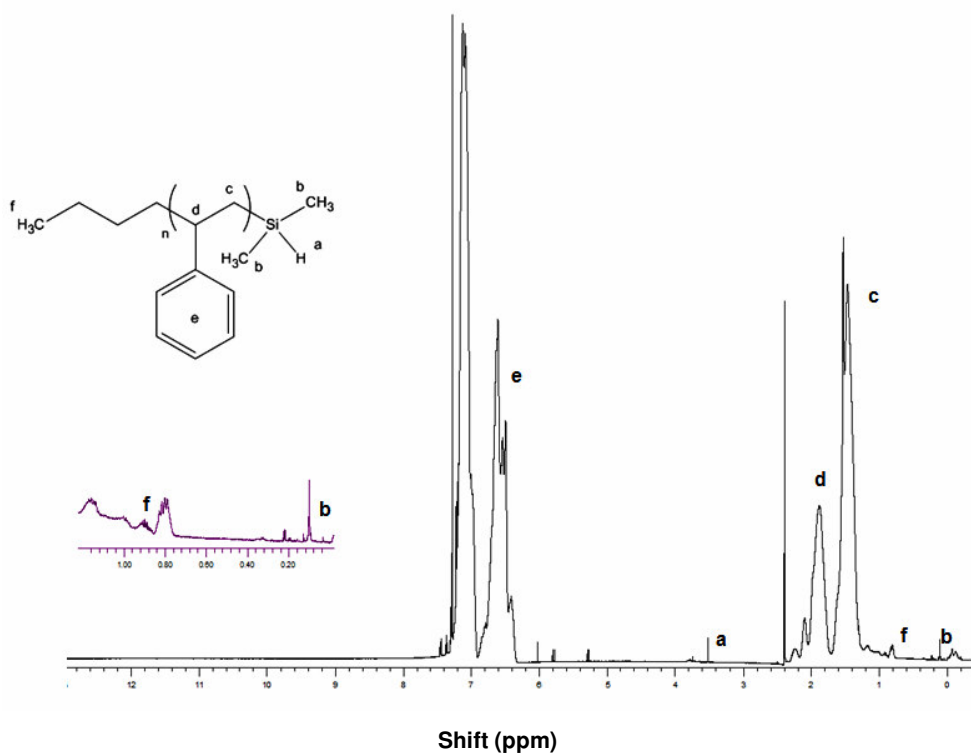


Figure 4.66: Typical ^1H -NMR spectrum for PSty with a silane endgroup.

High termination efficiencies were obtained (see Table 4.17) for the PSty-prepolymers. Each of these PSty prepolymers was reacted with the various commercial PDMS-macromonomers as summarized in Table 4.14. In the next section the results of the coupling of the prepolymers via a hydrosilylation reaction will be discussed.

Table 4.15: Termination efficiency of PSty silane functional end-groups

Code	PSty-silane functionality (-Si-H)	
	M_n (g/mol)	Termination efficiency
Psty_hn_2_20	22345	88%
Psty_hn_2_10	10915	98%
Psty_hn_1_5	5884	96%

4.2.2.2 Hydrosilylation – PDMS-g-PSty

4.2.2.2.1 LCCC results

The coupling of the prepolymers (hence polystyrene with a silane functionality and PDMS macromonomer with a vinyl functionality) proved to be challenging. At this point it should be stated that the grafting efficiencies were very low for the VDT 954, 731 and 131 series and therefore the SEC chromatograms together with summarized values were omitted as it was extremely difficult to integrate the true graft peak. The LCCC chromatograms of the VDT 954 series are shown in Figures 4.67-4.69.

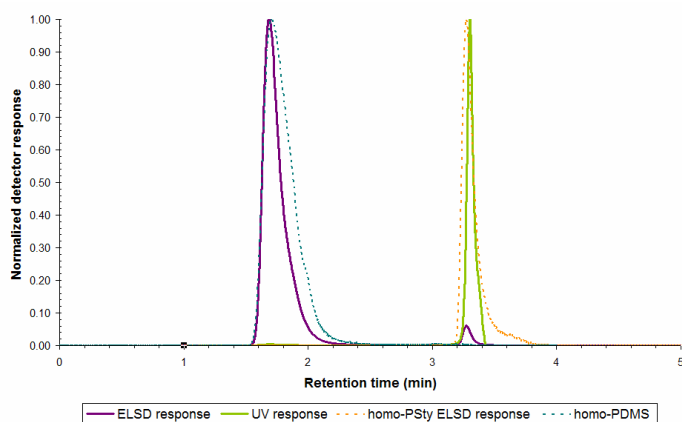


Figure 4.67: LCCC chromatogram of VDT 954_20.

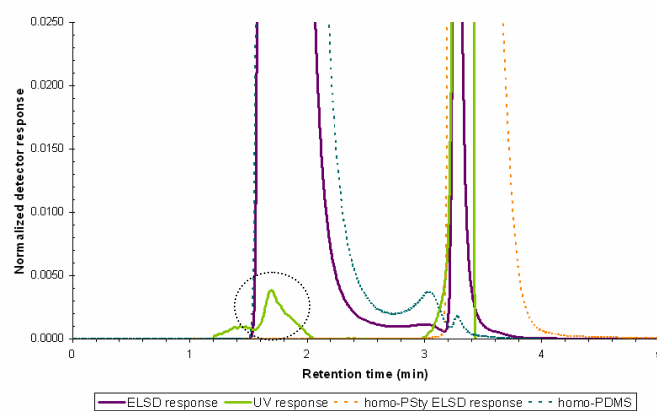


Figure 4.68: Magnified LCCC chromatogram of VDT 954_20.

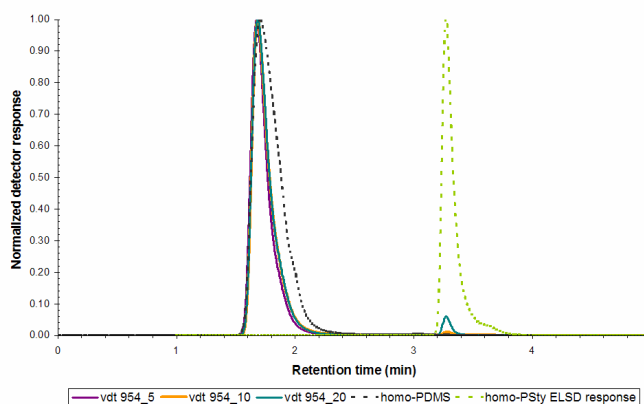


Figure 4.69: LCCC chromatogram of VDT 954 series.

At first glance of Figure 4.67 it seems that the first peak, at lower retention times, does not exhibit any UV response at 254 nm. Figure 4.68 is the magnified view of Figure 4.67. From this figure a UV response is detectable at lower retention times (hence not only for residual homo-PSty

prepolymer). One can only conclude from these results that grafting did take place, but the effectiveness of these grafting reactions is extremely low for the VDT 954 series. This is most likely due to the fact that chain mobility is severely compromised as this PDMS-prepolymer had an extremely high viscosity (see Table 4.14). The high molecular mass also results in the vinyl functional group being less accessible as the grafting reaction takes place in solution. The VDT 731 and VDT 131 gave similar results (see Figure 4.70 -74).

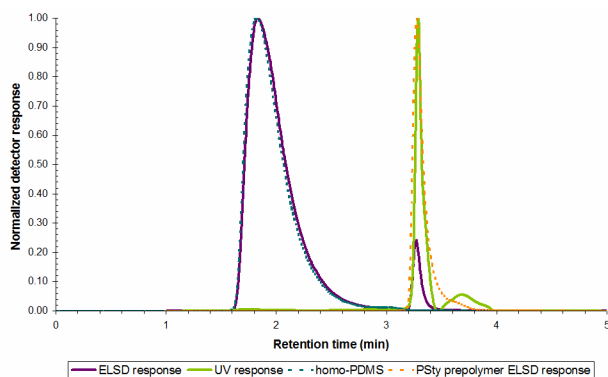


Figure 4.70: LCCC chromatogram of VDT 731_20.

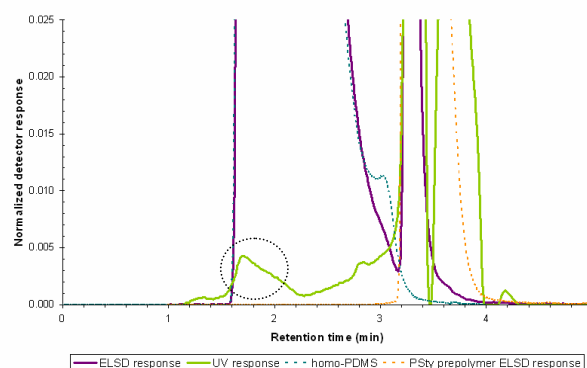


Figure 4.71: Magnified LCCC chromatogram of VDT 731_20.

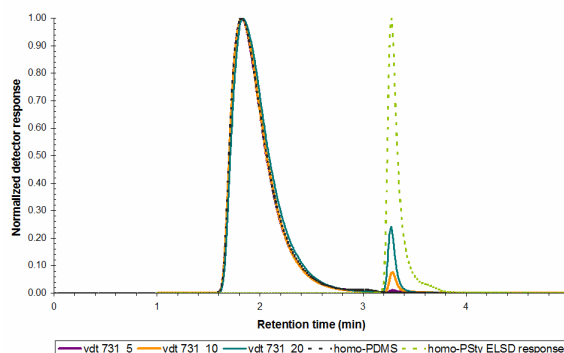


Figure 4.72: LCCC chromatogram of VDT 731 series.

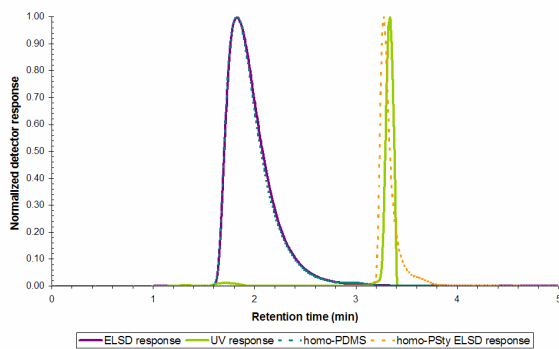


Figure 4.73: LCCC chromatogram of VDT 131_10

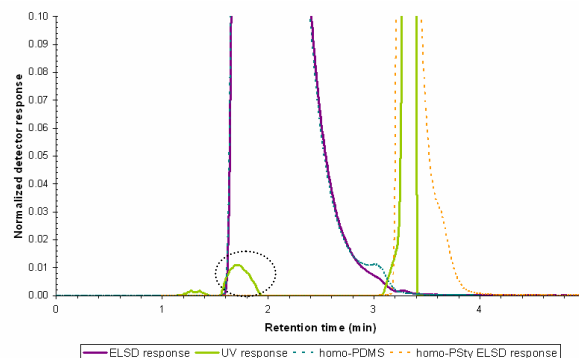


Figure 4.74: Magnified LCCC chromatogram of VDT 131_10.

Unlike for the PDMS-*g*-PSty series where the PSty prepolymer had the vinyl functional group and the PDMS macromonomer had the silane functional group (hence reversal of functional groups on the prepolymers), very low grafting efficiencies were obtained for this series. The low grafting effectiveness is not likely caused by the reversal of functional groups but more likely due to hindered chain mobility as the viscosity of the PDMS-macromonomers were extremely high. Furthermore, the very low percentage functional groups present on the backbone also contributed to the low grafting efficiencies.

4.3 Grafting from – PDMS-*g*-PSty

PDMS-*g*-PSty was also synthesised via the grafting from approach. What this entails is the synthesis of a PDMS macroinitiator from which styrene branches can be grown with a desired molecular weight (hence branch length). This method will also give a control over the structure of the graft material, i.e. branches will be homogeneously distributed and will have the same molecular weight (branch length).

4.3.1 Synthesis of PDMS macroinitiator

The PDMS macroinitiators were synthesised by converting the silane functional groups on the macromonomer-PDMS backbone to bromoisobutyrate functional groups. This is achieved by means of a hydrosilylation reaction where a Pt catalyst (Karstedt catalyst) is used. These types of reactions have been well documented^[18, 19] and have shown to give great efficiencies.

In this project the HMS commercial polymers were used to form the desired functional macroinitiators. During the hydrosilylation reaction, however, the HMS 301 and HMS 071 series crosslinked. This crosslinking which occurred is not well understood. The HMS 031 formed the desired bromoisobutyrate functional group.

¹H-NMR was used to monitor the formation of the allyl-2-bromo-2-methyl propionate molecules. Figure 4.75 is the proton spectra for a typical bromoisobutyrate PDMS macroinitiator (Figure 4.75 (a)) and the silane functional PDMS before hydrosilylation (Figure 4.75 (b)). One clearly sees a singlet at 2.02 ppm. This peak is representative of the methyl group protons (a in Figure 4.75(a)). Furthermore, one notes the peaks at 0.8 ppm (d) and 1.3 ppm (e) indicative of the new bromoisobutyrate functional group. The silane peak at 4.7 ppm (see Figure 4.75(b)) is still present in ¹H-NMR spectrum of bromoisobutyrate PDMS, implying that not all of the silane functional groups on the PDMS-macromonomer functionalised. Integration of this shift (at 4.7 ppm) to that of the methyl protons at 2.02 ppm, yielded the functionalisation efficiency.

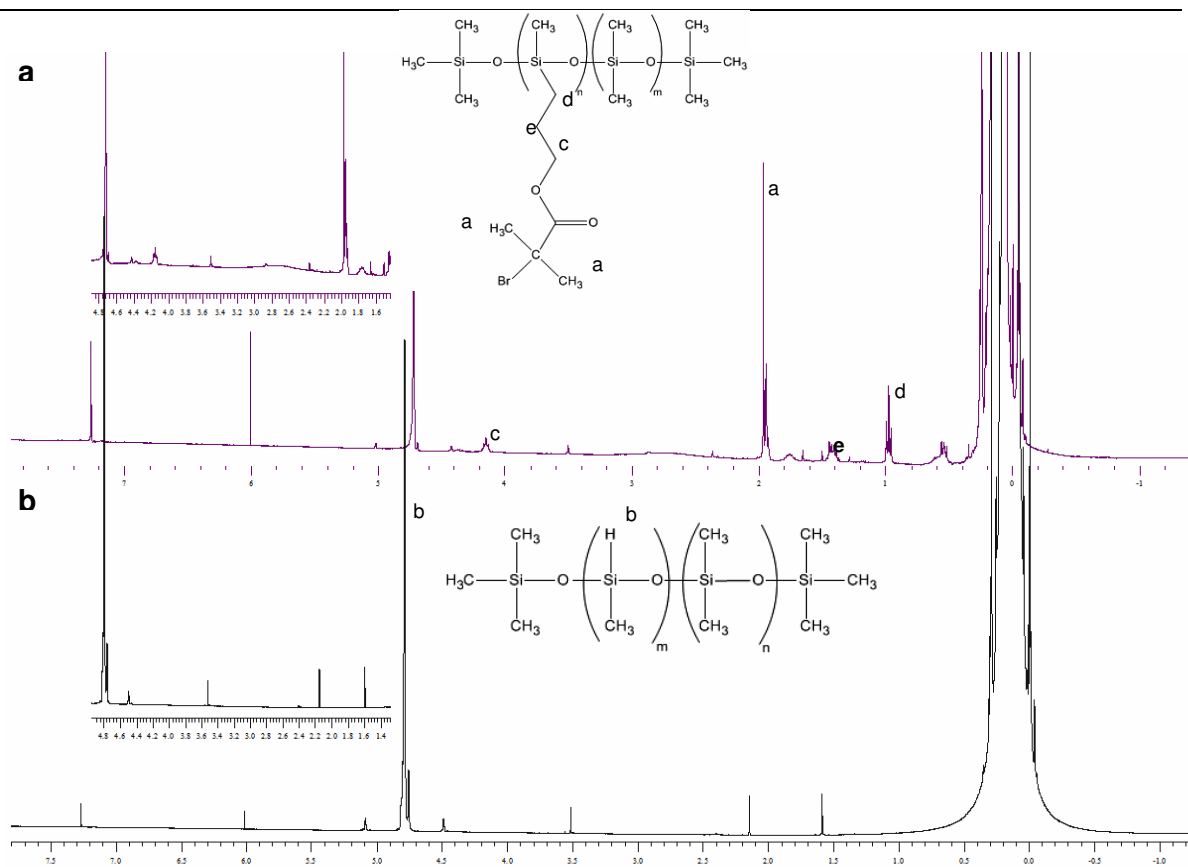


Figure 4.75 (a), (b): $^1\text{H-NMR}$ spectra obtained for bromoisbutyrate PDMS macroinitiator for the ATRP of styrene and silane functional PDMS before hydrosilylation respectively.

The results are summarized in Table 4.16. Termination efficiencies between 50-70% were obtained, which is not very high for these types of reactions. The three different macroinitiators were synthesised with styrene via ATRP to give branch chain lengths of 5000, 10 000, and 20 000. This was achieved by using a suitable catalyst-ligand system (see **section 3.1.6**).

Table 4.16: Termination efficiency of PSty allyl functional prepolymers calculated from $^1\text{H-NMR}$.

Code	M_n (g/mol)	Functionality (MeHSiO) before hydrosilylation	Functionality after hydrosilylation ($\text{CH}_2\text{COOC}(\text{CH}_3)_2\text{Br}$)	PSty aimed (ATRP reaction)
HMS 031_1B	1900 -2000	3–4 %	52 %	5 000
HMS 031_2B	1900 -2000	3–4%	56%	10 000
HMS 031_3B	1900 -2000	3–4%	69%	20 000

4.3.2 ATRP – PDMS-g-PSty

The grafting reactions were carried out as explained in **section 3.1.6.1**. As mentioned elsewhere, three different polystyrene lengths were aimed for; 20 000, 10 000 and 5 000 g/mol. The SEC chromatograms obtained for these polymers ATRP 1, ATRP 2 and ATRP 3 are illustrated in Figure 4.76. It is apparent that there is a very strong ELSD response, but that the UV response at 254 nm is very weak. This indicates that the grafting efficiency is low, as the UV response at 254 nm will exhibit a strong response if there is a large amount of PSty molecules present, which is not the case.

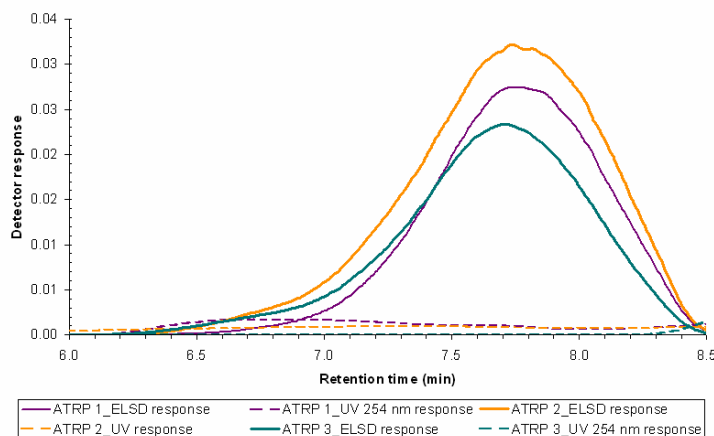


Figure 4.76: SEC chromatogram of PDMS-g-PSty

The LCCC chromatograms for this series are illustrated in Figure 4.77. None of the samples, hence ATRP 1 (aimed for PSty with a M_n of 5000), ATRP 2 (aimed for PSty with a M_n of 10 000) or ATRP 3 (aimed for PSty with a M_n of 20 000) show any significant UV response at 254 nm and have therefore been omitted from the LCCC chromatogram. The weak UV response at 254 nm implies that there is little formation of the graft copolymer. ATRP 2 and ATRP 3 do exhibit a shoulder at lower retention times which is not exhibited by the macroinitiator. Essentially this implies that some graft material did form, but the efficiency of the grafting reaction was very low.

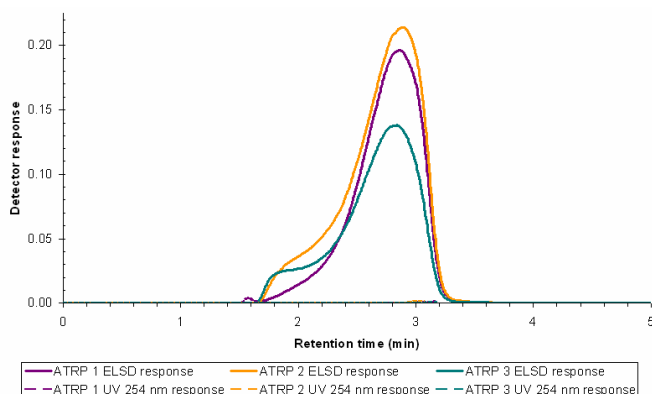


Figure 4.77: LCCC-chromatograms of PDMS-g-PSty

As the crosslinking during hydrosilylation of the highly functional macroinitiator is not well understood, this leaves open the possibility for further investigation and optimisation as ATRP has shown to form graft copolymers with high efficiencies which have a controlled structure. In addition results indicate that the conditions used in the ATRP synthesis have not been optimized since results show a partial success in forming the multi-functional PDMS macroinitiator.

This concludes chapter 4. Chapter 5 will give a summary of the conclusions as well as recommendation for further work.

4.4 References

- [1] S. G. Roos, B. Schmitt, A. H. E. Muller, *Polymer Preprints (ACS, Div. Polym. Chem.)* **40**, 984 **1999**.
- [2] P. Harald, A. Martina, R. Frank, B. Stefan, *Macromolecular Rapid Communications* **26**, 438 **2005**.
- [3] C. L. Elkins, T. E. Long, *Macromolecules* **37**, 6657 **2004**.
- [4] H. Shinoda, K. Matyjaszewski, L. Okrasa, M. Mierzwa, T. Pakula, *Macromolecules* **36**, 4772 **2003**.
- [5] K. Ito, S. Kawaguchi, *Advances in Polymer Science* **142**, 130 **1999**.
- [6] S. C. Hong, D. Neugebauer, Y. Inoue, J.-F. Lutz, K. Matyjaszewski, *Macromolecules* **36**, 27 **2002**.
- [7] F. Meijs, E. Rizzardo, *Journal of Molecular Science, Reviews in Macromolecular Chemistry and Physics* **C30 (3&4)**, 305 **1990**.
- [8] J. G. Zilliox, J. E. L. Roovers, S. Bywater, *Macromolecules* **8**, 573 **1975**.
- [9] D. Berek, *Progress in Polymer Science* **25**, 873 **2000**.
- [10] T. Macko, D. Hunkeler, *Advances in Polymer Science* **163**, 61 **2003**.
- [11] S. J. Kok, N. C. Arentsen, P. J. C. H. Cools, T. Hankemeier, P. J. Schoenmakers, *Journal of Chromatography A* **948**, 257 **2002**.
- [12] H. Shinoda, P. J. Miller, K. Matyjaszewski, *Macromolecules* **34**, 3186 **2001**.
- [13] S. G. Roos, A. H. E. Muller, K. Matyjaszewski, *American Chemical Society Symposium Series* **768**, 361 **2000**.
- [14] S. J. Kok, C. A. Wold, T. Hankemeier, P. J. Schoenmakers, *Journal of Chromatography A* **1017**, 83 **2003**.
- [15] J. C. Saam, D. J. Gordon, S. Lindsey, *Macromolecules* **3**, 1 **1970**.
- [16] S. D. Smith, J. M. DeSimone, H. Huang, G. York, D. W. Dwight, G. L. Wilkes, J. E. McGrath, *Macromolecules* **25**, 2575 **1992**.
- [17] M. Lazzari, G. Liu, S. Lecommandoux, *Block Copolymers in Nanoscience* (Wiley-VCH verlag GmbH & Co. KGaA, 2006), pp. 428.
- [18] L. N. Lewis, J. Stein, Y. Gao, R. E. Colborn, G. Hutchins, *Platinum Metals Reviews* **41**, 66 **1997**.
- [19] J. Huang, Z. Liu, X. Liu, C. He, S. Y. Chow, J. Pan, *Langmuir* **21**, 699 **2004**.

Chapter 5

Conclusions and Recommendations

*I may not have gone where I intended to go, but I think I have ended up where I intended to be –
Douglas Adams*

5.1 Conclusions

The summarized conclusions of this research study are as follow:

- PSty-*g*-PDMS was successfully synthesised by means of a conventional FRP using the grafting through technique.
 - 1.1 The synthesis of a series of PSty-*g*-PDMS materials, by means of varying the PDMS macromonomer feed ratio as well as graft lengths gave great insight to the significant role that viscosity and chain mobility of the macromonomer plays in the formation of the graft material using the grafting through technique.
 - 1.2 It was determined that the short series, hence the macromonomer with the lowest viscosity and branching length, showed the greatest chemical uniformity with the least amount of unreacted macromonomer and formation of homo-polymers.
- PDMS-*g*-PSty were successfully synthesised using two grafting approaches. The grafting onto approach was successful only if the PDMS macromonomer had sufficient functional groups and adequate chain mobility (hence a low viscosity).
 - 2.1 Polystyrene prepolymers with either an allyl or silane functional group were successfully synthesised by means of anionic polymerization. The grafting onto of these polystyrene prepolymers was more successful with the vinyl functional PSty prepolymer than the silane functional prepolymer mostly due to the respective functionality and molar mass of the respective functional PDMS prepolymers. It was shown that if the prepolymers had sufficiently low molecular weights (hence sufficient branch length) and the PDMS macromonomer had a sufficient amount of functional groups on the backbone from which the polystyrene prepolymer can be graft onto, this approach to form the graft copolymers (PDMS-*g*-PSty) can be used.
 - 2.2 The grafting from approach, using a PDMS macroinitiator and ATRP, showed limited success. This is most probably due to the lack of optimization of the ATRP reaction since results show at least partial successful formation of the bromo-isobutyrate PDMS macroinitiator.
- Chromatographic techniques for the analysis of the complex material were extremely successful and gave great insight to the CCD and MMD of the graft copolymer.

-
- 3.1 LCCC at the critical point of PSty, for the evaluation of the CCD of the graft copolymer, was successfully developed. This method provides a very quick chromatographic method for the analysis of the grafting reaction.
 - 3.2 Two-dimensional chromatography, where LCCC is used in the first dimension of separation and SEC as the second dimension of separation was also successfully developed and used for a comprehensive understanding of the CCD and MMD. The two-dimensional analysis revealed information which was not evident in the one dimensional results. The short series showed no apparent formation of homo-PDMS or unreacted macromonomer, whilst the medium and long series had an array of species formed. Not only was the graft material evident, but the formation of a one-arm star polymer as well as PDMS homo-macromonomer were also made apparent.
 - 3.3 The coupling of chromatographic technique offline to FTIR and TEM was successful and proved to be very insightful. A greater understanding of the microstructure of the graft copolymer was derived from the LC-FTIR results whilst the LC-TEM results gave insight to the morphological nature of the graft material. It is the latter technique which was extremely useful as this technique avoids the difficult homopolymer extraction and sample preparation.

5.2 Recommendations

It should be noted that one of the main aims of the study was to apply positron annihilation lifetime spectroscopy (PALS) to study the free volume properties of the graft copolymers synthesised. However, due to several problems with the instrument, the measurements could not be performed. It is recommended that this is done in the future as this technique would provide insight into the fundamental relationship between the structure and property of the multiphase materials.